A New Method of Time-Discretization for Nonlinear Systems

Graduate School of Systems and Information Engineering

University of Tsukuba

March 2015

Nguyen Van Triet

Abstract

A series of new discretization methods is proposed for obtaining discrete-time models of non-linear continuous-time systems, based on the continualization technique. This concept sheds new light to the discretization problems from an opposite angle, so to say, by highlighting a connection between a given discrete-time system and a corresponding continuous-time system. This concept is proposed and used in this thesis to derive a sufficient condition for a given discrete-time system to be an exact discretization of a continuous-time system. It is shown that this condition can be solved exactly for linear and certain nonlinear systems, in which case exact discrete-time models can be found. More importantly, perhaps, it is also shown that a variety of new models may be created by approximately solving this condition. A new model is proposed by using a linear relationship in solving this condition equation, which can always be found as long as a Jacobian matrix of the nonlinear system exists. The proposed discretization method can be applied to both autonomous and non-autonomous systems. It is proven that when Jacobian matrix of the nonlinear autonomous system is invertible, the equilibrium points of the model are identical to those of the original continuous-time system, and their asymptotic stability and instability are retained for any sampling period. A variety of self-excited and forced nonlinear oscillators, such as van der Pol and Lorenz oscillators, as well as an inverted pendulum subjected to high-frequency excitation, are examined and simulated. They show that the proposed discrete-time models perform better than all existing discrete-time models that the author is aware as on-line computable, and retain such key features as stability, limit cycles, and chaos, even for relatively large sampling periods.

The discretization method mentioned above, which is based on linear approximation, can be improved by using a Riccati approximation and is shown to have a smaller norm of the approximation error than the one based on linear approximation. Simulation results are presented for a Lotka-Volterra system to demonstrate that the proposed model has better performances than the existing methods obtained by the forward-difference, Kahan's, Mickens', and the author's previous models.

As an application of the proposed discretization methods, a new discrete-time feedback control is proposed for scalar nonlinear systems with constant parameters. It is shown that the proposed control law preserves the asymptotic stability of the desired linear system at sampling instants, while the popular forward difference and accurate Mickens methods do not, in general. As an example, the proposed control law is applied for discrete-time feedback linearization of a scalar Riccati system. Simulation results demonstrate that the proposed method has better accuracy and tends to retain the desired dynamics for larger sampling intervals, than the other two methods.

Acknowledgements

I would like to thank the people who have given their time and support, and have made it possible for me to work on and finish this thesis. First, my utmost appreciation goes to my principal research supervisor Professor Noriyuki Hori, for his guidance, unlimited continuous support and advice throughout this research. His willingness to share his vast knowledge and experience helped me learn to further develop my understanding on how to become a researcher. My respect for him as a researcher, engineer and human being is unparalleled.

I would also like to express my gratitude to my thesis committee members, Prof. Hiroshi Yabuno, Prof. Hiromi Mochiyama, Prof. Hajime Nobuhara, and Prof. Naoto Wakatsuki for their willing review, valuable and helpful suggestions to improve my thesis

I would like to thank all the members of Digital Control Laboratory, for their help and advice concerning this work.

I would like to acknowledge the financial support provided by the Honjo International Scholarship Foundation for the course of this study.

I extend my deepest thanks to my parents and brother in Vietnam, who always sincerely pray for my success in life and study, for their never ending love and care.

Last, but not least, I would like to dedicate this thesis to my family, my wife Huong and daughter MinhHa, for their love, patience, and understanding-they allowed me to spend most of the time on this thesis.

Contents

Abstract i
Acknowledgements iii
Symbols and Acronyms vii
List of figures viii
List of tables xi
1 Introduction 1
1.1 Digital control and discretization 1
1.2 Problem statement 2
1.3 Thesis overview 2
2 Discretization and continualization 3
2.1 Delta and shift operator 3
2.2 Discretization 3
2.3 Continualization 5
2.4 Summary 6
3 Discrete-time model of autonomous nonlinear systems 7
3.1 Discrete-time integration gain 7
3.2 Mapping model for a linear system 10
3.3 Exact discretization 11
3.4 Proposed discrete-time model 12
3.5 Examples of discrete-time models 14
3.5.1 Discrete-time model for van der Pol oscillator 14
3.5.2 Discrete-time model for Lorenz oscillator 17
3.6 Stability of Equilibria 22
3.6.1 Equilibrium points and their stability 22
3.6.2 Simulation results for Lotka-Volterra system 23
3.7 Summary 29
4 Discrete-time model of forced nonlinear oscillators 30
4.1 Proposed discrete-time model of forced nonlinear oscillators 30
4.2 Discrete-time models of a forced van der Pol oscillator 35
4.3 Summary 43
5 Discrete-time model of non-autonomous nonlinear systems 44
5.1 Proposed discrete-time model for non-autonomous nonlinear systems 44
5.2 Discrete-time for an inverted pendulum subjected to high frequency excitations 49
5.3 Summary 54
6 Improved nonlinear discrete-time models based on Riccati approximation of integration gains 55
6.1 Proposed model 55
6.2 Simulation results 61
6.3 Summary 67

7 A new discrete-time feedback control for scalar nonlinear systems **68**
7.1 Discrete-time feedback control 68
7.2 Discrete-time linearization feedback control for Riccati System 71
7.3 Simulation results 72
7.4 Summary 76
8 Conclusions **77**
References 79
Associated publications 82

Symbols and Acronyms

t : time

T : sampling interval

$\bar{\boldsymbol{\Gamma}}$: continuous-time system function

$\boldsymbol{\Gamma}$: discrete-time system function

$\bar{\mathbf{x}}$: continuous-time system state

$\bar{\mathbf{x}}_0$: initial value

$\bar{\mathbf{x}}^*$: continualized system state

$\mathbf{x}_k$: discrete-time system state

$\bar{\mathbf{u}}$: system input

$\mathbf{G}$: discrete-time integration gain

δ : delta operator

q : shift-left operator

$\frac{d}{dt}$: time derivative operator

$\dot{\bar{\mathbf{x}}}$: 1st order derivation of $\bar{\mathbf{x}}$

$\ddot{\bar{\mathbf{x}}}$: 2nd order derivation of $\bar{\mathbf{x}}$

D : Jacobian matrix operator

A^T : transpose of matrix or vector A

A^{-1} : inverse of matrix A

$\| \ \|$: norm

$\mathbf{I}$: identify matrix

R^n : nth order real number space

R^+ : positive real number set

ZOH: zero order hold

List of figures

Fig. 3.1: Discrete-time integration gain ……... 9

Fig. 3.2: Phase plane and time response of the four models, for $\varepsilon = 1.5$, $T = 0.1\,\text{s}$, and the initial condition of $\bar{x}_0 = -1$ and $\bar{y}_0 = -1.5$ ……... 16

Fig. 3.3: Phase plane and time response of the four models for $\varepsilon = 1.5$, $T = 0.3\,\text{s}$, and the initial condition of $\bar{x}_0 = -1$, and $\bar{y}_0 = -1.5$ ……... 17

Fig. 3.4: $x_1 - x_3$ plane of four models for $\sigma = 10,\ b = 8/3,\ r = 28$, $T = 0.05\,\text{s}$ ……... 20

Fig. 3.5: Time responses x_1 of four models for $\sigma = 10,\ b = 8/3,\ r = 28$, $T = 0.05\,\text{s}$ …… 20

Fig. 3.6: $x_1 - x_3$ plane of four models for $\sigma = 10,\ b = 8/3,\ r = 17$, $T = 0.05\,\text{s}$ ……... 21

Fig. 3.7: Time responses x_1 of four models for $\sigma = 10,\ b = 8/3,\ r = 17$, $T = 0.05\,\text{s}$ …… 21

Fig. 3.8: Time-responses of the forward-difference discrete-time model for the initial condition of $\bar{x}_1(0) = 0.2$ and $\bar{x}_2(0) = 0.4$ with different values of T …… 27

Fig. 3.9: Time-responses of Mickens' discrete-time model for the initial condition of $\bar{x}_1(0) = 0.2$ and $\bar{x}_2(0) = 0.4$ with different values of T …… 27

Fig. 3.10: Time-responses of Kahan's discrete-time model for the initial condition of $\bar{x}_1(0) = 0.2$ and $\bar{x}_2(0) = 0.4$ with different values of T …… 28

Fig. 3.11: Time-responses of the proposed discrete-time model for the initial condition of $\bar{x}_1(0) = 0.2$ and $\bar{x}_2(0) = 0.4$ with different values of T …….. 28

Fig. 4.1 Self-Sustained Oscillation (C1(s)): Phase plane and time response of the continuous-time, the forward-difference, and the proposed models, for $\bar{x}_0 = -1$, $\bar{y}_0 = -1.5$, $\varepsilon = 1.5$, $A = 1$, $\omega = 2$, $T = 0.1$ …… 38

Fig. 4.2 Quasi-Periodic Oscillation (C(1(b)): Phase plane and time response of the continuous-time, the forward-difference, and the proposed models, for $\bar{x}_0 = -1$, $\bar{y}_0 = -1.5$, $\varepsilon = 1.5$, $A = 3$, $\omega = 2$, $T = 0.1$ …… 38

Fig. 4.3 Fundamental Oscillation (C1(c)): Phase plane and time response of the continuous-time, the forward-difference, and the proposed models, for $\bar{x}_0 = -1$, $\bar{y}_0 = -1.5$, $\varepsilon = 1.5$, $A = 3$, $\omega = 3$, $T = 0.1$ 39
Fig. 4.4 Harmonic Oscillation (C1(d)): Phase plane and time response of the continuous-time, the forward-difference, and the proposed models, for $\bar{x}_0 = -1$, $\bar{y}_0 = -1.5$, $\varepsilon = 1.5$, $A = 8$, $\omega = 3$, $T = 0.1$ 39
Fig. 4.5 (C2(a)): Phase plane and time response of the continuous-time, the forward-difference, and the proposed models, for $\bar{x}_0 = -1$, $\bar{y}_0 = -1.5$, $\varepsilon = 3$, $A = 1$, $\omega = 2$, $T = 0.1$ 40
Fig. 4.6 (C2(b)): Phase plane and time response of the continuous-time and the proposed models, for $\bar{x}_0 = -1$, $\bar{y}_0 = -1.5$, $\varepsilon = 4$, $A = 1$, $\omega = 2$, $T = 0.1$ 40
Fig. 4.7 (C2(c)): Phase plane and time response of the continuous-time, and the proposed models, for $\bar{x}_0 = -1$, $\bar{y}_0 = -1.5$, $\varepsilon = 5$, $A = 1$, $\omega = 2$, $T = 0.1$ 41
Fig. 4.8 (C3(a)): Phase plane and time response of the continuous-time, the forward-difference, and the proposed models, for $\bar{x}_0 = -1$, $\bar{y}_0 = -1.5$, $\varepsilon = 1.5$, $A = 1$, $\omega = 2$, $T = 0.2$ 41
Fig. 4.9 (C3(a)): Phase plane and time response of the continuous-time, and the proposed models, for $\bar{x}_0 = -1$, $\bar{y}_0 = -1.5$, $\varepsilon = 1.5$, $A = 1$, $\omega = 2$, $T = 0.3$ 42
Fig. 4.10 (C3(b)): Phase plane and time response of the continuous-time, 4th order Runge-Kutta, and the proposed models, for $\bar{x}_0 = -1$, $\bar{y}_0 = -1.5$, $\varepsilon = 1.5$, $A = 1$, $\omega = 2$, $T = 0.3$ 42
Fig. 4.11 (C3(c)): Phase plane and time response of the continuous-time, 4th order Runge-Kutta, and the proposed models, for $\bar{x}_0 = -1$, $\bar{y}_0 = -1.5$, $\varepsilon = 1.5$, $A = 1$, $\omega = 2$, $T = 0.5$ 43
Fig. 5.1: The inverted pendulum subjected to high-frequency excitation at the base 50
Fig. 5.2: Responses of the continuous-time, the proposed, and the forward difference discrete-time models for $T = 0.001\text{s}$, $i = 1$ 52
Fig. 5.3: Responses of the continuous-time, the proposed, and the forward difference discrete-time models for $T = 0.0025\text{s}$, $i = 1$ 52
Fig. 5.4: Responses of the continuous-time, the proposed, and the forward difference discrete-time models for $T = 0.005\text{s}$, $i = 1$ 53
Fig. 5.5: Responses of the continuous-time, the proposed, and the forward difference discrete-time models for $T = 0.005\text{s}$, $i = 3$ 53
Fig. 5.6: Errors with the proposed and the forward difference discrete-time models for different values of sampling periods 54
Fig. 6.1: State response x_1 of continuous-time, Mickens, Kahan, former and proposed models for $T = 0.1s$ and $T = 0.5s$ 64

Fig. 6.2: State response x_2 of continuous-time, Mickens, Kahan, former and proposed models for $T = 0.1s$ and $T = 0.5s$ …… 65
Fig. 6.3: State response x_1 of continuous-time, Mickens, Kahan, former and proposed models for $T = 1.0s$ …… 65
Fig. 6.4: State response x_2 of continuous-time, Mickens, Kahan, former and proposed models for $T = 1.0s$ …… 66
Fig. 6.5: State response x_1 of continuous-time, Mickens, Kahan, former and proposed models for $T = 2.0s$ …… 66
Fig. 6.6: State response x_2 of continuous-time, Mickens, Kahan, former and proposed models for $T = 2.0s$ …… 67
Fig. 7.1: Structure of discrete-time feedback controller …… 71
Fig. 7.2: Responses of the desired closed-loop, forward difference, Mickens', and proposed methods for $T = 0.2$ seconds ……. 74
Fig. 7.3: Responses of the desired closed-loop, forward difference, Mickens', and proposed methods for $T = 0.4$ seconds ……. 74
Fig. 7.4: Responses of the desired closed-loop, forward difference, Mickens', and proposed methods for $T = 0.6$ seconds ……. 75
Fig. 7.5: Responses of the desired closed-loop and proposed methods for $T = 1$ second ……... 75
Fig. 7.6: Responses of the desired closed-loop, forward difference, Mickens', proposed and linearization-based methods for T=0.01 second …… 76
Fig. 8.1: Bridging the continuous-time and discrete-time domains for nonlinear system ……. 77

List of tables

Table 3.1: CPU-times elapsed during the first 100 seconds of simulation …… 29
Table 4.1: Conditions used for the simulations …….. 37
Table 6.1: Duration of computation time ……... 67

Chapter 1

Introduction

1.1 Digital control and discretization

Digital computations involving a continuous-time system require its conversion into a discrete-time format somewhere in the process, and a number of researchers have worked on this topic in a variety of fields, including engineering systems and control [1-7]. A large number of discretization methods have been proposed for linear systems [8, 9], while those available for nonlinear systems are still relatively rare [9]. A linearized discrete-time model is often used as an approximation of the given non-linear system, first by linearizing the continuous-time system around an operating point and then discretizing the resulting linear system, for which a number of discretization methods are available. Recent approaches are to obtain non-linear discrete-time models for non-linear continuous-time systems, and try to capture such key non-linear phenomena as limit cycles and chaos. Although accurate discretization methods are available for off-line simulations, those that lead to on-line computable algorithms are still relatively rare. Of those, the simplest discretization method is the forward-difference model, whose form and parameter values are chosen to be the same as those of the continuous-time system and only differentiation is replaced with its Euler discrete-time equivalent [9]. Owing to its simplicity and applicability, this model is widely used. However, its accuracy is usually poor even for linear cases unless a high sampling frequency is used. This is true also for non-linear digital control systems that are designed based on the forward-difference model, which can complicate a subsequent digital controller design in an effort to take the discretization error into account [10]. A discretization method was proposed in [2] based on bi-linearization. Although this technique seems to be applicable to some important classes of non-linear systems, it usually does not lead to an exact discrete-time model, which gives state responses that match those of the continuous-time system exactly at any discrete-time instant for any sampling period. The so-called non-standard models have been proposed in [4], which uses non-local discretization grids with constant gains based on the linear portion of the non-linear equation, and is applicable to a wide range of non-linear systems. It has been shown through simulations that the non-standard method is superior to the forward-difference model in terms of computational accuracy. However, care has to be exercised in determining the order in which the state equations are updated on-line. This formulation also makes the relationship between discrete-time and continuous-time systems less clear.

An approach that is based on exact linearization of non-linear systems has been presented for systems governed by a differential Riccati equation [11], where the gain called the discrete-time integration gain played an important role. This role is more visible using a delta-operator form [9] than the conventional shift form. The integration gain for linear systems is a function of

continuous-time parameters and a sampling interval [8], whereas that for non-linear systems, is also a function of system states [11]. Extensions of the exact gain to non-exact cases have been attempted for a non-linear oscillator [12], where the integration gain is chosen such that the system looks linear in form. However, this approach seems inapplicable for wide range of nonlinear systems, and the accuracy of derived discrete-time model is still poor.

1.2 Issues to tackle

The present thesis investigates the topics listed above, which are fundamental but long-standing issues in discretization of nonlinear systems, and tries to make important contributions in finding answers, in particular, to the following questions:

- Is there a way to look at the discretization process from a bilateral point of view with regard to the relationship between a continuous-time system and a discrete-time model?
- Is there a systematic method, exact or approximate, of discretization that is applicable to a wide range of nonlinear systems with high accuracy?
- Are the discrete-time models applicable to and effective in, the design of a digital control system, which has to be on-line computable?

The answers to these questions will be given in the thesis, in the affirmative.

1.3 Thesis organization

Based on an insight of discrete-time integration gained from the earlier attempts, the present study develops a sufficient condition for a given discrete-time system to be an exact discretization of a continuous-time system by using the concept of continualization. When this equation is solved exactly, exact discrete-time models are obtained, whereas when it is solved approximately, approximate models are derived.

The thesis is organized as follows: some definitions about the discrete-time model, the exact discrete-time model, and the continualization concept are presented in Chapter 2 [13, 14]. A brief review of the discrete-time model using the discrete-time integrator gain and the discrete-time model thus obtained for an autonomous nonlinear system with these examples for van der Pol and Lorenz oscillators are presented in Chapter 3 [14]. Investigations of equilibrium points and their stability are also presented in this chapter [15]. In Chapter 4, the models obtained for autonomous nonlinear system in Chapter 3 are extended to nonlinear forced oscillators, where the external forces are given functions of time [13]. The well-known forced van der Pol oscillator is used as an example. Chapter 5 presents the generalization of the discrete-time model of Chapter 4 to non-autonomous nonlinear systems, and an example of the inverted pendulum that is subjected to high frequency excitation [16]. An improvement of the model developed in Chapter 3 for autonomous nonlinear system is presented in Chapter 6 [17] based on Riccati approximation of integration gain. Chapter 7 treats an application of the proposed discrete-time models, which are used in the design of discrete-time linearization feedback control for scalar Riccati system [18]. Chapter 8 presents conclusions and suggests topics for future work.

Chapter 2

Discretization and continualization

In this chapter, some general concepts of discretization and discrete-time modeling are discussed. Throughout the thesis, a discrete-time model is expressed in delta operator, which has better numerical properties than that in shift operator. Definitions of exact discretization and less-stringent general discretization are presented. A process that can be considered as a sort of inverse operation of discretization is continualization. This concept will play a key role in the development of new discretization methods. A generalization of this concept is proposed by a definition of continualization for a given discrete-time model.

2.1 Delta and shift operator

In the time domain, the shift operator has been widely used for representing discrete-time systems. The reasons for its popularity are its simplicity in form and ease in understanding the mechanism of a derived algorithm and for implementing the algorithm using digital equipment. However, the relationship with continuous-time result becomes less clear. In fact, discrete-time results expressed in this form do not approach continuous-time results even if the discrete-time period approaches zero. The use of the delta operator fills the gap between continuous-time and discrete-time results. In addition, the discrete-time system expressed in this form has better numerical properties than that expressed in the shift form [9]. Therefore, the delta operator is used throughout this thesis to express discrete-time systems.

2.2 Discretization

Let a continuous-time model of a nonlinear system be given by the following state space equation:

$$\frac{d\,\bar{\mathbf{x}}(t)}{dt} = \bar{\mathbf{\Gamma}}\left(\bar{\mathbf{x}}(t), t\right), \quad \bar{\mathbf{x}}(t_0) = \bar{\mathbf{x}}_0, \tag{2.1}$$

where $\bar{\mathbf{x}} \in R^n$ is a state vector of continuous time variable t, and $\bar{\mathbf{x}}_0$ is an arbitrary initial value. $\bar{\mathbf{\Gamma}}$ is assumed to be expandable into Taylor series. This implied that $\bar{\mathbf{\Gamma}}$ satisfies the Lipschitz condition and eq. (2.1) has a unique solution for a given initial condition.

For the continuous-time system (2.1), a number of discrete-time systems can be associated. In the present study, they are expressed in delta form [9, 19] with a uniform discrete-time period of T, as

$$\delta \mathbf{x}_k = \frac{\mathbf{x}_{k+1} - \mathbf{x}_k}{T} = \mathbf{\Gamma}\left(\mathbf{x}_k, kT\right), \quad \mathbf{x}_{k_0} = \bar{\mathbf{x}}_0, \tag{2.2}$$

where $\mathbf{x}_k = \mathbf{x}(kT) \in R^n$ is the discrete-time state vector and δ is the delta operator defined as

$$\delta = \frac{q-1}{T} \tag{2.3}$$

with q being the shift-left operator such that $q\mathbf{x}_k = \mathbf{x}_{k+1}$. Since the present paper will be paying a close attention to relationships that exist between the continuous-time system and its discrete-time models, the delta operator form will be more convenient than the more conventional shift form [9]. It is assumed that the initial time k_0 is synchronized between the continuous-time and the discrete-time systems, such that

$$t_0 = k_0 T\ . \tag{2.4}$$

$\mathbf{\Gamma}$ is called discrete-time system function. Given an appropriate initial condition, the discrete-time equation (2.2) has a unique solution as long as $\mathbf{\Gamma}$ is defined for each of its arguments [20], which is a rather mild condition compared with the condition assumed on the continuous-time system.

Since discretization and continualization are the main topics of the present study, some definitions related to them are presented for clarification.

Definition 2.1 [Exact Discretization][4]: A discrete-time state $\mathbf{x}_k$ of system (2.2) is said to be an exact discretization of a continuous-time state $\bar{\mathbf{x}}(t)$ of system (2.1) if the following relationship holds for any k and T:

$$\mathbf{x}_k = \bar{\mathbf{x}}(kT) \tag{2.5}$$

In this case, a discrete-time system, whose state is $\mathbf{x}_k$, is said to be an exact discrete-time model of a continuous-time system, whose state is $\bar{\mathbf{x}}(t)$.□

The existence of an exact discrete-time model is guaranteed under the standard assumption of existence of a solution to eq. (2.1) [4]. The state of an exact discrete-time model satisfies eq. (2.5) for any T. When T is changed, $\mathbf{x}_k$ will represent a new discrete-time sequence.

The above definition is widely accepted as a proper discretization of a continuous-time signal and is sometimes called a sampled-data signal. However, discrete-time signals and systems are not always exact in the sense of Definition 2.1, but only "similar." This sense of similarity is accommodated in a more general definition given below:

Definition 2.2 [Discretization] [21]: The discrete-time state $\mathbf{x}_k$ is said to be a discretization of the continuous-time state $\bar{\mathbf{x}}(t)$ if the following relationship holds for any fixed instant τ:

$$\lim_{\substack{T\to 0 \\ kT\le\tau<(k+1)T}} \mathbf{x}_k = \bar{\mathbf{x}}(\tau). \tag{2.6}$$

Such a discrete-time system is said to be a discrete-time model of the original continuous-time system (2.1).□

It should be noted that time instant τ is fixed and kT is varied as T is changed, so the above definition uses a point-wise convergence. In this definition, τ can be anywhere between the two successive sampling instants and T approaches zero continuously. This is more general than the fixed-station-convergence used in [3], where T is limited to be such that τ/T is integer as it approaches zero.

2.3 Continualization

A process that can be considered as a sort of inverse operation of discretization is continualization, which is the role of hold devices, such as a zero-order-hold (ZOH) used in digital control. The definition proposed below is a generalization of this concept and will play a key role in the development of new discretization methods. It is more general in the sense that this does not have to be on-line computable, but is used to clarify conditions at the limit of T approaching zero.

Definition 2.3 [Signal Cotinualization]: Given the discrete-time state $\mathbf{x}_k$ of eq. (2.2), the following continuous-time signal $\bar{\mathbf{x}}^*(t)$ is said to be a continualization of $\mathbf{x}_k$: In each interval $kT \le t < (k+1)T$,

$$\bar{\mathbf{x}}^*(t) = \bar{\mathbf{x}}^*(kT) + (t-kT)\boldsymbol{\Gamma}\left(\bar{\mathbf{x}}^*(kT), t-kT\right), \tag{2.7}$$

where $\bar{\mathbf{x}}^*(kT) = \mathbf{x}_k$. □

Remark 2.1: The discrete-time state of system (2.2) is an exact discretization of the continualized signal (2.7), since $\bar{\mathbf{x}}^*(kT) = \mathbf{x}_k$ for any k and T. However, there are a number of continuous-time signals that can pass through the same discrete-time sequence for a finite T. It should be noted that this continuous-time signal is a function of both t and T.

The concept of a continualized signal can be extended to a system, as follows:

Definition 2.4 [System Continualization]: Using $\boldsymbol{\Gamma}$ of a given discrete-time system (2.2), the continuous-time system given by

$$\dot{\bar{\mathbf{x}}}^*(t) = \bar{\boldsymbol{\Gamma}}^*\left(\bar{\mathbf{x}}^*(t), t\right) = \frac{d}{dt}\left((t-kT)\boldsymbol{\Gamma}\left(\bar{\mathbf{x}}^*(kT), t-kT\right)\right) \tag{2.8}$$

where $\bar{\mathbf{x}}^*(t)$ is generated by eq. (2.7) in each $kT \le t < (k+1)T$, is said to be the continualized system of discrete-time system (2.2). □

Remark 2.2: Since $\mathbf{x}_k = \overline{\mathbf{x}}^*(kT)$ for all positive k and T, which satisfies Definition 2.1, the discrete-time system given by eq. (2.2) is an exact discrete-time model of the continualized system (2.8), but not necessarily of system (2.1).

2.4 Summary

For a given continuous-time model, the discrete-time model is expressed in delta form, which has better numerical properties than the expression using shift form. Definitions of exact discretization and more general discretization are presented. A process that can be considered as a sort of inverse operation of discretization is continualization. This concept will play a key role in the development of new discretization methods in this study. A generalization of this concept is proposed by a definition of continualization for a given discrete-time model.

Chapter 3

Discrete-time model of autonomous nonlinear systems

A new approach is proposed for obtaining discrete-time models of a nonlinear autonomous continuous-time system based on classification of, what is called in this study, a discrete-time integration gain. The models are expressed as a product of this gain and the system function that has the same structure as that of the continuous-time system. By using the continualization proposed in Chapter 2, sufficient conditions on this gain to make the model exact are presented. A new discrete-time model is proposed for nonlinear systems, which is approximate in general, but exact for linear systems. The method is applicable to any system that has a Jacobian matrix. It is shown that when Jacobian matrix of the nonlinear equation is invertible, the equilibrium points of the proposed discrete-time model are identical to those of the original continuous-time system, and their asymptotic stability and instability are retained for any sampling period. As examples, Lotka-Volterra system, van der Pol and Lorenz oscillators are examined and simulated to show that the proposed discrete-time models performs better than other discrete-time models that are known to the authors to be on-line computable such as the forward-difference, Mickens', Kahan's models.

3.1 Discrete-time integration gain

Consider an autonomous continuous-time system given by the following state space equation:

$$\frac{d\,\bar{\mathbf{x}}(t)}{dt} = \bar{\boldsymbol{\Gamma}}\left(\bar{\mathbf{x}}(t)\right), \quad \bar{\mathbf{x}}(t_0) = \bar{\mathbf{x}}_0, \tag{3.1}$$

Function $\bar{\boldsymbol{\Gamma}}: R^n \to R^n$ depends, in general, on state $\bar{\mathbf{x}}$ and is assumed to be expandable into Taylor series. In the present study, the discrete-time model is based on the use of the discrete-time integration gain expressed in delta operator form as [11]

$$\delta \mathbf{x}_k = \frac{\mathbf{x}_{k+1} - \mathbf{x}_k}{T} = \mathbf{G}\left(\mathbf{x}_k, T\right)\bar{\boldsymbol{\Gamma}}\left(\mathbf{x}_k\right), \quad \mathbf{x}_{k_0} = \bar{\mathbf{x}}_0, \tag{3.2}$$

where delta operator δ is defined eq. (2.3), and the discrete-time system function $\boldsymbol{\Gamma}$ in eq. (2.2) is expressed by a product of $\mathbf{G}$ and $\bar{\boldsymbol{\Gamma}}$.

It should be emphasized that function $\bar{\boldsymbol{\Gamma}}$ in eq. (3.2) is the same function as that in eq. (3.1). The matrix $\mathbf{G}\left(\mathbf{x}_k, T\right) \in R^{n\times n}$, which is called the discrete-time integration gain in the present study, is a bounded function of both, in general, T and $\mathbf{x}_k$, and is assumed to be differentiable with respect to

T . This gain plays a key role in the present study in the development of discrete-time models. The discrete-time system has a unique solution given an initial condition.

Remark 3.1: The integration gain can be used to classify various discrete-time models. For linear systems given by $\bar{\boldsymbol{\Gamma}}(\bar{\mathbf{x}}) = \mathbf{A}\bar{\mathbf{x}} + \mathbf{B}$, the so called step-invariant model is one given by $\mathbf{G}(\mathbf{x}_k, T) = \left(\int_0^T e^{\mathbf{A}\tau} d\tau \right) / T$, which is the average of the state-transition matrix over a discrete-time period, and is known to give state responses that match those of the continuous-time system under zero-order hold exactly at all discrete-time instants for any period T . For linear and nonlinear systems, the forward difference model is one with the integration gain set to identify matrix, or $\mathbf{G}(\mathbf{x}_k, T) = \mathbf{I}$, and can have good accuracy if T is sufficiently small.

For the purpose of comprehending the geometric role of discrete-time integration gain $\mathbf{G}$, consider a scalar system as

$$\frac{d\bar{x}(t)}{dt} = \bar{\Gamma}(\bar{x}(t)). \tag{3.3}$$

For the continuous-time system as eq. (3.3), most conventional methods, such as the forward-difference method for a scalar system, adjust only the difference on vertical axis $\bar{x}$, in a fixed time period T to approximate the exact slope of $\bar{x}(t)$. The drawback of these methods is the inability to compute online and their poor accuracy is at low sampling frequency. For example, the forward difference method, which is simple to compute only approximates the slope of continuous-time state $\bar{x}(t)$ by δx_k such that the discrete-time integrator gain in (3.2) is fixed at identity matrix. However, the idea of discrete-time integrator gain is that, the slope of $\bar{x}(t)$ can be discretized exactly also by using the discrete-time integration operator δ , which enables online computation, in a virtual space where the time period T between $\lfloor kT, (k+1)T \rceil$ is expanded by the discrete-time integrator gain $G(x_k, T)$ as illustrated in Fig. 3.1.

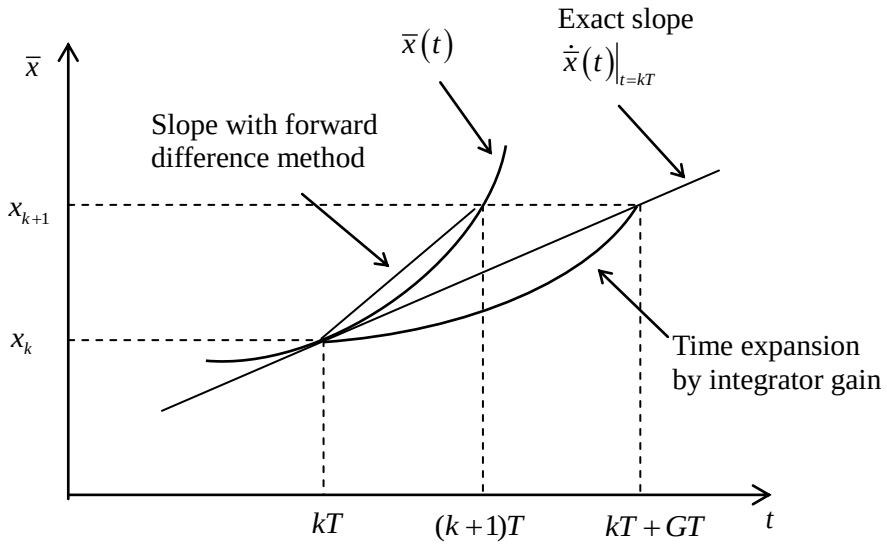

Fig. 3.1: Discrete-time integration gain

Insights obtained from [8, 21] for linear systems have hinted the following theorem for the above discrete-time integration gain:

Theorem 3.1: A discrete-time state $\mathbf{x}_k$ of system (3.2) is a discretization of the continuous-time state $\bar{\mathbf{x}}(t)$ of system (3.1), if the integration gain in (3.2) satisfies the following condition

$$\lim_{T\to 0}\mathbf{G}(\mathbf{x}_k, T) = \mathbf{I} \tag{3.4}$$

where $\mathbf{I}$ is an identity matrix. When this condition is satisfied, system (3.2) is a discrete-time model of continuous-time system (3.1).□

Proof: From Definition 2.3, the discrete-time state $\mathbf{x}_k$ of (3.2) is an exact discretization of a continuous-time state $\bar{\mathbf{x}}^*(t)$ that satisfies eq. (2.7) for $t \in \lfloor kT, (k+1)T)$. Therefore, letting $t = \tau$ in eq. (2.7), one has

$$\frac{\bar{\mathbf{x}}^*(\tau) - \bar{\mathbf{x}}^*(kT)}{\tau - kT} = \mathbf{G}\left(\bar{\mathbf{x}}^*(kT), \tau - kT\right)\bar{\mathbf{\Gamma}}\left(\bar{\mathbf{x}}^*(kT)\right) \tag{3.5}$$

for any fixed τ. On the other hand, since

$$\lim_{\substack{T\to 0 \\ kT\le\tau<(k+1)T}} kT = \tau \tag{3.6}$$

and the limit of (3.4) is satisfied for arbitrary values of k, the continuous-time gain satisfies

$$\lim_{\substack{T\to 0 \\ kT\le T<(k+1)T}} \mathbf{G}\left(\bar{\mathbf{x}}^*(kT), \tau - kT\right) = \lim_{(\tau - kT)\to 0} \mathbf{G}\left(\bar{\mathbf{x}}^*(kT), \tau - kT\right) = \mathbf{I} \tag{3.7}$$

Noting that

$$\lim_{\substack{T\to 0\\ kT\le T<(k+1)T}} \bar{\mathbf{x}}^*(kT)=\bar{\mathbf{x}}^*(\tau) \tag{3.8}$$

the limit of (3.5) yields

$$\begin{aligned}\lim_{\substack{T\to 0\\ kT\le T<(k+1)T}} \frac{\bar{\mathbf{x}}^*(\tau)-\bar{\mathbf{x}}^*(kT)}{\tau-kT} &= \lim_{\substack{T\to 0\\ kT\le T<(k+1)T}} \mathbf{G}\left(\bar{\mathbf{x}}^*(kT),\tau-kT\right)\bar{\mathbf{\Gamma}}\left(\bar{\mathbf{x}}^*(kT)\right)\\ &= \lim_{\substack{T\to 0\\ kT\le T<(k+1)T}} \bar{\mathbf{\Gamma}}\left(\bar{\mathbf{x}}^*(kT)\right)\\ &= \bar{\mathbf{\Gamma}}\left(\lim_{\substack{T\to 0\\ kT\le T<(k+1)T}} \bar{\mathbf{x}}^*(kT)\right)=\bar{\mathbf{\Gamma}}\left(\bar{\mathbf{x}}^*(\tau)\right)\end{aligned} \tag{3.9}$$

As T approaches zero, so that condition (3.4) holds, the above gives

$$\frac{d\bar{\mathbf{x}}^*(\tau)}{dt}=\bar{\mathbf{\Gamma}}\left(\bar{\mathbf{x}}^*(\tau)\right) \tag{3.10}$$

for all τ in the limit. Since there is only one solution of eq. (3.1) at any time instant, it follows that

$$\bar{\mathbf{x}}^*(\tau)=\bar{\mathbf{x}}(\tau) \tag{3.11}$$

while the exactness of discretization of $\mathbf{x}_k$ to $\bar{\mathbf{x}}^*(t)$ gives

$$\mathbf{x}_k=\bar{\mathbf{x}}^*(kT) \tag{3.12}$$

Finally, for eq. (3.12), take the limit of T approaching zero and choosing k such that $kT\le\tau<(k+1)T$, and use (3.8) and (3.11), to obtain

$$\lim_{\substack{T\to 0\\ kT\le T<(k+1)T}} \mathbf{x}_k = \lim_{\substack{T\to 0\\ kT\le T<(k+1)T}} \bar{\mathbf{x}}^*(kT)=\bar{\mathbf{x}}^*(\tau)=\bar{\mathbf{x}}(\tau) \tag{3.13}$$

for any τ. Therefore, system (3.2) is a discrete-time model of the continuous-time system (3.1) in the sense of Definition 2.2.

3.2 Mapping model for a linear system

A linear, time invariant, continuous-time system is given as (3.1) with

$$\bar{\mathbf{\Gamma}}\left(\bar{\mathbf{x}}(t)\right)=\mathbf{A}\bar{\mathbf{x}}(t)+\mathbf{B} \tag{3.14}$$

where $\mathbf{A}$, $\mathbf{B}$ are system parameters. The mapping models [21], which are based on approximations of numerical differentiation or integration, for the above continuous-time system are given by (3.2), where discrete-time integration gain is given as

$$\mathbf{G}\left(\mathbf{x}_k,T\right)=\left(\mathbf{I}-\mu T\mathbf{A}\right)^{-1} \tag{3.15}$$

Depending on the value chosen for parameter μ, different mapping models can be obtained. The forward-difference model is obtained by setting $\mu=0$, the backward- difference model by $\mu=1$,

and the Tustin' s model by $\mu = 1/2$. The value of μ is not limited to these values as long as the inverse matrix in (3.15) exists and the discrete-time integration gain $\mathbf{G}(\mathbf{x}_k, T)$ approaches the continuous-time integration gain or the identity matrix $\mathbf{I}$ as the discrete-time period T goes to zero. However, these models can cause large errors in their results as the discrete-time period increases.

3.3 Exact discretization

The following theorem states that any discrete-time system (3.2) can be an exact model of a continuous-time system (3.1) if the integration gain $\mathbf{G}$ is chosen in a certain manner.

Theorem 3.2: A discrete-time system (3.2), is an exact model of a continuous-time system (3.1), if the discrete-time integration gain $\mathbf{G}$ in (3.2) is chosen to satisfy the following three conditions:

(i) $\mathbf{G}(\mathbf{x}_k, s)$, $\partial \mathbf{G}(\mathbf{x}_k, s)/\partial \mathbf{x}_k$, $\partial\left(\partial \mathbf{G}(\mathbf{x}_k, s)/\partial s\right)/\partial \mathbf{x}_k$ are continuous functions of $\mathbf{x}_k$, where $s \in R^+$

(ii) $\dfrac{\partial\left[\mathbf{G}(\mathbf{x}_k, s)\bar{\mathbf{\Gamma}}(\mathbf{x}_k)\right]}{\partial \mathbf{x}_k} \neq -1$

(iii) $\dot{\mathbf{H}}\left(\bar{\mathbf{x}}^*(kT), t-kT\right)\bar{\mathbf{\Gamma}}\left(\bar{\mathbf{x}}^*(kT)\right) = \bar{\mathbf{\Gamma}}\left(\bar{\mathbf{x}}^*(kT) + \mathbf{H}\left(\bar{\mathbf{x}}^*(kT), t-kT\right)\bar{\mathbf{\Gamma}}\left(\bar{\mathbf{x}}^*(kT)\right)\right)$ (3.16)

for each interval $kT \le t < (k+1)T$, where $\bar{\mathbf{x}}^*(t)$ is the continualization of discrete-time state $\mathbf{x}_k$ as Definition 2.3, and the continuous-time function $\mathbf{H}\left(\bar{\mathbf{x}}^*(kT), t-kT\right)$ is defined as

$$\mathbf{H}\left(\bar{\mathbf{x}}^*(kT), t-kT\right) = (t-kT)\mathbf{G}\left(\bar{\mathbf{x}}^*(kT), t-kT\right). \square \tag{3.17}$$

Proof: A sufficient condition for eq. (2.8) to have a unique solution in each interval is that $\bar{\mathbf{\Gamma}}^*\left(\bar{\mathbf{x}}^*(t), t\right)$ in eq. (2.8) is a continuous function of $\bar{\mathbf{x}}^*$. Since

$$\begin{aligned}\frac{\partial \bar{\mathbf{\Gamma}}^*\left(\bar{\mathbf{x}}^*(t), t\right)}{\partial \bar{\mathbf{x}}^*(t)} &= \frac{\partial\left[\dot{\mathbf{H}}\left(\bar{\mathbf{x}}^*(kT), t-kT\right)\bar{\mathbf{\Gamma}}\left(\bar{\mathbf{x}}^*(kT)\right)\right]/\partial \bar{\mathbf{x}}^*(kT)}{\partial\left[\bar{\mathbf{x}}^*(kT) + \mathbf{H}\left(\bar{\mathbf{x}}^*(kT), t-kT\right)\bar{\mathbf{\Gamma}}\left(\bar{\mathbf{x}}^*(kT)\right)\right]/\partial \bar{\mathbf{x}}^*(kT)} \\ &= \frac{\partial\left[\dot{\mathbf{H}}\left(\bar{\mathbf{x}}^*(kT), t-kT\right)\bar{\mathbf{\Gamma}}\left(\bar{\mathbf{x}}^*(kT)\right)\right]/\partial \bar{\mathbf{x}}^*(kT)}{1 + \partial\left[\mathbf{H}\left(\bar{\mathbf{x}}^*(kT), t-kT\right)\bar{\mathbf{\Gamma}}\left(\bar{\mathbf{x}}^*(kT)\right)\right]/\partial \bar{\mathbf{x}}^*(kT)}\end{aligned} \tag{3.18}$$

$\bar{\mathbf{\Gamma}}^*\left(\bar{\mathbf{x}}^*(t), t\right)$ is a continuous function of $\bar{\mathbf{x}}^*$ if condition (i) and (ii) are met.

Thus, $\mathbf{x}_k$ is an uniquely exact discretization of continualization $\bar{\mathbf{x}}^*(t)$. Condition (iii) implies that,

for each $kT \le t < (k+1)T$, the state $\bar{\mathbf{x}}^*(t)$ is a unique solution of the original continuous-time (3.1), and discrete-time system (3.2) is an exact discretization of continuous-time system (3.1).

Remark 3.2: For a logistic system be given by

$$\dot{\bar{x}}(t) = \bar{x}(t)\left(1 - \varepsilon \bar{x}(t)\right) = \bar{x}(t) - \varepsilon\left(\bar{x}(t)\right)^2 \tag{3.19}$$

where ε is a positive parameter, the expansion (3.16) terminates after three terms, as

$$\begin{aligned} \dot{\mathrm{H}}\left(\bar{x}^*(kT), t-kT\right) = 1 + \left(1 - 2\varepsilon \bar{x}^*(kT)\right)\mathrm{H}\left(\bar{x}^*(kT), t-kT\right) \\ - \varepsilon \bar{x}^*(kT)\left(1 - \varepsilon \bar{x}^*(kT)\right)\left[\mathrm{H}\left(\bar{x}^*(kT), t-kT\right)\right]^2 \end{aligned} \tag{3.20}$$

which can be solved exactly, using $\mathrm{H}\left(\bar{x}^*(kT), t-kT\right) = 0$ at $t = kT$, as

$$\mathrm{H}\left(\bar{x}^*(kT), t-kT\right) = \frac{e^{t-kT} - 1}{1 + \varepsilon \bar{x}^*(kT)\left(e^{t-kT} - 1\right)} \tag{3.21}$$

Therefore, we have

$$G\left(\bar{x}^*(kT), t-kT\right) = \frac{1}{t-kT} \frac{e^{t-kT} - 1}{1 + \varepsilon \bar{x}^*(kT)\left(e^{t-kT} - 1\right)}. \tag{3.22}$$

In eq. (3.22), when t is taken as $t = (k+1)T$, one obtains

$$G\left(\bar{x}^*(kT), T\right) = \frac{1}{T} \frac{e^{T} - 1}{1 + \varepsilon \bar{x}^*(kT)\left(e^{T} - 1\right)}, \tag{3.23}$$

which leads to the exact discrete-time integration gain given by

$$G\left(x_k, T\right) = \frac{1}{T} \frac{e^{T} - 1}{1 + \varepsilon x_k \left(e^{T} - 1\right)} \quad \to I\,(T \to 0). \tag{3.24}$$

Exact discrete-time models of logistic systems can be obtained via exact linearization using variable transformation [11]. However, the present method is easier.

3.4 Proposed discrete-time model

The following model is widely applicable to nonlinear systems given in the form of (3.1) and will be called the proposed discrete-time model.

Theorem 3.3 [The proposed model]: A nonlinear discrete-time system given by (3.2) with the discrete-time integrator gain given by

$$\mathbf{G}\left(\mathbf{x}_k, T\right) = \frac{1}{T} \int_o^T e^{\left[D\bar{\mathbf{f}}(\mathbf{x}_k)\right]\tau} d\tau \tag{3.25}$$

where $D\bar{\mathbf{\Gamma}}(\mathbf{x}_k)$ is a Jacobian matrix of $\bar{\mathbf{\Gamma}}$ at $\mathbf{x}_k$, is a discrete-time model of the continuous-time model given by (3.1). When Jacobian $D\bar{\mathbf{\Gamma}}(\bar{\mathbf{x}}_k)$ is non-singular, the gain can be written as

$$\mathbf{G}(\mathbf{x}_k, T) = \frac{e^{\left[D\bar{\mathbf{\Gamma}}(\mathbf{x}_k)\right]T} - \mathbf{I}}{T}\left[D\bar{\mathbf{\Gamma}}(\mathbf{x}_k)\right]^{-1}.\square \tag{3.26}$$

Proof: Using l'Hospital's Rule, one obtain

$$\lim_{T\to 0}\mathbf{G}(\mathbf{x}_k, T) = \lim_{T\to 0}\frac{1}{T}\int_0^T e^{\left[D\bar{\mathbf{\Gamma}}(\mathbf{x}_k)\right]\tau}d\tau = \mathbf{I} \tag{3.27}$$

so that a discrete-time system (3.2) is a discrete-time model of continuous-time system in the sense of Definition 2.2.

The derivation for eq. (3.25) is as follows: When the Taylor series expansion around $\bar{\mathbf{x}}^*(kT)$ of eq. (3.16) is truncated with the first two terms, one requires,

$$\dot{\mathbf{H}}(\bar{\mathbf{x}}^*(kT), t-kT) = \mathbf{I} + \left[D\bar{\mathbf{\Gamma}}(\bar{\mathbf{x}}^*(kT))\right]\mathbf{H}(\bar{\mathbf{x}}^*(kT), t-kT) \tag{3.28}$$

Noting that $\mathbf{H}(\bar{\mathbf{x}}^*(kT), t-kT)$ is, in general, a function of $\bar{\mathbf{x}}^*(kT)$ and $(t-kT)$, and that $\mathbf{H}(\bar{\mathbf{x}}^*(kT), t-kT) = 0$ when $t = kT$, a solution to the above linear differential equation is found to be

$$\mathbf{H}(\bar{\mathbf{x}}^*(kT), t-kT) = \int_0^{t-kT} e^{\left[D\bar{\mathbf{\Gamma}}(\bar{\mathbf{x}}^*(kT))\right]\tau}d\tau \tag{3.29}$$

Substituting the above into eq. (3.17) gives the following continuous-time gain function:

$$\mathbf{G}(\bar{\mathbf{x}}^*(kT), t-kT) = \frac{1}{t-kT}\int_0^{t-kT} e^{\left[D\bar{\mathbf{\Gamma}}(\bar{\mathbf{x}}^*(kT))\right]\tau}d\tau \tag{3.30}$$

In eq. (3.30), when t is taken as $t = (k+1)T$, we have

$$\mathbf{G}(\bar{\mathbf{x}}^*(kT), T) = \frac{1}{T}\int_0^T e^{\left[D\bar{\mathbf{\Gamma}}(\bar{\mathbf{x}}^*(kT))\right]\tau}d\tau \tag{3.31}$$

Using the same form of function $\mathbf{G}$, the discrete-time integration gain is obtained as

$$\mathbf{G}(\mathbf{x}_k, T) = \frac{1}{T}\int_0^T e^{\left[D\bar{\mathbf{\Gamma}}(\bar{\mathbf{x}}_k)\right]\tau}d\tau \tag{3.32}$$

The proposed model can be found for any nonlinear system (3.1) as long as its Jacobian matrix exists. The fact that this model gives good results for many nonlinear systems and retain important features for van der Pol and Lorentz oscillators will be shown by simulations shortly.

Remark 3.3: For a linear system, $\bar{\mathbf{\Gamma}}$ in eq. (3.1) is given by

$$\bar{\mathbf{\Gamma}}(\bar{\mathbf{x}}) = \mathbf{A}\bar{\mathbf{x}} + \mathbf{B} \tag{3.33}$$

where $\mathbf{A}$, $\mathbf{B}$ are system parameters of compatible dimensions. In this case, eq. (3.16) can be written exactly as a linear equation $\dot{\mathbf{H}}\left(\bar{\mathbf{x}}^*\left(kT\right),t-kT\right)=\mathbf{I}+\mathbf{A}\mathbf{H}\left(\bar{\mathbf{x}}^*\left(kT\right),t-kT\right)$, which is independent of $\bar{\mathbf{x}}^*\left(kT\right)$ and whose solution is $\mathbf{H}\left(\bar{\mathbf{x}}^*\left(kT\right),t-kT\right)=\int_0^{t-kT}e^{\mathbf{A}\tau}d\tau$. This leads to the integration gain of the exact discrete-time model [8] as

$$\mathbf{G}\left(\mathbf{x}_k,T\right)=\frac{1}{T}\int_o^T e^{\mathbf{A}\tau}d\tau \tag{3.34}$$

When $\mathbf{A}$ is invertible, this gain can be written as

$$\mathbf{G}\left(\mathbf{x}_k,T\right)=\frac{e^{\mathbf{A}T}-\mathbf{I}}{T}\mathbf{A}^{-1}. \tag{3.35}$$

3.5 Examples of discrete-time models

3.5.1 Discrete-time model for van der Pol oscillator

Van der Pol oscillator was proposed by Balthasar van der Pol in 1920 to describe an electronic circuit that appeared in very early radios, modeled by following nonlinear differential equation [22]

$$\ddot{\bar{x}}=-\bar{x}+\varepsilon\left(1-\bar{x}^2\right)\dot{\bar{x}} \tag{3.36}$$

where ε is a positive parameter that characterizes a degree of nonlinearity. This can be rewritten in a form of

$$\begin{cases}\dot{\bar{x}}=\bar{y}\\ \dot{\bar{y}}=-\bar{x}+\varepsilon\left(1-\bar{x}^2\right)\bar{y}\end{cases}, \tag{3.37}$$

whose Jacobian matrix is non-singular and given by

$$D\bar{\mathbf{\Gamma}}\left(\bar{\mathbf{x}}\right)=\begin{bmatrix}0 & 1\\ -1-2\varepsilon\bar{x}\bar{y} & \varepsilon\left(1-\bar{x}^2\right)\end{bmatrix}. \tag{3.38}$$

Using the discrete-time integration gain given by eq. (3.25), the proposed discrete-time model is obtained as

$$\begin{bmatrix}\delta x_k\\ \delta y_k\end{bmatrix}=\frac{e^{\left[D\bar{\mathbf{\Gamma}}(\mathbf{x}_k)\right]T}-\mathbf{I}}{T}\left[D\bar{\mathbf{\Gamma}}\left(\mathbf{x}_k\right)\right]^{-1}\begin{bmatrix}y_k\\ -x_k+\varepsilon\left(1-x_k^2\right)y_k\end{bmatrix}, \tag{3.39}$$

where

$$D\bar{\mathbf{\Gamma}}\left(\mathbf{x}_k\right)=\begin{bmatrix}0 & 1\\ -1-2\varepsilon x_k y_k & \varepsilon\left(1-x_k{}^2\right)\end{bmatrix}. \tag{3.40}$$

Mickens' model for the van der Pol oscillator [4] is given by

$$\begin{bmatrix} \delta x_k \\ \delta y_k \end{bmatrix} = \phi \begin{bmatrix} y_k \\ -x_k + \varepsilon\left(1 - x_{k+1}^2\right) y_k \end{bmatrix} + \varphi \begin{bmatrix} x_k \\ y_k \end{bmatrix}, \tag{3.41}$$

where ϕ and φ are given by

$$\varphi = \frac{e^{T\frac{\varepsilon}{2}} \left\{ \cos\sqrt{1-\left(\frac{\varepsilon}{2}\right)^2}\, T - \frac{\varepsilon \sin\sqrt{1-\left(\frac{\varepsilon}{2}\right)^2}\, T}{2\sqrt{1-\left(\frac{\varepsilon}{2}\right)^2}} \right\} - 1}{T}, \tag{3.42}$$

$$\phi = e^{\frac{\varepsilon}{2}T} \frac{\sin\sqrt{1-\left(\frac{\varepsilon}{2}\right)^2}\, T}{\sqrt{1-\left(\frac{\varepsilon}{2}\right)^2}\, T}. \tag{3.43}$$

In this discretization scheme, the eigenvalues λ_1 and λ_2 of a linear part of the nonlinear function must be distinct, and the parameter be such that $\varepsilon < 2$. It should be noted that the right-hand-side of the above equation for δy_k contains the term x_{k+1}, which makes this method nonlocal and nonstandard [4]. Therefore, variable x_k must be updated before y_k in computations.

The forward difference model is obtained simply as

$$\begin{bmatrix} \delta x_k \\ \delta y_k \end{bmatrix} = \begin{bmatrix} y_k \\ -x_k + \varepsilon\left(1 - x_k^2\right) y_k \end{bmatrix}. \tag{3.44}$$

Extensive simulations have been carried out with the van der Pol oscillator (3.37) and some typical results of phase-planes and time responses are shown in Figs. 3.2 and 3.3. They compare the original continuous-time oscillator computed using the Runge-Kutta method, the proposed model, Micken's model, and the forward-difference models.

In Fig. 3.2, the phase plane plots are traced from 0 to 1,000 seconds and the time response for the first 10 seconds, for $\varepsilon = 1.5$, $T = 0.1$s, and the initial condition of $\bar{x}_0 = -1.0$ and $\bar{y}_0 = -1.5$, which is inside the limit cycle. At this sampling interval, all discrete-time models give responses that are more or less results similar to those of the continuous-time model, although the proposed model is closest.

Fig. 3.3 shows the results under the same conditions except for the sampling interval, which is increased to 0.3 seconds. At this sampling interval, neither Mickens' model nor the forward-difference model could give steady results, while the proposed model is still very close to the continuous-time model. Although not shown here, in all simulation tests for larger nonlinear parameter values of ε and ranges of T and the initial conditions, it was found that the proposed discrete-time model

consistently gave results closer to the continuous-time van der Pol model than the forward-difference and Mickens models.

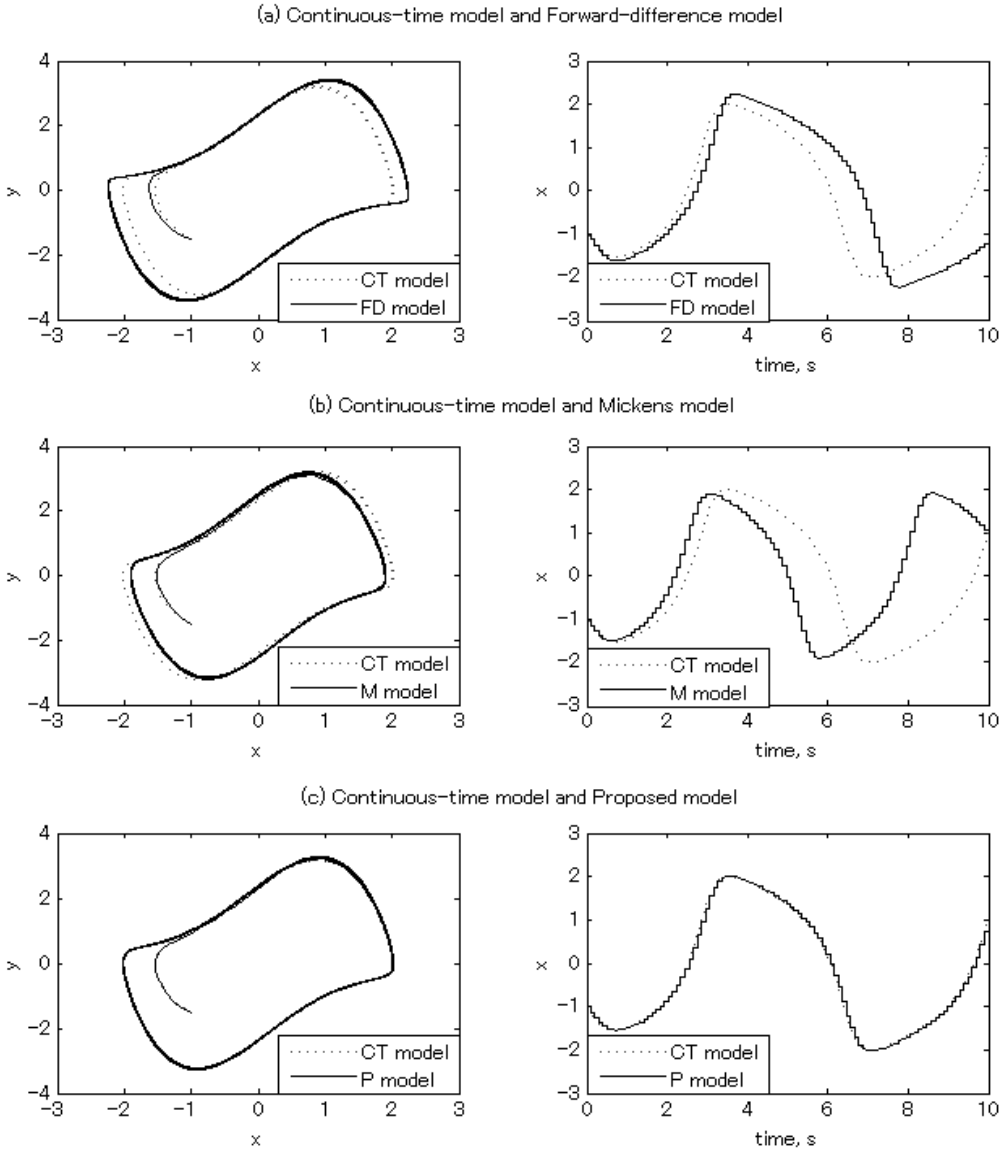

Fig. 3.2: Phase plane and time response of the four models, for $\varepsilon = 1.5$, $T = 0.1$s, and the initial condition of $\bar{x}_0 = -1$ and $\bar{y}_0 = -1.5$

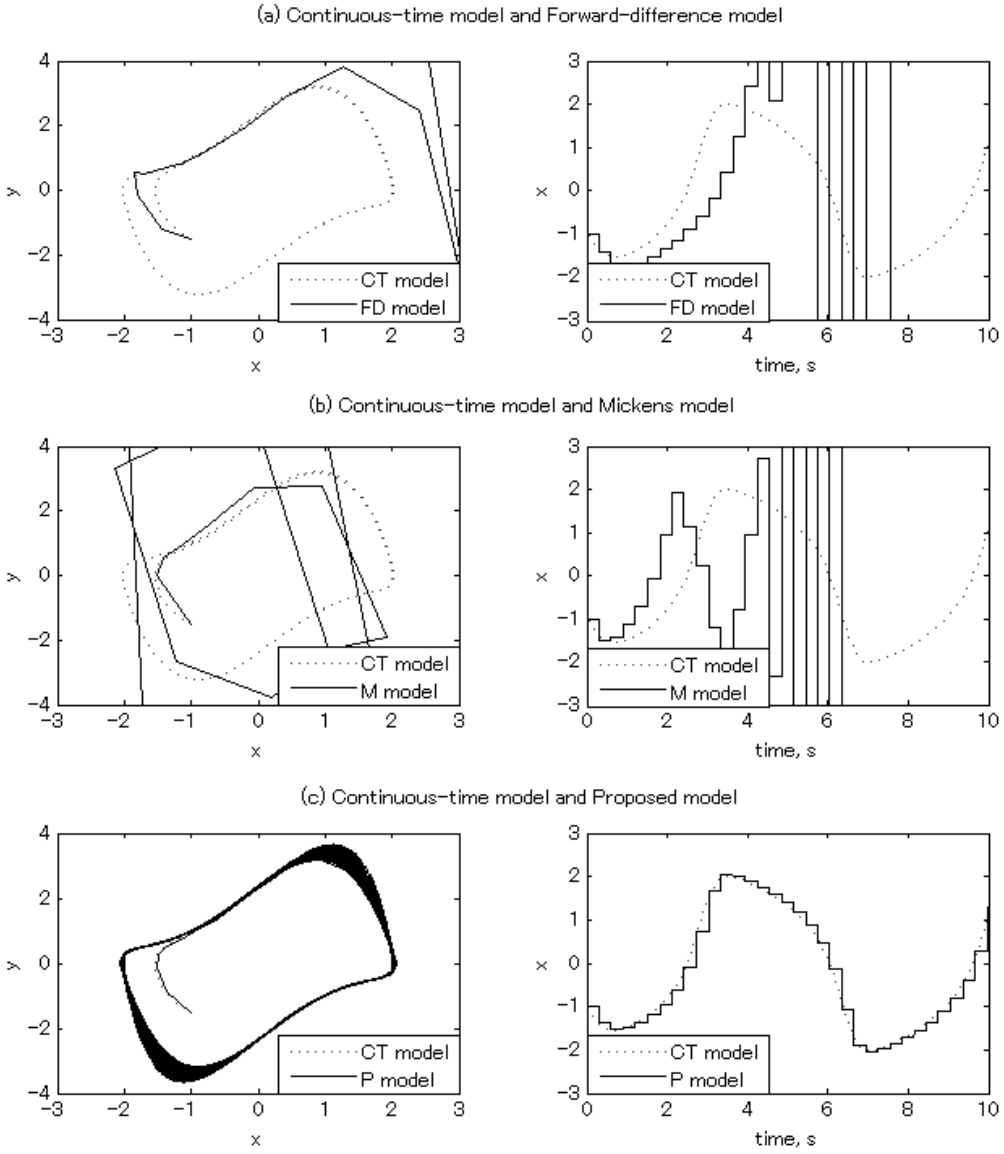

Fig. 3.3: Phase plane and time response of the four models for $\varepsilon = 1.5$, $T = 0.3$ s, and the initial condition of $\bar{x}_0 = -1$, and $\bar{y}_0 = -1.5$

3.5.2 Discrete-time model for Lorenz oscillator

Consider the Lorenz oscillator [23] given by the following equation:

$$\begin{cases} \dot{\bar{x}}_1 = \sigma\left(\bar{x}_2 - \bar{x}_1\right) \\ \dot{\bar{x}}_2 = r\bar{x}_1 - \bar{x}_2 - \bar{x}_1\bar{x}_3 \\ \dot{\bar{x}}_3 = -b\bar{x}_3 + \bar{x}_1\bar{x}_2 \end{cases} \tag{3.45}$$

where all parameters are positive; i.e., $\sigma, r, b > 0$. In particular, σ is the Prandtl number and r the Rayleigh number. Jacobian matrix of this system is

$$D\bar{\mathbf{\Gamma}}(\bar{\mathbf{x}}) = \begin{bmatrix} -\sigma & \sigma & 0 \\ r - \bar{x}_3 & -1 & -\bar{x}_1 \\ \bar{x}_2 & \bar{x}_1 & -b \end{bmatrix} \tag{3.46}$$

The proposed discrete-time model can be obtained as

$$\begin{bmatrix} \delta x_{1,k} \\ \delta x_{2,k} \\ \delta x_{3,k} \end{bmatrix} = \frac{e^{\left[D\bar{\mathbf{\Gamma}}(\mathbf{x}_k)\right]T} - \mathbf{I}}{T} \left[D\bar{\mathbf{\Gamma}}(\mathbf{x}_k) \right]^{-1} \begin{bmatrix} \sigma(x_{2,k} - x_{1,k}) \\ r x_{1,k} - x_{2,k} - x_{1,k} x_{3,k} \\ -b x_{3,k} + x_{1,k} x_{2,k} \end{bmatrix} \tag{3.47}$$

where

$$D\bar{\mathbf{\Gamma}}(\mathbf{x}_k) = \begin{bmatrix} -\sigma & \sigma & 0 \\ r - x_{3,k} & -1 & -x_{1,k} \\ x_{2,k} & x_{1,k} & -b \end{bmatrix}. \tag{3.48}$$

Mickens' discrete-time model [24] is given by

$$\begin{bmatrix} \delta x_{1,k} \\ \delta x_{2,k} \\ \delta x_{3,k} \end{bmatrix} = \begin{bmatrix} \frac{1 - e^{-\sigma T}}{\sigma T} & 0 & 0 \\ 0 & 1 - e^{-T} & 0 \\ 0 & 0 & \frac{1 - e^{-bT}}{bT} \end{bmatrix} \begin{bmatrix} -\sigma x_{1,k} + \sigma x_{2,k} \\ r x_{1,k+1} - x_{2,k} - x_{1,k+1} x_{3,k} \\ -b x_{3,k} + x_{1,k+1} x_{2,k+1} \end{bmatrix}. \tag{3.49}$$

It can be seen that there are such nonlinear terms as $x_{1,k+1}x_{3,k}$ and $x_{1,k+1}x_{2,k+1}$ in the above.

The forward difference model is obtained as

$$\begin{bmatrix} \delta x_{1,k} \\ \delta x_{2,k} \\ \delta x_{3,k} \end{bmatrix} = \begin{bmatrix} \sigma(x_{2,k} - x_{1,k}) \\ r x_{1,k} - x_{2,k} - x_{1,k} x_{3,k} \\ -b x_{3,k} + x_{1,k} x_{2,k} \end{bmatrix}. \tag{3.50}$$

Simulations have been carried also for the Lorenz system (3.45), where $\sigma = 10$ and $b = 8/3$. For a Rayleigh number r smaller than 24.06, the system state approaches one of two fixed-point attractors. Otherwise the system is chaotic. Fig. 3.4 and 3.5 show the $x_1 - x_3$ plane and time response x_1 of the continuous model, the proposed model, Mickens' model, and the forward-difference model, for $r = 28$, $T = 0.0075s$, and the initial condition of $\bar{x}_1(0) = 1, \bar{x}_2(0) = 2, \bar{x}_3(0) = 3$, for the first 1,000 seconds.

The forward-difference model does not produce reasonable results, while both the Mickens' and the proposed models retain the chaotic behavior of the continuous-time model. The proposed model is closer, however, to the continuous-time model than the Micken's model. Fig. 3.6 and 3.7 is for the

same system under the same conditions except that $r = 17$ and $T = 0.05s$. Although not shown, Mickens' model becomes divergent for a sampling interval greater than $0.072s$, while the proposed model still retains the general shape of the continuous-time trajectory.

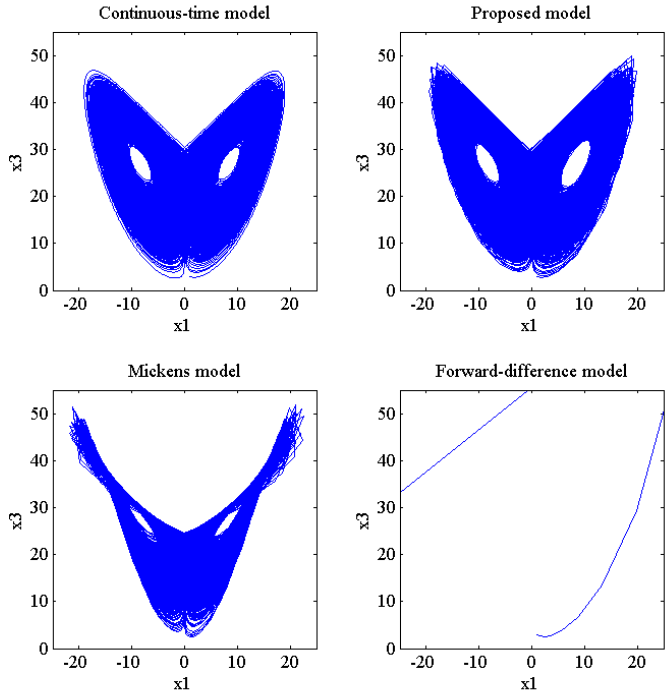

Fig. 3.4: $x_1 - x_3$ plane of four models for $\sigma = 10,\ b = 8/3,\ r = 28,\ T = 0.05\,\mathrm{s}$

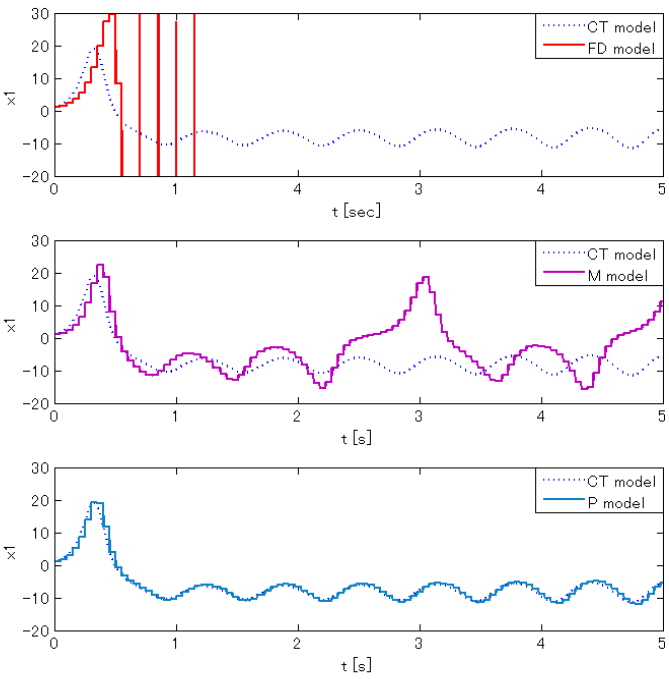

Fig. 3.5: Time responses x_1 of four models for $\sigma = 10,\ b = 8/3,\ r = 28,\ T = 0.05\,\mathrm{s}$

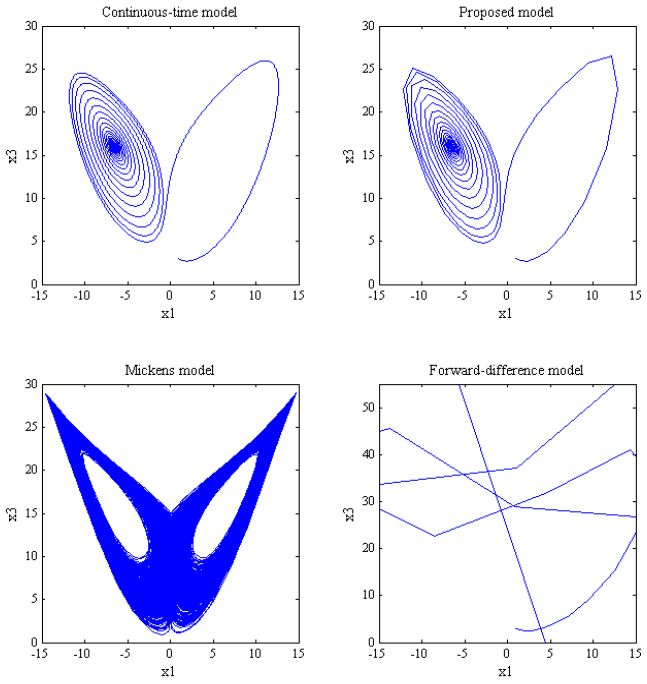

Fig. 3.6: $x_1 - x_3$ plane of four models for $\sigma = 10,\ b = 8/3,\ r = 17,\ T = 0.05\,\mathrm{s}$

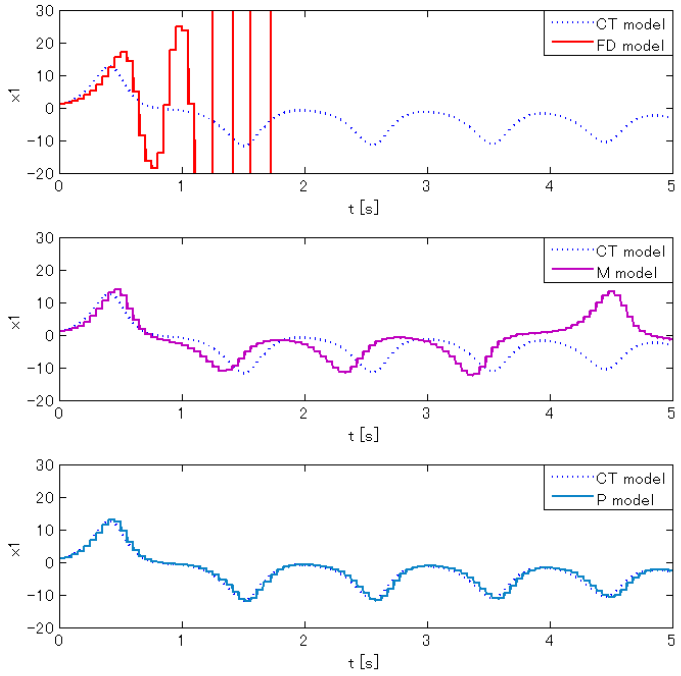

Fig. 3.7: Time responses x_1 of four models for $\sigma = 10,\ b = 8/3,\ r = 17,\ T = 0.05\,\mathrm{s}$

3.6 Stability of Equilibria

3.6.1 Equilibrium points and their stability

The following theories state the properties of proposed discrete-time model on equilibrium points and their stability.

Theorem 3.4: When $D\bar{\mathbf{\Gamma}}(\bar{\mathbf{x}})$ is non-singular, the equilibrium points of the discrete-time model (3.2) with the discrete-time integrator gain given by eq. (3.25) are identical to those of the continuous-time model (3.1).□

Proof: If $\bar{\mathbf{x}}_e$ is an equilibrium point of discrete-time model (3.2), then it follows that

$$\delta\mathbf{x}_e = \frac{e^{\left[D\bar{\mathbf{\Gamma}}(\bar{\mathbf{x}}_e)\right]T} - \mathbf{I}}{T}\left[D\bar{\mathbf{\Gamma}}(\bar{\mathbf{x}}_e)\right]^{-1}\bar{\mathbf{\Gamma}}(\bar{\mathbf{x}}_e) = \mathbf{0}, \tag{3.51}$$

which is equivalent to

$$\left[D\bar{\mathbf{\Gamma}}(\bar{\mathbf{x}}_e)\right]e^{\left[D\bar{\mathbf{\Gamma}}(\bar{\mathbf{x}}_e)\right]T}\left[D\bar{\mathbf{\Gamma}}(\bar{\mathbf{x}}_e)\right]^{-1}\bar{\mathbf{\Gamma}}(\bar{\mathbf{x}}_e) = \bar{\mathbf{\Gamma}}(\bar{\mathbf{x}}_e). \tag{3.52}$$

Noting that

$$\left[D\bar{\mathbf{\Gamma}}(\bar{\mathbf{x}}_e)\right]e^{\left[D\bar{\mathbf{\Gamma}}(\bar{\mathbf{x}}_e)\right]T}\left[D\bar{\mathbf{\Gamma}}(\bar{\mathbf{x}}_e)\right]^{-1} = e^{\left[D\bar{\mathbf{\Gamma}}(\bar{\mathbf{x}}_e)\right]\left[D\bar{\mathbf{\Gamma}}(\bar{\mathbf{x}}_e)\right]^{-1}T} = e^{\left[D\bar{\mathbf{\Gamma}}(\bar{\mathbf{x}}_e)\right]T}, \tag{3.53}$$

eq. (3.51) can be written as

$$\left(e^{\left[D\bar{\mathbf{\Gamma}}(\bar{\mathbf{x}}_e)\right]T} - \mathbf{I}\right)\bar{\mathbf{\Gamma}}(\bar{\mathbf{x}}_e) = \mathbf{0}. \tag{3.54}$$

Using a non-singular matrix $\mathbf{P}$, Jacobian matrix can be transformed into Jordan form such that $D\bar{\mathbf{\Gamma}}(\bar{\mathbf{x}}) = \mathbf{P}\mathbf{\Lambda}\mathbf{P}^{-1}$ and that

$$e^{\left[D\bar{\mathbf{\Gamma}}(\bar{\mathbf{x}}_e)T\right]} - \mathbf{I} = e^{P\Lambda P^{-1}T} - \mathbf{I} = P(e^{\Lambda T} - \mathbf{I})P^{-1}. \tag{3.55}$$

When $D\bar{\mathbf{\Gamma}}(\bar{\mathbf{x}})$ is non-singular, none of its eigenvalues is non-zero and $e^{\Lambda T} - \mathbf{I}$ is non-singular and so is $\left(e^{\left[D\bar{\mathbf{\Gamma}}(\bar{\mathbf{x}}_e)\right]T} - \mathbf{I}\right)$.

Thus, eq. (3.54) is equivalent to

$$\bar{\mathbf{\Gamma}}(\bar{\mathbf{x}}_e) = \mathbf{0}. \tag{3.56}$$

Lemma 3.1 [25]: The asymptotic stability of an equilibrium point of discrete-time system given by

$$\delta\mathbf{x}_k = \frac{1}{T}\left(\int_0^T e^{\mathbf{A}\tau}d\tau\right)\mathbf{A}\mathbf{x}_k \tag{3.57}$$

is equivalent to that of continuous-time system

$$\dot{\bar{\mathbf{x}}} = \mathbf{A}\bar{\mathbf{x}} \,.\square \tag{3.58}$$

Theorem 3.5: When $D\bar{\mathbf{\Gamma}}(\bar{\mathbf{x}})$ is non-singular, an asymptotically stable equilibrium point of continuous-time model (3.1) is also an asymptotically stable equilibrium point of discrete-time model (3.2), where the discrete-time integrator gain is given by (3.25). □

Proof: When $D\bar{\mathbf{\Gamma}}(\bar{\mathbf{x}})$ is non-singular, Theorem 3.4 implies that if $\bar{\mathbf{x}}_e$ is an equilibrium point of continuous-time model (3.1), then it also is an equilibrium of discrete-time model of discrete-time model (3.2). Linearizing system (3.1) around equilibrium point $\bar{\mathbf{x}}_e$ yields the linear system

$$\dot{\bar{\mathbf{x}}} = \left[D\bar{\mathbf{\Gamma}}(\bar{\mathbf{x}}_e) \right] \bar{\mathbf{x}} \,. \tag{3.59}$$

If all the eigenvalues of $D\bar{\mathbf{\Gamma}}(\bar{\mathbf{x}}_e)$ are in the left-half complex plane, then $\bar{\mathbf{x}}_e$ is an asymptotically stable equilibrium point, while if one or more eigenvalues of $D\bar{\mathbf{\Gamma}}(\bar{\mathbf{x}}_e)$ are in the right-half complex plane, then $\bar{\mathbf{x}}_e$ is an unstable equilibrium [26].

The linearization of eq. (3.2) around equilibrium point $\bar{\mathbf{x}}_e$ is given by

$$\begin{aligned} \delta\mathbf{x}_k &= \left[\frac{\partial}{\partial \mathbf{x}_k} \left(\mathbf{G}(\mathbf{x}_k, T) \bar{\mathbf{\Gamma}}(\mathbf{x}_k) \right) \Big|_{\mathbf{x}_k = \bar{\mathbf{x}}_e} \right] \mathbf{x}_k \\ &= \left[\frac{\partial \mathbf{G}(\mathbf{x}_k, T)}{\partial \mathbf{x}_k} \bar{\mathbf{\Gamma}}(\mathbf{x}_k) + \mathbf{G}(\mathbf{x}_k, T) \frac{d\bar{\mathbf{\Gamma}}(\mathbf{x}_k)}{d\mathbf{x}_k} \Big|_{\mathbf{x}_k = \bar{\mathbf{x}}_e} \right] \mathbf{x}_k \end{aligned} \,. \tag{3.60}$$

Noting that $\bar{\mathbf{x}}_e$ and integrator gain is given by (3.25), eq. (3.60) can be written as

$$\delta\mathbf{x}_k = \frac{1}{T} \int_0^T e^{\left[D\bar{\mathbf{\Gamma}}(\bar{\mathbf{x}}_e) \right] \tau} d\tau \left[D\bar{\mathbf{\Gamma}}(\bar{\mathbf{x}}_e) \right] \mathbf{x}_k \,. \tag{3.61}$$

Lemma 3.1 implies that the asymptotic stability of discrete-time system (3.61) is equivalent to that of continuous-time system (3.59), which proves Theorem 3.5.

3.6.2 Simulation results for Lotka-Volterra system

The Lotka-Volterra models [27, 28] are those differential equations that can be written in the form of

$$\frac{d\bar{x}_i}{dt} = \Gamma_i\left(\bar{\mathbf{x}}(t)\right) = \bar{x}_i(t) \left(r_i + \sum_{j=1}^{n} a_{ij} \bar{x}_j(t) \right), \; 1 \le i \le n \tag{3.62}$$

where $\bar{x}_i(t)$ is the state variables, and r_i and a_{ij} are constant parameters. Depending on how these parameters are chosen, this model can represent three distinctive cases; the competitive, the cooperative, and the predator-prey cases. The discretization method to be proposed below can be applied to any of these cases, while some others cannot be. Theorem 3.3 can be applied to any Lotka-Volterra type differential equation, as long as its Jacobian matrix is non-singular. This is presented as lemma below:

Lemma 3.2: For the Lotka-Volterra differential equation expressed as eq. (3.62), the proposed discrete-time model is given by eqs. (3.2) and (3.25), where

$$D\bar{\boldsymbol{\Gamma}}(\bar{\mathbf{x}}) = \begin{bmatrix} r_1 + 2a_{11}x_1 + \sum_{j=2}^{n} a_{1j}\bar{x}_j & a_{11}\bar{x}_1 & \cdots & a_{1n}\bar{x}_n \\ a_{21}\bar{x}_2 & r_2 + 2a_{22}\bar{x}_2 + \sum_{\substack{j=1 \\ j\neq 2}}^{n} a_{2j}\bar{x}_j & \cdots & a_{2n}\bar{x}_2 \\ \vdots & \vdots & \ddots & \vdots \\ a_{n1}\bar{x}_n & a_{n2}\bar{x}_n & \cdots & r_n + 2a_{nn}\bar{x}_n + \sum_{\substack{j=1 \\ j\neq n}}^{n} a_{nj}\bar{x}_j \end{bmatrix}. \square \tag{3.63}$$

Remark 3.4: As a consequence of Theorems 3.4 and 3.5, the proposed discrete-time model preserves the locations of equilibrium points and their asymptotic stability of the original continuous-time system.

For ease of exposition, the following two-species Lotka-Volterra system is considered below:

$$\begin{cases} \dot{\bar{x}}_1 = \bar{x}_1\left(r_1 + a_{11}\bar{x}_1 + a_{12}\bar{x}_2\right) \\ \dot{\bar{x}}_2 = \bar{x}_2\left(r_2 + a_{21}\bar{x}_1 + a_{22}\bar{x}_2\right) \end{cases}. \tag{3.64}$$

The proposed discrete-time model is given by eqs. (3.2) and (3.25) with discrete-time Jacobian matrix given by

$$D\boldsymbol{\Gamma}(\mathbf{x}_k) = \begin{bmatrix} r_1 + 2a_{11}x_{1,k} + a_{12}x_{2,k} & a_{12}x_{1,k} \\ a_{21}x_{2,k} & r_2 + a_{21}x_{1,k} + 2a_{22}x_{2,k} \end{bmatrix}. \tag{3.65}$$

The discrete-time integration gain is given by eq. (3.25). For comparison, the forward-difference model is given by

$$\begin{cases} \delta x_{1,k} = x_{1,k}\left(r_1 + a_{11}x_{1,k} + a_{12}x_{2,k}\right) \\ \delta x_{2,k} = x_{2,k}\left(r_2 + a_{21}x_{1,k} + a_{22}x_{2,k}\right) \end{cases}, \tag{3.66}$$

whose integration gain is unity matrix independently of the sampling interval. Kahan' s model is given by [24]

$$\begin{cases} \delta x_{1,k} = r_1\left(\dfrac{x_{1,k}+x_{1,k+1}}{2}\right) + a_{11}x_{1,k}x_{1,k+1} + a_{12}\left(\dfrac{x_{1,k}x_{2,k+1}+x_{1,k+1}x_{2,k}}{2}\right) \\ \delta x_{2,k} = r_2\left(\dfrac{x_{2,k}+x_{2,k+1}}{2}\right) + a_{21}\left(\dfrac{x_{1,k}x_{2,k+1}+x_{k+1}x_{2,k}}{2}\right) + a_{22}x_{2,k}x_{2,k+1} \end{cases}, \tag{3.67}$$

where $\bar{x}_1$, $\bar{x}_2$, $\bar{x}_1\bar{x}_2$, $\bar{x}_1^{\,2}$, and $\bar{x}_2^{\,2}$ in continuous-time model are replaced, respectively, by $\left(x_{1,k}+x_{1,k+1}\right)/2$, $\left(x_{2,k}+x_{2,k+1}\right)/2$, $\left(x_{1,k}x_{2,k+1}+x_{1,k+1}x_{2,k}\right)/2$, $x_{1,k}x_{1,k+1}$, and $x_{2,k}x_{2,k+1}$. The right-hand-side of the above equation contains variable at $k+1$ time-step and needs to be converted in the standard delta form. The integration gain is as given by

$$\mathbf{G}\left(\mathbf{x}_k,T\right) = \left(\mathbf{I} - \frac{T}{2}\left[D\bar{\mathbf{\Gamma}}\left(\mathbf{x}_k\right)\right]\right)^{-1}, \tag{3.68}$$

where the same Jacobian matrix, eq. (3.65), of the proposed model is used.

Mickens' model takes a different form depending on whether the system is of the predator-prey [24], the competitive, and the cooperative type [29]. For example, Mickens' model for the competitive-species case, which will be used for simulations below, is given by

$$\begin{cases} \dfrac{x_{1,k+1}-x_{1,k}}{\varphi_1} = r_1x_{1,k} + a_{11}x_{1,k}x_{1,k+1} + a_{12}x_{1,k+1}x_{2,k} \\ \dfrac{x_{2,k+1}-x_{2,k}}{\varphi_2} = r_2x_{2,k} + a_{21}x_{1,k}x_{2,k+1} + a_{12}x_{2,k}x_{2,k+1} \end{cases} \tag{3.69}$$

where $\varphi_1 = \left(e^{r_1T}-1\right)/r_1$, $\varphi_2 = \left(e^{r_2T}-1\right)/r_2$. This yields the discrete-time integration gain given by

$$\mathbf{G}\left(\mathbf{x}_k,T\right) = \begin{bmatrix} \dfrac{\varphi_1}{1-\varphi_1\left(a_{11}x_{1,k}+a_{12}x_{2,k}\right)} & 0 \\ 0 & \dfrac{\varphi_2}{1-\varphi_2\left(a_{21}x_{1,k}+a_{22}x_{2,k}\right)} \end{bmatrix}. \tag{3.70}$$

Simulations have been carried also for the two-species Lotka-Volterra system (3.64) to compare the original continuous-time model, which is computed using Runge-Kutta method in Matlab/Simulink environment, with discrete-time models obtained by the forward-difference, Mickens', Kahan's, and the proposed discretization methods. Parameters used for simulations are $r_1=5$, $r_2=6$, $a_{11}=-1$, $a_{12}=-2$, $a_{21}=-3$, and $a_{22}=-4$, which make the system to be of the competitive type and yields four equilibrium points at $(0,0)$, $(5,0)$, $(0,1.5)$, and $(-4,4.5)$. The initial condition used is $\bar{x}_1(0)=0.2$ and $\bar{x}_2(0)=0.4$. This type of model often leads to extinction of one species, such as Neanderthal man vs early modern man.

Fig. 3.8 shows the time-responses of the popular forward-difference discrete-time model for $T = 0.1,\ 0.25$, and 0.5 seconds and the response of the continuous-time system. It can be seen that at the sampling period of 0.1s, which gives reasonable 20 samples per settling time, the response converges to the correct equilibrium point of $(5,0)$, although the difference with the continuous-time response is visible on the plot. As the sampling period increases, the response becomes slower during the transient and at $T = 0.2\text{s}$ it starts to oscillate around the equilibrium point. The response becomes chaotic at about $T = 0.28\text{s}$ and divergent for T larger than about 0.29 s.

Fig. 3.9 is for Mickens' model under the same conditions as in Fig. 3.8. With this method, the transient response becomes slower as the sampling period increases, but without becoming oscillatory, and remains convergent to the correct equilibrium point at least up to $T = 50\text{s}$.

Fig. 3.10 is the result obtained with Kahan's discrete-time model. Although not clear from the figures, Kahan's method gives results that are closer to the continuous-time result than Mickens' method. However, it was found that Kahan's model can change its domain of attraction suddenly as the discrete-time period is changed. In the present example, the response reaches the equilibrium point of $(5,0)$ using $T = 0.486\text{s}$ but it suddenly changes its reaching point to another equilibrium of $(-4,4.5)$ using $T = 0.487\text{s}$. Such a change in fundamental property can be detrimental in numerical investigations. The response starts to diverge at about $T = 3.0\text{s}$.

Fig. 3.11 shows the response with the proposed discrete-time model. Among the four discrete-time models compared in this section, the proposed method and Kahan's model give the response that matches the continuous-time response almost exactly at discrete-time instants for $T = 0.1$ and 0.25 seconds. While the proposed model calls for heavier computational efforts, there is no sudden change in the steady-state value as in Kahan's method. The response becomes, however, divergent at about $T = 2.0s$.

The four discrete-time models used for simulations can be compared in terms of the discrete-time integration gains, since the system function to which the gain is multiplied is the same sampled version of the continuous-time system, as seen in eq. (3.2). The proposed discrete-time model requires computation of the exponential of Jacobian matrix at each time instant, while the forward-difference, Kahan, and Mickens models are only quadratic in their computations. Table 3.1 shows the actual computation time elapsed in a Simulink simulation run for 100 seconds, as measured by Matlab's cputime command. Comparing relative values, it may be concluded that, while the proposed model uses the longest CPU time, the differences are not highly significant.

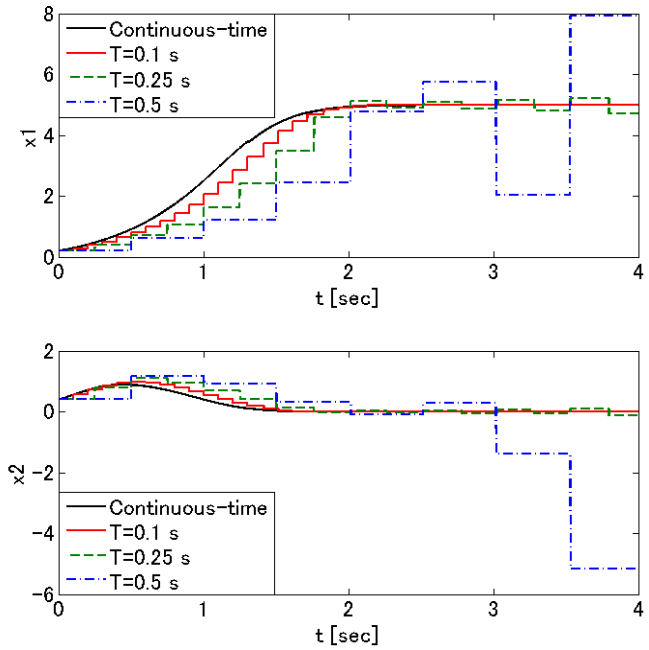

Fig. 3.8: Time-responses of the forward-difference discrete-time model for the initial condition of $\bar{x}_1(0) = 0.2$ and $\bar{x}_2(0) = 0.4$ with different values of T

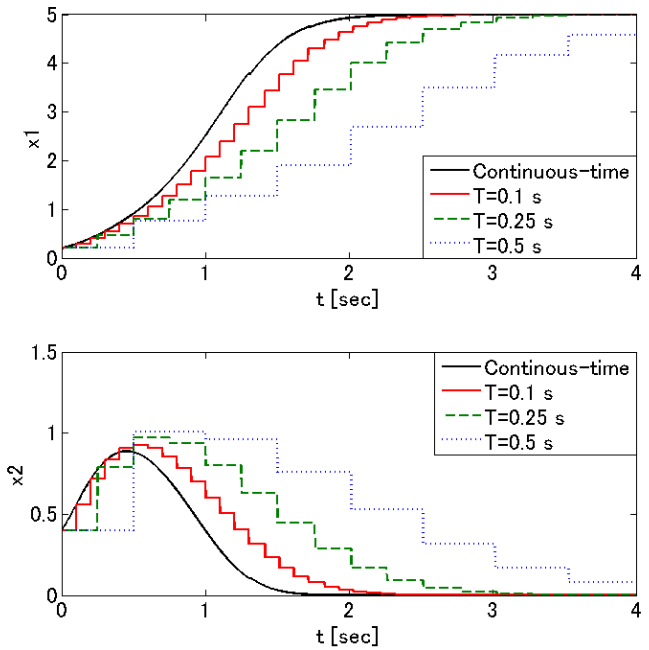

Fig. 3.9: Time-responses of Mickens' discrete-time model for the initial condition of $\bar{x}_1(0) = 0.2$ and $\bar{x}_2(0) = 0.4$ with different values of T

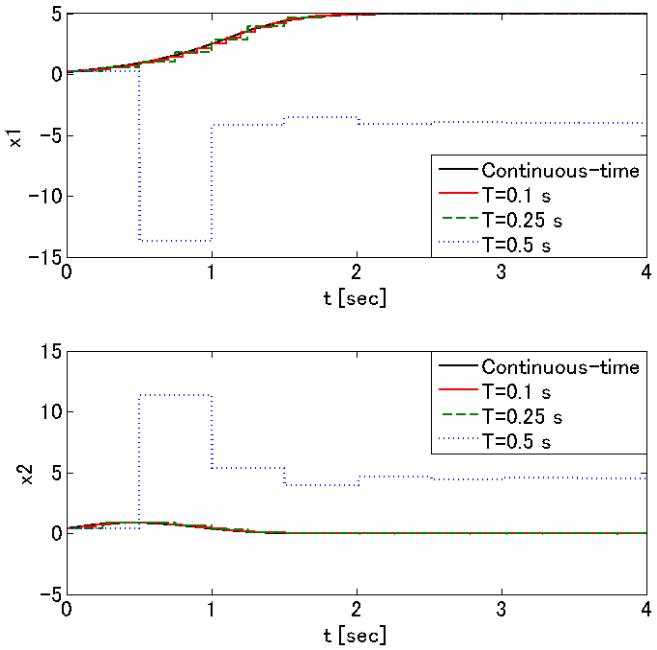

Fig. 3.10: Time-responses of Kahan's discrete-time model for the initial condition of $\bar{x}_1(0) = 0.2$ and $\bar{x}_2(0) = 0.4$ with different values of T

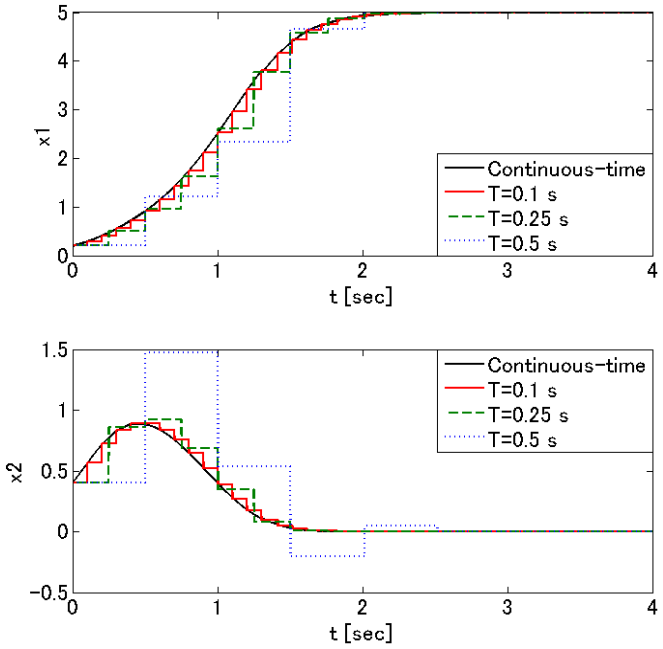

Fig. 3.11: Time-responses of the proposed discrete-time model for the initial condition of $\bar{x}_1(0) = 0.2$ and $\bar{x}_2(0) = 0.4$ with different values of T

Table 3.1: CPU-times elapsed during the first 100 seconds of simulation

	$T = 0.1s$	$T = 0.25s$	$T = 0.5s$	$T = 1s$
Proposed	0.9828	0.9048	0.8268	0.8112
Kahan	0.9048	0.8268	0.8112	0.78
Micken	0.8892	0.8112	0.8268	0.7956
Forward. diff	0.8736	0.8268	Divergent	Divergent

3.7 Summary

Discrete-time models for autonomous nonlinear systems have been looked at from the view-point of discrete-time integration gains, which led to new models. The form of models is fixed to be the product of this gain and the system function that has the same structure as that of the continuous-time original. Sufficient conditions for this gain to make the discrete-time model exact are presented. The model is exact when the gain is exact, while it is approximate when the gain is approximate. The main contribution of the present paper is the development of a systematic procedure to obtain discrete-time models based on approximated gains, even when the exact gain is unknown. As long as a Jacobian matrix exists for the nonlinear state equation, the gain can be found approximately and the proposed model derived. When Jacobian matrix is non-singular, it can be shown that the asymptotic stability and instability of equilibrium points that correspond to the original system are preserved in the proposed discrete-time model. Simulations show that the proposed models give performances that are superior to on-line computable methods such as the forward-difference, Mickens, and Kahan models as applied to Lotka-Volterra system, van der Pol and Lorentz nonlinear oscillators.

Although the proposed model is developed based on the Taylor expansion of the nonlinear function, it is used to determine the integration gain and the form of the model is nonlinear. This is different from the linearization of a system itself based on the Taylor expansion. The proposed model corresponds to one with the first two terms in the series expansion in a differential equation concerning this gain, and can always be found as long as the expansion exists, whereas the well-known forward difference model corresponds to one with the first term only.

Chapter 4

Discrete-time model of forced nonlinear oscillators

In this chapter, a discrete-time model is proposed for forced nonlinear oscillators, which is a class of non-autonomous nonlinear system. By implementing the continualization technique to a given discrete-time system, sufficient conditions are derived so that the obtained model is exact for any sampling periods. In fact, this condition can be solved exactly for linear and certain nonlinear systems, and thus, their exact discrete-time model can be found. Furthermore, new models can be developed by approximately solving this condition. One such model, which can always be found as long as a Jacobian matrix of the nonlinear system exists, is presented. As an example, a van der Pol oscillator driven by a forcing sinusoidal function is discretized and simulated under various conditions. They show that the proposed model tends to retain such key features as limit cycles and space-filling oscillations even for large sampling periods, and out-performs the forward difference model, which is a well-known, widely-used, and on-line computable model.

4.1 Proposed discrete-time model of forced nonlinear oscillator

Let a continuous-time model of a forced nonlinear oscillator be given by the following state space equation:

$$\frac{d\,\bar{\mathbf{x}}(t)}{dt} = \bar{\mathbf{\Gamma}}\left(\bar{\mathbf{x}}(t), t\right) = \bar{\mathbf{f}}\left(\bar{\mathbf{x}}(t)\right) + \bar{\mathbf{g}}(t), \quad \bar{\mathbf{x}}(t_0) = \bar{\mathbf{x}}_0, \tag{4.1}$$

where $\bar{\mathbf{x}} \in R^n$ is a state vector of continuous time variable t, $\bar{\mathbf{f}} : R^n \to R^n$ is a function of the state vector, and $\bar{\mathbf{g}} \in R^n$ is a known forcing function. Function $\bar{\mathbf{f}}$ is assumed to be expandable into Taylor series, so that $\bar{\mathbf{\Gamma}}$ satisfies the Lipschitz condition and eq. (4.1) has a unique solution for a given initial condition.

The discrete-time model is expressed in delta form with a uniform discrete-time period of T, as

$$\delta \mathbf{x}_k = \frac{\mathbf{x}_{k+1} - \mathbf{x}_k}{T} = \mathbf{\Gamma}\left(\mathbf{x}_k, T\right), \quad \mathbf{x}_{k_0} = \bar{\mathbf{x}}_0 \tag{4.2}$$

The following theorem states that any discrete-time system (4.2) can be an exact model of a continuous-time system (4.1) if the discrete-time function $\mathbf{\Gamma}$ is chosen in a certain manner.

Theorem 4.1 [Exact Discretization]: A discrete-time system given by eq. (4.2) is an exact discrete-time model of system (4.1) if function $\mathbf{\Gamma}\left(\mathbf{x}_k, T\right)$ satisfies the following three conditions:

(i) $\dfrac{\partial \boldsymbol{\Gamma}(\mathbf{x}_k, s)}{\partial \mathbf{x}_k}$, $\dfrac{\partial}{\partial \mathbf{x}_k}\left(\dfrac{\partial(\boldsymbol{\Gamma}(\mathbf{x}_k, s))}{\partial s}\right)$ are continuous functions of $\mathbf{x}_k$, where $s \in R^+$

(ii) $s\dfrac{\partial \boldsymbol{\Gamma}(\mathbf{x}_k, s)}{\partial \mathbf{x}_k} \neq -1.$

(iii) $$\frac{d}{dt}\left((t-kT)\boldsymbol{\Gamma}\left(\bar{\mathbf{x}}^*(kT), t-kT\right)\right) = \bar{\mathbf{f}}\left(\bar{\mathbf{x}}^*(kT) + (t-kT)\boldsymbol{\Gamma}\left(\bar{\mathbf{x}}^*(kT), t-kT\right)\right) + \bar{\mathbf{g}}(t) \tag{4.3}$$

for each interval $kT \le t < (k+1)T$, where $\bar{\mathbf{x}}^*(t)$ is the continualization of discrete-time state $\mathbf{x}_k$ as Definition 2.3.□

The proof of the above theorem will be shown using the following lemma:

Lemma 4.1: When the conditions (i) and (ii) are met, the continualization state $\bar{\mathbf{x}}^*(t)$ that satisfies eq. (2.7) is a unique solution of eq. (2.8) in each interval $kT \le t < (k+1)T$. □

Proof: A sufficient condition for eq. (2.8) to have a unique solution in each interval is that $\bar{\boldsymbol{\Gamma}}^*\left(\bar{\mathbf{x}}^*(t), t\right)$ is a continuous function of $\bar{\mathbf{x}}^*$. Since

$$\begin{aligned}\frac{\partial \bar{\boldsymbol{\Gamma}}^*\left(\bar{\mathbf{x}}^*(t), t\right)}{\partial \bar{\mathbf{x}}^*(t)} &= \frac{\dfrac{\partial}{\partial \bar{\mathbf{x}}^*(kT)}\dfrac{\partial}{\partial t}\left((t-kT)\boldsymbol{\Gamma}\left(\bar{\mathbf{x}}^*(kT), t-kT\right)\right)}{\dfrac{\partial\left[\bar{\mathbf{x}}^*(kT) + (t-kT)\boldsymbol{\Gamma}\left(\bar{\mathbf{x}}^*(kT), t-kT\right)\right]}{\partial \bar{\mathbf{x}}^*(kT)}} \\ &= \frac{\dfrac{\partial \boldsymbol{\Gamma}\left(\bar{\mathbf{x}}^*(kT), t-kT\right)}{\partial \bar{\mathbf{x}}^*(kT)} + (t-kT)\dfrac{\partial}{\partial \bar{\mathbf{x}}^*(kT)}\dfrac{\partial \boldsymbol{\Gamma}\left(\bar{\mathbf{x}}^*(kT), t-kT\right)}{\partial t}}{1 + (t-kT)\dfrac{\partial \boldsymbol{\Gamma}\left(\bar{\mathbf{x}}^*(kT), t-kT\right)}{\partial \bar{\mathbf{x}}^*(kT)}},\end{aligned} \tag{4.4}$$

$\bar{\boldsymbol{\Gamma}}^*\left(\bar{\mathbf{x}}^*(t), t\right)$ is a continuous function of $\bar{\mathbf{x}}^*$ if conditions (i) and (ii) are met. □

Proof of Theorem 4.1: From Remark 2.1 and Lemma 4.1, discrete-time system (4.2) is an exact discretization of continualized system (2.8). Condition (iii) implies that, for each $kT \le t < (k+1)T$, the state $\bar{\mathbf{x}}^*(t)$ of the continualized system (2.8) is a unique solution of the original continuous-time system (4.1). Thus, discrete-time system (4.2) is an exact discretization of original continuous-time system (4.1).□

Remark 4.1: Condition (iii) is a requirement that function $\boldsymbol{\Gamma}\left(\bar{\mathbf{x}}^*(kT), t-kT\right)$ be such that eq. (2.8) equals eq. (4.1); that is, using eq. (2.7), in each interval,

$$\frac{d}{dt}\Big((t-kT)\boldsymbol{\Gamma}\left(\bar{\mathbf{x}}^*(kT),t-kT\right)\Big)=\dot{\bar{\mathbf{x}}}^*(t)$$
$$=\bar{\mathbf{f}}\left(\bar{\mathbf{x}}^*(t)\right)+\bar{\mathbf{g}}(t) \tag{4.5}$$
$$=\bar{\mathbf{f}}\left(\bar{\mathbf{x}}^*(kT)+(t-kT)\boldsymbol{\Gamma}\left(\bar{\mathbf{x}}^*(kT),t-kT\right)\right)+\bar{\mathbf{g}}(t).$$

When eq. (4.3) can be solved for $\boldsymbol{\Gamma}$, the exact discrete-time model is found. However, eq. (4.3) is a nonlinear differential equation, which is generally unsolvable analytically. By solving it approximately, an approximate discrete-time model may be obtained. One such model is proposed below, which is applicable to a class of non-autonomous nonlinear and linear systems, as long as they have a Jacobian matrix.

Theorem 4.2 [The Proposed Model]: A discrete-time system given by eq. (4.2) where function $\boldsymbol{\Gamma}$ is chosen as

$$\boldsymbol{\Gamma}\left(\mathbf{x}_k,T\right)=\frac{1}{T}\left(\int_0^T e^{\left[D\bar{\mathbf{f}}(\mathbf{x}_k)\right](T-\lambda)}d\lambda\right)\bar{\mathbf{f}}\left(\mathbf{x}_k\right)+\frac{1}{T}\int_0^T e^{\left[D\bar{\mathbf{f}}(\mathbf{x}_k)\right](T-\lambda)}\bar{\mathbf{g}}\left(\lambda+kT\right)d\lambda \tag{4.6}$$

with $D\bar{\mathbf{f}}\left(\mathbf{x}_k\right)$ being a Jacobian matrix of $\bar{\mathbf{f}}$ at $\mathbf{x}_k$, is a discrete-time model, in the sense of Definition 2.2, of the continuous-time system given by eq. (4.1).□

Proof: Eq. (2.7) with $\boldsymbol{\Gamma}$ given by (4.6) holds for a fixed time $t=\tau$ in each sampling interval such that

$$\frac{\bar{\mathbf{x}}^*(\tau)-\bar{\mathbf{x}}^*(kT)}{\tau-kT}=\frac{1}{\tau-kT}\left(\int_0^{\tau-kT} e^{\left[D\bar{\mathbf{f}}\left(\bar{\mathbf{x}}^*(kT)\right)\right](\tau-kT-\lambda)}d\lambda\right)\bar{\mathbf{f}}\left(\bar{\mathbf{x}}^*(kT)\right)$$
$$+\frac{1}{\tau-kT}\int_0^{\tau-kT} e^{\left[D\bar{\mathbf{f}}\left(\bar{\mathbf{x}}^*(kT)\right)\right](\tau-kT-\lambda)}\bar{\mathbf{g}}\left(\lambda+kT\right)d\lambda \tag{4.7}$$

and this also holds at the limit of T approaching zero while k is chosen such that $kT\le\tau<(k+1)T$. Thus, noting that, for a fixed τ,

$$\lim_{\substack{T\to 0\\ kT\le\tau<(k+1)T}} kT=\tau, \tag{4.8}$$

and $\bar{\mathbf{f}}\left(\bar{\mathbf{x}}^*(\tau)\right)$ and $\bar{\mathbf{g}}(\tau)$ are finite, the use of l'Hospital's Rule on the right-hand-side of eq. (4.7) yields

$$\lim_{\substack{T\to 0\\ kT\le\tau<(k+1)T}}\left[\frac{1}{\tau-kT}\left(\int_0^{\tau-kT} e^{\left[D\bar{\mathbf{f}}\left(\bar{\mathbf{x}}^*(kT)\right)\right](\tau-kT-\lambda)}d\lambda\right)\bar{\mathbf{f}}\left(\bar{\mathbf{x}}^*(kT)\right)\right]$$
$$+\lim_{\substack{T\to 0\\ kT\le\tau<(k+1)T}}\left[+\frac{1}{\tau-kT}\int_0^{\tau-kT} e^{\left[D\bar{\mathbf{f}}\left(\bar{\mathbf{x}}^*(kT)\right)\right](\tau-kT-\lambda)}\bar{\mathbf{g}}\left(\lambda+kT\right)d\lambda\right]. \tag{4.9}$$
$$=\bar{\mathbf{f}}\left(\bar{\mathbf{x}}^*(\tau)\right)+\bar{\mathbf{g}}(\tau)$$

The left-hand-side, on the other hand, gives

$$\lim_{\substack{T\to 0\\ kT\le\tau<(k+1)T}} \frac{\bar{\mathbf{x}}^*(\tau)-\bar{\mathbf{x}}^*(kT)}{\tau-kT}=\frac{d\bar{\mathbf{x}}^*(\tau)}{d\tau}. \tag{4.10}$$

Therefore, at the limit of T approaching zero and for all τ such that $kT\le\tau<(k+1)T$, eq. (4.7) gives

$$\frac{d\bar{\mathbf{x}}^*(\tau)}{d\tau}=\bar{\mathbf{f}}\left(\bar{\mathbf{x}}^*(\tau)\right)+\bar{\mathbf{g}}(\tau). \tag{4.11}$$

Since eq. (4.1) has a unique solution given an initial condition, it follows that

$$\lim_{\substack{T\to 0\\ kT\le\tau<(k+1)T}} \bar{\mathbf{x}}^*(\tau)=\bar{\mathbf{x}}(\tau). \tag{4.12}$$

Therefore, $\mathbf{x}_k=\bar{\mathbf{x}}^*(kT)$, eq. (4.8), and eq. (4.12) lead, for any τ with $kT\le\tau<(k+1)T$, to

$$\lim_{\substack{T\to 0\\ kT\le\tau<(k+1)T}} \mathbf{x}_k=\lim_{\substack{T\to 0\\ kT\le\tau<(k+1)T}} \bar{\mathbf{x}}^*(kT)=\lim_{\substack{T\to 0\\ kT\le\tau<(k+1)T}} \bar{\mathbf{x}}^*(\tau)=\bar{\mathbf{x}}(\tau). \tag{4.13}$$

In view of Definition 2.2, system (4.2) is a discrete-time model of continuous-time system (4.1). □

Since the proposed model has been shown above to be a valid model in the sense of Definition 2.2, a more constructive procedure is shown below. When function $\bar{\mathbf{f}}$ in eq. (4.3) is expanded into the Taylor series and truncated with the first two terms as

$$\begin{aligned}&\bar{\mathbf{f}}\left(\bar{\mathbf{x}}^*(kT)+(t-kT)\boldsymbol{\Gamma}\left(\bar{\mathbf{x}}^*(kT),t-kT\right)\right)\\ &\quad=\bar{\mathbf{f}}\left(\bar{\mathbf{x}}^*(kT)\right)+\left[D\bar{\mathbf{f}}\left(\bar{\mathbf{x}}^*(kT)\right)\right](t-kT)\boldsymbol{\Gamma}\left(\bar{\mathbf{x}}^*(kT),t-kT\right),\end{aligned} \tag{4.14}$$

eq. (4.3) can always be solved and an approximate discrete-time model obtained. That is, for arbitrary $\bar{\mathbf{x}}^*(kT)$, eq. (4.3) be expressed as

$$\begin{aligned}\frac{d}{dt}\left((t-kT)\boldsymbol{\Gamma}\left(\bar{\mathbf{x}}^*(kT),t-kT\right)\right)&=\left[D\bar{\mathbf{f}}\left(\bar{\mathbf{x}}^*(kT)\right)\right](t-kT)\boldsymbol{\Gamma}\left(\bar{\mathbf{x}}^*(kT),t-kT\right)\\ &\quad+\bar{\mathbf{f}}\left(\bar{\mathbf{x}}^*(kT)\right)+\bar{\mathbf{g}}(t)\end{aligned} \tag{4.15}$$

Defining ζ as $\zeta=t-kT$, eq. (4.15) can be written as

$$\frac{d}{d\zeta}\left(\zeta\boldsymbol{\Gamma}\left(\bar{\mathbf{x}}^*(kT),\zeta\right)\right)=\left[D\bar{\mathbf{f}}\left(\bar{\mathbf{x}}^*(kT)\right)\right]\zeta\boldsymbol{\Gamma}\left(\bar{\mathbf{x}}^*(kT),\zeta\right)+\bar{\mathbf{f}}\left(\bar{\mathbf{x}}^*(kT)\right)+\bar{\mathbf{g}}(\zeta+kT) \tag{4.16}$$

where $0\le\zeta<T$. Noting that $\zeta\boldsymbol{\Gamma}\left(\bar{\mathbf{x}}^*(kT),\zeta\right)=0$ at $\zeta=0$, a solution to the above linear differential equation in $\zeta\boldsymbol{\Gamma}\left(\bar{\mathbf{x}}^*(kT),\zeta\right)$ gives the following continuous-time function [30]:

$$\begin{aligned}\zeta\boldsymbol{\Gamma}\left(\bar{\mathbf{x}}^*(kT),\zeta\right)&=\int_0^{\zeta} e^{\left[D\bar{\mathbf{f}}\left(\bar{\mathbf{x}}^*(kT)\right)\right](\zeta-\lambda)}\left(\bar{\mathbf{f}}\left(\bar{\mathbf{x}}^*(kT)\right)+\bar{\mathbf{g}}(kT+\lambda)\right)d\lambda\\ &=\int_0^{\zeta} e^{\left[D\bar{\mathbf{f}}\left(\bar{\mathbf{x}}^*(kT)\right)\right](\zeta-\lambda)}d\lambda\,\bar{\mathbf{f}}\left(\bar{\mathbf{x}}^*(kT)\right)+\int_0^{\zeta} e^{\left[D\bar{\mathbf{f}}\left(\bar{\mathbf{x}}^*(kT)\right)\right](\zeta-\lambda)}\bar{\mathbf{g}}(kT+\lambda)d\lambda\end{aligned}. \tag{4.17}$$

Adopting this form of function, the discrete-time function is obtained as

$$\boldsymbol{\Gamma}(\mathbf{x}_k,T)=\frac{1}{T}\int_o^T e^{\left[D\mathbf{f}(\mathbf{x}_k)\right](T-\lambda)}d\lambda\cdot\mathbf{f}(x_k)+\frac{1}{T}\int_o^T e^{\left[D\mathbf{f}(\mathbf{x}_k)\right](T-\lambda)}\bar{\mathbf{g}}(kT+\lambda)d\lambda\,, \tag{4.18}$$

which is eq. (3.25).

Remark 4.2: When eq. (4.3) can be solved exactly, an exact discrete-time model can be found. For instance for a linear system, the proposed method gives the exact discrete-time model; i.e., for $\bar{\boldsymbol{\Gamma}}$ in eq. (4.1) given by

$$\bar{\boldsymbol{\Gamma}}(\bar{\mathbf{x}}(t),t)=\mathbf{A}\bar{\mathbf{x}}+\bar{\mathbf{g}}(t)\,, \tag{4.19}$$

where $\mathbf{A}$ is system matrix of compatible dimension, eq. (4.3) can be written exactly as a linear differential equation as

$$\frac{d}{dt}\Big((t-kT)\boldsymbol{\Gamma}\left(\bar{\mathbf{x}}^*(kT),t-kT\right)\Big)-\mathbf{A}(t-kT)\boldsymbol{\Gamma}\left(\bar{\mathbf{x}}^*(kT),t-kT\right)-\mathbf{A}\bar{\mathbf{x}}^*(kT)-\bar{\mathbf{g}}(t)=0\,, \tag{4.20}$$

whose solution is [31]

$$(t-kT)\boldsymbol{\Gamma}\left(\bar{\mathbf{x}}^*(kT),t-kT\right)=\int_0^{t-kT}e^{\mathbf{A}(t-kT-\tau)}d\tau\cdot\mathbf{A}\bar{\mathbf{x}}^*(kT)+\int_0^{t-kT}e^{\mathbf{A}(t-kT-\tau)}\bar{\mathbf{g}}(kT+\tau)d\tau$$

This leads to the exact discrete-time model [31] as

$$\boldsymbol{\Gamma}(\mathbf{x}_k,T)=\frac{1}{T}\int_0^T e^{\mathbf{A}(T-\tau)}d\tau\cdot\mathbf{A}\mathbf{x}_k+\frac{1}{T}\int_0^T e^{\mathbf{A}(T-\tau)}\bar{\mathbf{g}}(\tau+kT)d\tau\,. \tag{4.21}$$

Remark 4.3: When the Taylor series expansion of $\bar{\mathbf{f}}\left(\bar{\mathbf{x}}^*(kT)+(t-kT)\boldsymbol{\Gamma}\left(\bar{\mathbf{x}}^*(kT),t-kT\right)\right)$ is truncated after the first term and $\mathbf{g}(t)$ is constant in the interval $\left[kT,(k+1)T\right)$, eq. (4.3) yields $d\left((t-kT)\boldsymbol{\Gamma}\left(\bar{\mathbf{x}}^*(kT),t-kT\right)\right)\big/dt=\bar{\mathbf{f}}\left(\bar{\mathbf{x}}^*(kT)\right)+\bar{\mathbf{g}}(kT)$, so that

$$\boldsymbol{\Gamma}\left(\bar{\mathbf{x}}^*(kT),t-kT\right)=\bar{\mathbf{f}}\left(\bar{\mathbf{x}}^*(kT)\right)+\bar{\mathbf{g}}(kT)\,. \tag{4.22}$$

This is known as the forward difference model.

Remark 4.4: When $\bar{\mathbf{g}}(t)$ is a stair-case function given by

$$\bar{\mathbf{g}}(t)=\alpha_k,\quad kT\le t<(k+1)T\,, \tag{4.23}$$

integration of eq. (4.18) gives

$$\boldsymbol{\Gamma}(\mathbf{x}_k,T)=\frac{1}{T}\int_0^T e^{\left[D\mathbf{f}(\mathbf{x}_k)\right](T-\tau)}d\tau\left\{\mathbf{f}(\mathbf{x}_k)+\alpha_k\right\}. \tag{4.24}$$

Furthermore, when Jacobian matrix $D\mathbf{f}(\mathbf{x}_k)$ is non-singular, (4.24) can be written as

$$\boldsymbol{\Gamma}(\mathbf{x}_k,T)=\frac{e^{\left[D\mathbf{f}(\mathbf{x}_k)\right]T}-\mathbf{I}}{T}\left[D\mathbf{f}(\mathbf{x}_k)\right]^{-1}\left\{\mathbf{f}(\mathbf{x}_k)+\alpha_k\right\}. \tag{4.25}$$

Remark 4.5: When the Jacobian matrix is non-singular and a specific form is given for $\bar{\mathbf{g}}(t)$, the model (4.18) can be written in a more specific form. For instance, for a sinusoidal function given by

$$\bar{\mathbf{g}}(t) = \mathbf{A}\cos(\omega t), \tag{4.26}$$

the second term in eq. (4.18) can be integrated by parts. Noting $d^2\bar{\mathbf{g}}(t)/dt^2 = -\omega^2\bar{\mathbf{g}}(t)$, it yields

$$\begin{aligned}\boldsymbol{\Gamma}(\mathbf{x}_k, T) = &\frac{e^{\left[D\mathbf{f}(\mathbf{x}_k)\right]T} - \mathbf{I}}{T}\left[D\mathbf{f}(\mathbf{x}_k)\right]^{-1}\mathbf{f}(x_k) \\ &-\left(\omega^2\mathbf{I} + \left[D\mathbf{f}(\mathbf{x}_k)\right]^2\right)^{-1}\left\{D\mathbf{f}(\mathbf{x}_k)\left(\bar{\mathbf{g}}_{k+1} - e^{\left[D\mathbf{f}(\mathbf{x}_k)\right]T}\bar{\mathbf{g}}_k\right) + \left(\dot{\bar{\mathbf{g}}}_{k+1} - e^{\left[D\mathbf{f}(\mathbf{x}_k)\right]T}\dot{\bar{\mathbf{g}}}_k\right)\right\}\end{aligned}, \tag{4.27}$$

where $\bar{\mathbf{g}}_k$ and $\dot{\bar{\mathbf{g}}}_k$ are defined as

$$\bar{\mathbf{g}}_k = \bar{\mathbf{g}}(kT) = \mathbf{A}\cos(\omega kT), \quad \dot{\bar{\mathbf{g}}}_k = \dot{\bar{\mathbf{g}}}(kT) = -\mathbf{A}\omega\sin(\omega kT). \tag{4.28}$$

4.2 Discrete-time models of a forced van der Pol oscillator

Consider the forced van der Pol oscillator modeled by [22]

$$\ddot{\bar{x}} + \bar{x} - \varepsilon\left(1 - \bar{x}^2\right)\dot{\bar{x}} - A\cos(\omega t) = 0, \tag{4.29}$$

where ε is a positive parameter, A the amplitude of the forcing function, and ω its angular velocity. This can be rewritten in the form of state-space equation given by

$$\frac{d\,\bar{\mathbf{x}}(t)}{dt} = \bar{\mathbf{f}}\left(\bar{\mathbf{x}}(t)\right) + \bar{\mathbf{g}}(t) \tag{4.30}$$

where

$$\bar{\mathbf{x}} = \begin{bmatrix}\bar{x} \\ \bar{y}\end{bmatrix} \tag{4.31}$$

$$\bar{\mathbf{f}}\left(\bar{\mathbf{x}}(t)\right) = \begin{bmatrix}\bar{y} \\ -\bar{x} + \varepsilon\left(1 - \bar{x}^2\right)\bar{y}\end{bmatrix} \tag{4.32}$$

$$\bar{\mathbf{g}}(t) = \begin{bmatrix}0 \\ A\cos(\omega t)\end{bmatrix}. \tag{4.33}$$

This system reduces to the relaxation oscillator when $A = 0$, which yields a stable limit cycle. When the system is excited with $A \neq 0$, it exhibits various types of behaviors such as chaos and stable orbit with more than one closed cycle [32]. Jacobian matrix of $\bar{\mathbf{f}}$ for this system is non-singular and given by

$$D\bar{\mathbf{f}}(\bar{\mathbf{x}}) = \begin{bmatrix}0 & 1 \\ -1 - 2\varepsilon\bar{x}\bar{y} & \varepsilon\left(1 - \bar{x}^2\right)\end{bmatrix}. \tag{4.34}$$

The Proposed Model: Using the discrete-time function given by (4.27), the proposed discrete-time model is obtained as

$$\delta\mathbf{x}_k = \frac{e^{\left[D\bar{\mathbf{f}}(\mathbf{x}_k)\right]T} - \mathbf{I}}{T}\left[D\bar{\mathbf{f}}(\mathbf{x}_k)\right]^{-1}\bar{\mathbf{f}}(\mathbf{x}_k) - \left(\omega^2\mathbf{I} + \left[D\bar{\mathbf{f}}(\mathbf{x}_k)\right]^2\right)^{-1}\left\{D\bar{\mathbf{f}}(\mathbf{x}_k)\left(\bar{\mathbf{g}}_{k+1} - e^{\left[D\bar{\mathbf{f}}(\mathbf{x}_k)\right]T}\bar{\mathbf{g}}_k\right) + \left(\dot{\bar{\mathbf{g}}}_{k+1} - e^{\left[D\bar{\mathbf{f}}(\mathbf{x}_k)\right]T}\dot{\bar{\mathbf{g}}}_k\right)\right\} \tag{4.35}$$

where

$$\bar{\mathbf{g}}_k = \bar{\mathbf{g}}(t)\big|_{t=kT} = \begin{bmatrix} 0 \\ A\cos(\omega kT) \end{bmatrix}, \tag{4.36}$$

and

$$\dot{\bar{\mathbf{g}}}_k = \dot{\bar{\mathbf{g}}}(t)\big|_{t=kT} = \begin{bmatrix} 0 \\ -A\omega\sin(\omega kT) \end{bmatrix}. \tag{4.37}$$

The Forward-Difference Model: This model is obtained as

$$\begin{bmatrix} \delta x_k \\ \delta y_k \end{bmatrix} = \begin{bmatrix} y_k \\ -x_k + \varepsilon\left(1 - x_k^2\right)y_k \end{bmatrix} + \begin{bmatrix} 0 \\ A\cos(\omega kT) \end{bmatrix}. \tag{4.38}$$

Extensive simulations have been carried out for the forced van der Pol oscillator (4.29). While the unforced oscillator has a stable limit cycle, the forced oscillator exhibits several interesting phenomena, such as periodic and space-filling responses [32]. The conditions used for simulations are summarized in Table 4.1, where Cases C1(a) to C(d) cover basic four conditions; namely, Self-Sustained, Quasi-Periodic, Fundamental, and Harmonic Oscillations.

All figures given below show typical phase-planes (for the first 1,000 seconds) and time responses (for the first 30 seconds) starting from the initial condition of $\bar{x}_0 = -1.0$ and $\bar{y}_0 = -1.5$. Fig. 4.1 to 4.4 are for the case of $\varepsilon = 1.5$ and $T = 0.1$s, covering four types of oscillations caused under different combinations of input amplitudes ($A = 1, 3, 8$) and frequencies ($\omega = 2, 3$). The proposed model and the forward-difference model are compared with those of the original continuous-time oscillator that is computed using ode45 (Dormand-Prince). The input is assumed to be applied through a ZOH in all discrete-time models.

To see if the proposed method gives consistently better results than others, simulations under different conditions have been carried out. For instance, Fig. 4.1 and 4.5 to 4.7 are for the case of $A = 1$, $\omega = 2, T = 0.1$, covering different values of nonlinearity parameter $\varepsilon = 1.5, 3, 4, 5$. Fig. 4.1, 4.8, and 4.9 are for the case of $\varepsilon = 1.5, A = 1, \omega = 2$, covering different values of $T = 0.1, 0.2, 0.3$. It can be seen that the forward-difference model is not capable of yielding satisfactory results, and becomes unstable for cases 4.6, 4.7, and 4.9. In contrast, the proposed model gives responses that are very close to those of the continuous-time model in all cases.

Comparisons have also been made between the proposed method and 4th-order Runge-Kutta (R-K), as shown in Fig. 4.10 and 4.11. It was found that the R-K method has a better performance than the proposed method up to about *T*=0.4 seconds. However, when the sampling interval increases to 0.5

seconds, 4th order Runge-Kutta method suddenly becomes numerically unstable and the computations stops at about 13.7 seconds. However, the proposed method remains stable at this sampling interval. For the forced van der Pol system under consideration, both the bilinear method of Hirota [2] and the non-standard method of Mickens [4] do not seem to be applicable.

Table 4.1: Conditions used for the simulations

<table>
<tr><th>Conditions</th><th>Initial State</th><th>ε</th><th>A</th><th>ω</th><th>T</th></tr>
<tr><td>C1(a)
Self-Sustained
Oscillation</td><td rowspan="12">$\bar{x}_0 = -1$
$\bar{y}_0 = -1.5$</td><td rowspan="4">$\varepsilon = 1.5$</td><td>$A = 1$</td><td rowspan="2">$\omega = 2$</td><td rowspan="9">$T = 0.1$</td></tr>
<tr><td>C1(b)
Quasi-Periodic
Oscillation</td><td rowspan="2">$A = 3$</td></tr>
<tr><td>C1(c)
Fundamental
Oscillation</td><td rowspan="2">$\omega = 3$</td></tr>
<tr><td>C1(d)
Harmonic
Oscillation</td><td>$A = 8$</td></tr>
<tr><td>C2(a)</td><td>$\varepsilon = 3$</td><td rowspan="4">$A = 1$</td><td rowspan="4">$\omega = 2$</td></tr>
<tr><td>C2(b)</td><td>$\varepsilon = 4$</td></tr>
<tr><td>C2(c)</td><td>$\varepsilon = 5$</td></tr>
<tr><td>C3(a)</td><td rowspan="3">$\varepsilon = 1.5$</td><td>$T = 0.2$</td></tr>
<tr><td>C3(b)</td><td>$T = 0.3$</td></tr>
<tr><td>C3(c)</td><td>$T = 0.5$</td></tr>
</table>

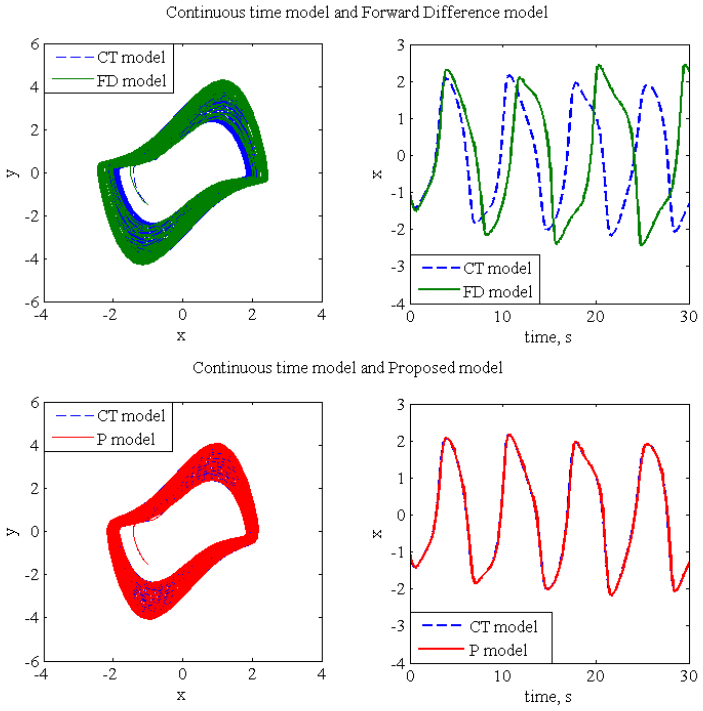

Fig. 4.1 Self-Sustained Oscillation (C1(s)): Phase plane and time response of the continuous-time, the forward-difference, and the proposed models, for $\bar{x}_0 = -1,\ \bar{y}_0 = -1.5,\ \varepsilon = 1.5,\ A = 1,\ \omega = 2,\ T = 0.1$

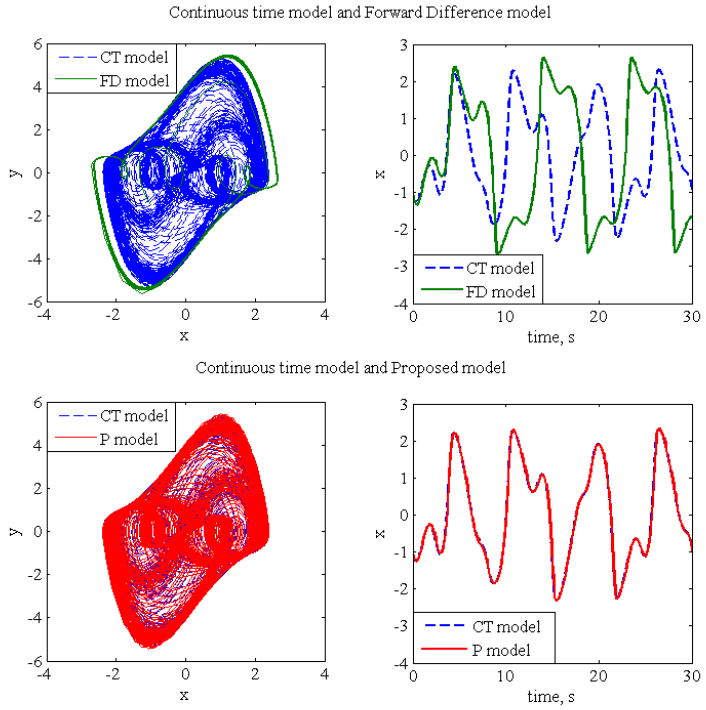

Fig. 4.2 Quasi-Periodic Oscillation (C(1(b)): Phase plane and time response of the continuous-time, the forward-difference, and the proposed models, for $\bar{x}_0 = -1,\ \bar{y}_0 = -1.5,\ \varepsilon = 1.5,\ A = 3,\ \omega = 2,\ T = 0.1$

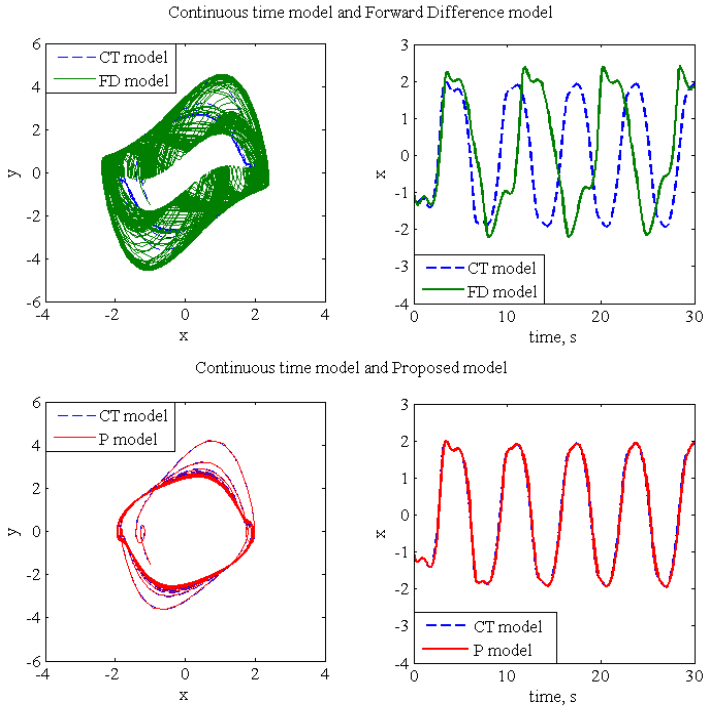

Fig. 4.3 Fundamental Oscillation (C1(c)): Phase plane and time response of the continuous-time, the forward-difference, and the proposed models, for $\bar{x}_0 = -1,\ \bar{y}_0 = -1.5,\ \varepsilon = 1.5,\ A = 3,\ \omega = 3,\ T = 0.1$

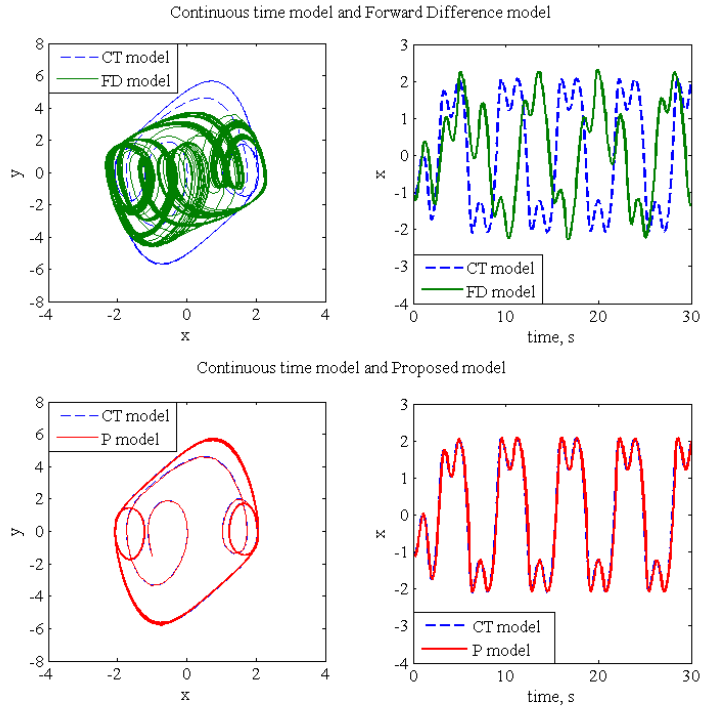

Fig. 4.4 Harmonic Oscillation (C1(d)): Phase plane and time response of the continuous-time, the forward-difference, and the proposed models, for $\bar{x}_0 = -1,\ \bar{y}_0 = -1.5,\ \varepsilon = 1.5,\ A = 8,\ \omega = 3,\ T = 0.1$

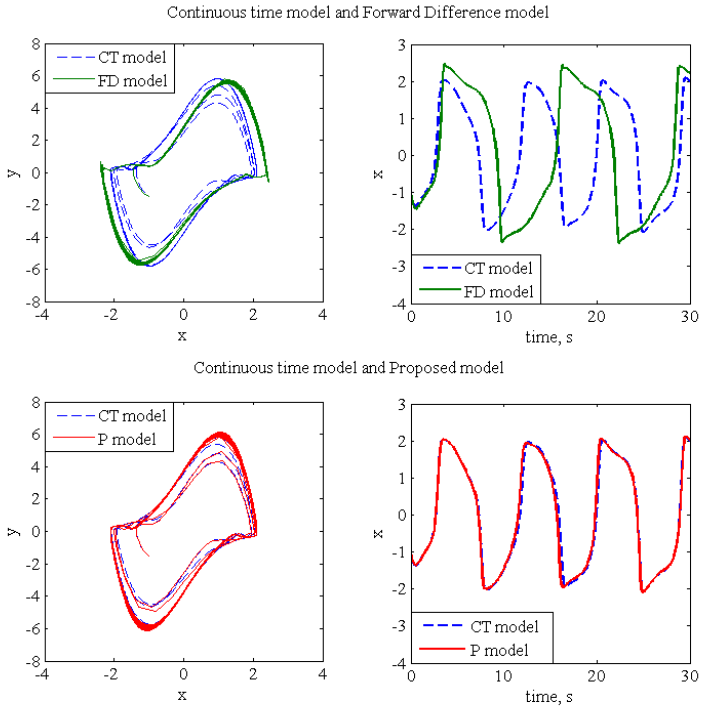

Fig. 4.5 (C2(a)): Phase plane and time response of the continuous-time, the forward-difference, and the proposed models, for $\bar{x}_0 = -1,\ \bar{y}_0 = -1.5,\ \varepsilon = 3,\ A = 1,\ \omega = 2,\ T = 0.1$

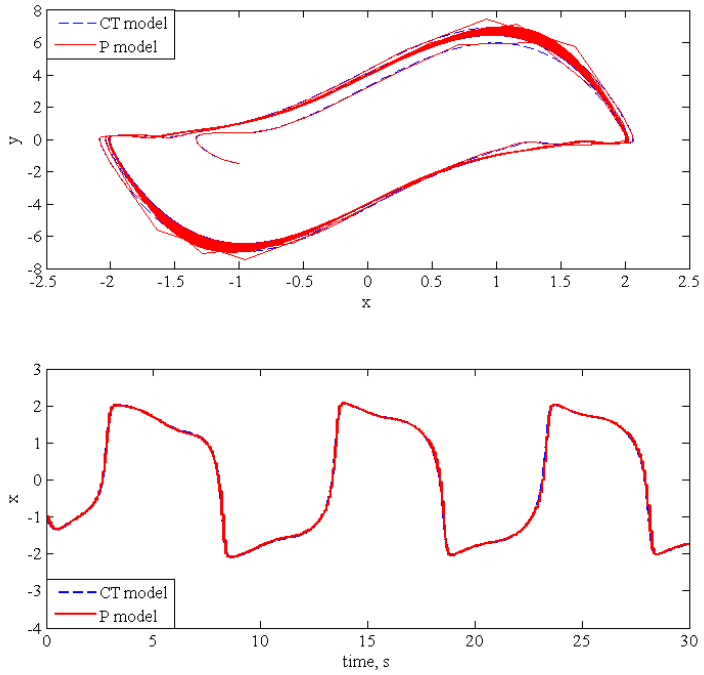

Fig. 4.6 (C2(b)): Phase plane and time response of the continuous-time and the proposed models, for $\bar{x}_0 = -1,\ \bar{y}_0 = -1.5,\ \varepsilon = 4,\ A = 1,\ \omega = 2,\ T = 0.1$

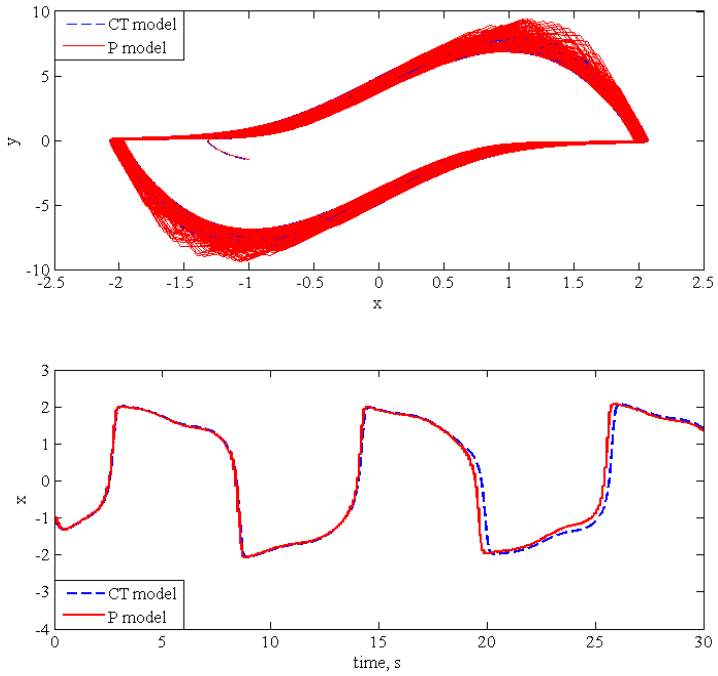

Fig. 4.7 (C2(c)): Phase plane and time response of the continuous-time, and the proposed models, for

$$\bar{x}_0 = -1,\ \bar{y}_0 = -1.5,\ \varepsilon = 5,\ A = 1,\ \omega = 2,\ T = 0.1$$

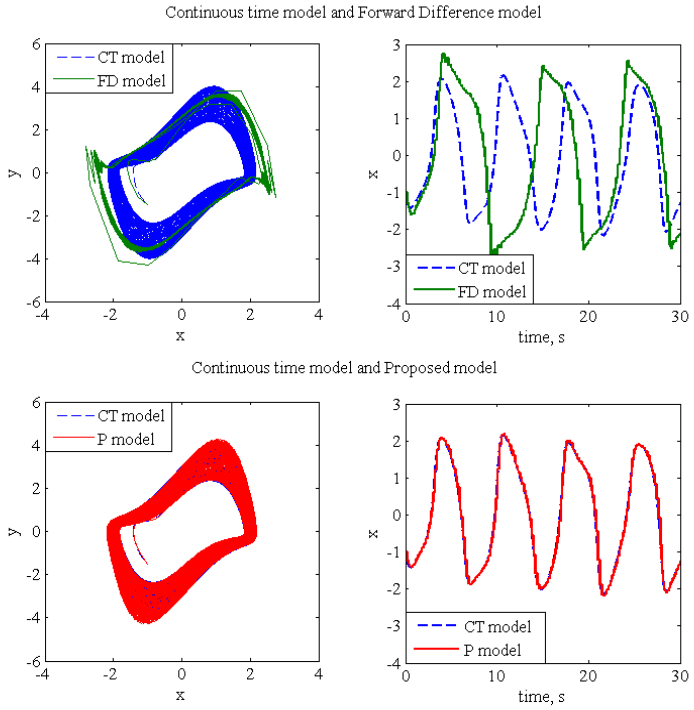

Fig. 4.8 (C3(a)): Phase plane and time response of the continuous-time, the forward-difference, and the proposed models, for $\bar{x}_0 = -1,\ \bar{y}_0 = -1.5,\ \varepsilon = 1.5,\ A = 1,\ \omega = 2,\ T = 0.2$

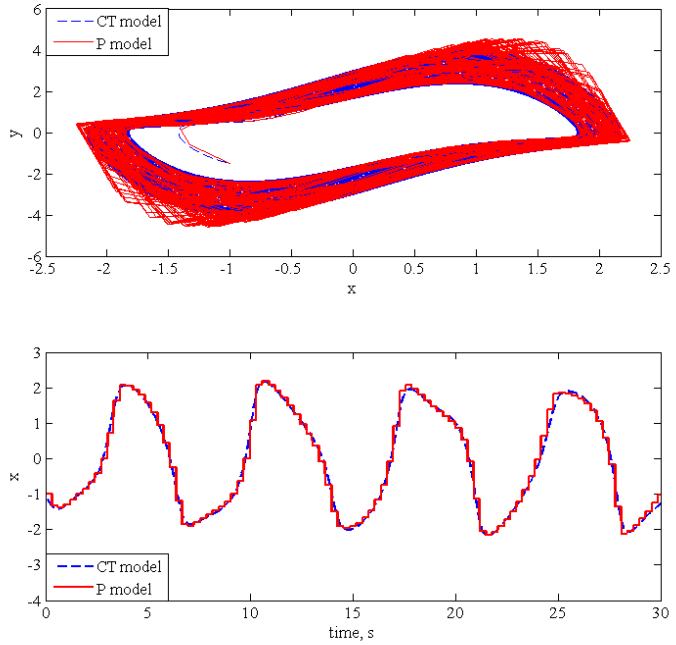

Fig. 4.9 (C3(a)): Phase plane and time response of the continuous-time, and the proposed models, for

$$\bar{x}_0 = -1,\ \bar{y}_0 = -1.5,\ \varepsilon = 1.5,\ A = 1,\ \omega = 2,\ T = 0.3$$

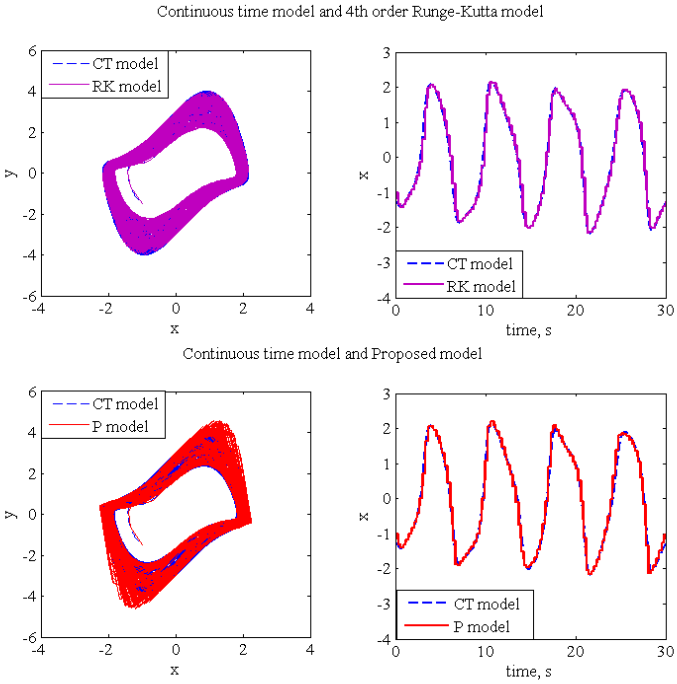

Fig. 4.10 (C3(b)): Phase plane and time response of the continuous-time, 4th order Runge-Kutta, and the proposed models, for $\bar{x}_0 = -1,\ \bar{y}_0 = -1.5,\ \varepsilon = 1.5,\ A = 1,\ \omega = 2,\ T = 0.3$

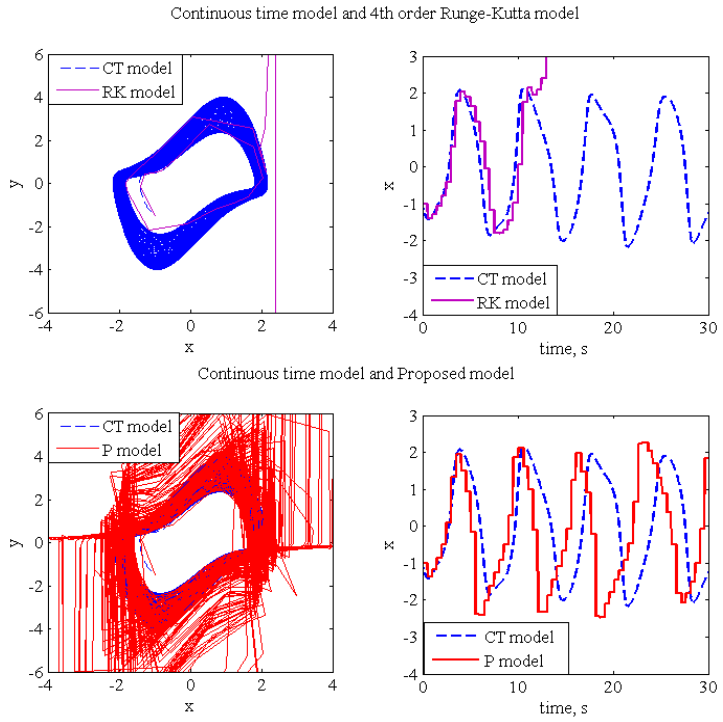

Fig. 4.11 (C3(c)): Phase plane and time response of the continuous-time, 4th order Runge-Kutta, and the proposed models, for $\bar{x}_0 = -1,\ \bar{y}_0 = -1.5,\ \varepsilon = 1.5,\ A = 1,\ \omega = 2,\ T = 0.5$

4.3 Summary

Discrete-time models of forced nonlinear oscillators and their relationships with continuous-time systems have been investigated such that a certain differential equation is obtained as a sufficient condition for the model to be exact. When the solution of this equation can be obtained exactly, such as linear and certain nonlinear systems, the discrete-time model will be exact. When an exact model is not known, the proposed model can always be obtained as an approximate model as long as a Jacobian matrix exists for the given continuous-time system. However, the model is not a linear approximation based on this Jacobian matrix, but a nonlinear approximation. The method is applied to a van der Pol oscillator driven by a sinusoidal input. Simulations show that the proposed model gives performances that are superior to the popular on-line computable method known as the forward-difference model.

Chapter 5

Discrete-time model of non-autonomous nonlinear systems

A discretization method is proposed in this chapter for continuous-time, non-autonomous, and nonlinear systems. The concept of continualization proposed in Chapter 2 is used to derive a sufficient condition for a given discrete-time system to be an exact discretization of the original continuous-time system. The proposed discretization method is based on an approximate solution to this condition, which is computed using Peano-Baker series. As an example, an inverted pendulum subjected to high-frequency excitation is considered. Simulation results show that the proposed method has good performances even with a relatively large sampling interval.

5.1 Proposed discrete-time model for non-autonomous nonlinear systems

Let a continuous-time model of a non-autonomous nonlinear system be given by the following state space equation:

$$\frac{d\,\bar{\mathbf{x}}(t)}{dt} = \bar{\mathbf{\Gamma}}\left(\bar{\mathbf{x}}(t), t\right), \quad \bar{\mathbf{x}}(t_0) = \bar{\mathbf{x}}_0 \tag{5.1}$$

where $\bar{\mathbf{x}} \in R^n$ is a state vector of continuous-time variable t and $\bar{\mathbf{\Gamma}}$ assumed to be expandable into Taylor series. This implies that $\bar{\mathbf{\Gamma}}$ satisfies the Lipschitz condition and (5.1) has a unique solution for a given initial condition.

The discrete-time model is expressed in delta form with a uniform discrete-time period of T, as

$$\delta \mathbf{x}_k = \frac{\mathbf{x}_{k+1} - \mathbf{x}_k}{T} = \mathbf{\Gamma}\left(\mathbf{x}_k, kT\right), \quad \mathbf{x}_{k_0} = \bar{\mathbf{x}}_0 \tag{5.2}$$

The following theorem states that any discrete-time system (5.2) can be an exact model of a continuous-time system (5.1) if the discrete-time function $\mathbf{\Gamma}$ is chosen in a certain manner.

Theorem 5.1 [Exact Discretization]: A discrete-time system given by (5.2) is an exact discrete-time model of system (5.1) if $\mathbf{\Gamma}$ satisfies the following: In each interval $kT \le t < (k+1)T$,

$$\frac{d}{dt}\Big((t-kT)\mathbf{\Gamma}\left(\bar{\mathbf{x}}^*(kT), t-kT\right)\Big) = \bar{\mathbf{\Gamma}}\left(\bar{\mathbf{x}}^*(kT) + (t-kT)\mathbf{\Gamma}\left(\bar{\mathbf{x}}^*(kT), t-kT\right), t\right), \tag{5.3}$$

where $\bar{\mathbf{x}}^*(t)$ is the continualization of discrete-time state $\mathbf{x}_k$ as Definition 2.3.□

Proof: For the state $\bar{\mathbf{x}}^*(t)$ to be a solution of (5.1), $\boldsymbol{\Gamma}\left(\bar{\mathbf{x}}^*(kT), t-kT\right)$ must be such that (2.8) equals (5.1); that is, using (2.7), in each interval,

$$\begin{aligned}
&\frac{d}{dt}\left((t-kT)\boldsymbol{\Gamma}\left(\bar{\mathbf{x}}^*(kT), t-kT\right)\right) \\
&= \dot{\bar{\mathbf{x}}}^*(t) \\
&= \bar{\boldsymbol{\Gamma}}\left(\bar{\mathbf{x}}^*(t), t\right) \\
&= \bar{\boldsymbol{\Gamma}}\left(\bar{\mathbf{x}}^*(kT) + (t-kT)\boldsymbol{\Gamma}\left(\bar{\mathbf{x}}^*(kT), t-kT\right), t\right)
\end{aligned} \quad , \tag{5.4}$$

which is (5.3).□

When (5.3) can be solved for $\boldsymbol{\Gamma}$, the exact discrete-time model can be found. When it is solved approximately, an approximate discrete-time model may be obtained. One such model is proposed below, which is applicable to a general class of non-autonomous nonlinear and linear systems, provided they have a Jacobian matrix.

Theorem 5.2 [The Proposed Model]: A discrete-time system given by (5.2), where $\boldsymbol{\Gamma}$ is chosen as

$$\boldsymbol{\Gamma}\left(\mathbf{x}_k, T\right) = \frac{1}{T}\int_0^T e^{\int_\lambda^T D\bar{\boldsymbol{\Gamma}}\left(\mathbf{x}_k, \gamma+kT\right)d\gamma} \bar{\boldsymbol{\Gamma}}\left(\mathbf{x}_k, \lambda+kT\right)d\lambda \tag{5.5}$$

with $D\bar{\boldsymbol{\Gamma}}$ being Jacobian matrix of $\bar{\boldsymbol{\Gamma}}$, is a discrete-time model of the continuous-time system given by (5.1).□

Proof: Equation (2.7) with $\boldsymbol{\Gamma}$ given by (5.5) holds for a fixed time $t=\tau$ in each sampling interval such that

$$\frac{\bar{\mathbf{x}}^*(\tau) - \bar{\mathbf{x}}^*(kT)}{\tau - kT} = \frac{1}{\tau - kT}\int_0^{\tau-kT} e^{\int_\lambda^{\tau-kT} D\bar{\boldsymbol{\Gamma}}\left(\bar{\mathbf{x}}^*(kT), \gamma+kT\right)d\gamma} \bar{\boldsymbol{\Gamma}}\left(\bar{\mathbf{x}}^*(kT), \lambda+kT\right)d\lambda \tag{5.6}$$

and this also holds at the limit of T approaching zero while k is chosen such that $kT \le \tau < (k+1)T$ holds. Thus, noting that, for a fixed τ and a suitable choice of k,

$$\lim_{\substack{T\to 0 \\ kT\le\tau<(k+1)T}} kT = \tau \tag{5.7}$$

and $\bar{\boldsymbol{\Gamma}}$ is finite, the use of l'Hospital's Rule on the right-hand-side of (5.6) yields

$$
\begin{aligned}
&\lim_{\substack{T\to 0\\ kT\le\tau<(k+1)T}}\left[\frac{1}{\tau-kT}\int_0^{\tau-kT} e^{\int_\lambda^{\tau-kT} D\bar{\boldsymbol{\Gamma}}\left(\bar{\mathbf{x}}^*(kT),\gamma+kT\right)d\gamma}\bar{\boldsymbol{\Gamma}}\left(\bar{\mathbf{x}}^*(kT),\lambda+kT\right)d\lambda\right]\\
&=\lim_{\substack{T\to 0\\ kT\le\tau<(k+1)T}}\left[D\bar{\boldsymbol{\Gamma}}\left(\bar{\mathbf{x}}^*(kT),\tau\right)(\tau-kT)\boldsymbol{\Gamma}\left(\bar{\mathbf{x}}^*(kT),\tau-kT\right)+\bar{\boldsymbol{\Gamma}}\left(\bar{\mathbf{x}}^*(kT),\tau\right)\right]\\
&=\lim_{\substack{T\to 0\\ kT\le\tau<(k+1)T}}\left[\bar{\boldsymbol{\Gamma}}\left(\bar{\mathbf{x}}^*(kT),\tau\right)\right]\\
&=\bar{\boldsymbol{\Gamma}}\left(\bar{\mathbf{x}}^*(\tau),\tau\right)
\end{aligned}
\tag{5.8}
$$

The left-hand-side, on the other hand, gives

$$
\lim_{\substack{T\to 0\\ kT\le\tau<(k+1)T}}\frac{\bar{\mathbf{x}}^*(\tau)-\bar{\mathbf{x}}^*(kT)}{\tau-kT}=\frac{d\bar{\mathbf{x}}^*(\tau)}{d\tau}. \tag{5.9}
$$

Therefore, at the limit of T approaching zero and for all τ such that $kT\le\tau<(k+1)T$, (5.6) gives

$$
\frac{d\bar{\mathbf{x}}^*(\tau)}{d\tau}=\bar{\boldsymbol{\Gamma}}\left(\bar{\mathbf{x}}^*(\tau),\tau\right). \tag{5.10}
$$

Since (5.1) has a unique solution given an initial condition, it follows that

$$
\lim_{\substack{T\to 0\\ kT\le\tau<(k+1)T}}\bar{\mathbf{x}}^*(\tau)=\bar{\mathbf{x}}(\tau). \tag{5.11}
$$

Therefore, the relationship of $\mathbf{x}_k=\bar{\mathbf{x}}^*(kT)$, (5.7), and (5.11) lead, for any τ with $kT\le\tau<(k+1)T$, to

$$
\lim_{\substack{T\to 0\\ kT\le\tau<(k+1)T}}\mathbf{x}_k=\lim_{\substack{T\to 0\\ kT\le\tau<(k+1)T}}\bar{\mathbf{x}}^*(kT)=\lim_{\substack{T\to 0\\ kT\le\tau<(k+1)T}}\bar{\mathbf{x}}^*(\tau)=\bar{\mathbf{x}}(\tau). \tag{5.12}
$$

In view of Definition 2.2, system (5.2) with (5.5) is a discrete-time model of the continuous-time system (5.1). □

Equation (5.5) can be derived as follows: When $\bar{\boldsymbol{\Gamma}}$ in (5.3) is expanded into the Taylor series and truncated with the first two terms as

$$
\begin{aligned}
&\bar{\boldsymbol{\Gamma}}\left(\left[\bar{\mathbf{x}}^*(kT)+(t-kT)\boldsymbol{\Gamma}\left(\bar{\mathbf{x}}^*(kT),t-kT\right)\right],t\right)\\
&=\bar{\boldsymbol{\Gamma}}\left(\bar{\mathbf{x}}^*(kT),t\right)+\left[D\bar{\boldsymbol{\Gamma}}\left(\bar{\mathbf{x}}^*(kT),t\right)\right](t-kT)\boldsymbol{\Gamma}\left(\bar{\mathbf{x}}^*(kT),t-kT\right)
\end{aligned},
\tag{5.13}
$$

eq. (5.3) can always be solved and an approximate discrete-time model obtained. That is, for arbitrary $\bar{\mathbf{x}}^*(kT)$, (5.3) can be expressed as

$$
\begin{aligned}
&\frac{d}{dt}\left((t-kT)\boldsymbol{\Gamma}\left(\bar{\mathbf{x}}^*(kT),t-kT\right)\right)\\
&=\left[D\bar{\boldsymbol{\Gamma}}\left(\bar{\mathbf{x}}^*(kT),t\right)\right](t-kT)\boldsymbol{\Gamma}\left(\bar{\mathbf{x}}^*(kT),t-kT\right)+\bar{\boldsymbol{\Gamma}}\left(\bar{\mathbf{x}}^*(kT),t\right)
\end{aligned}.
\tag{5.14}
$$

Defining $\zeta=t-kT$, (5.14) can be written as

$$\begin{aligned}&\frac{d}{d\zeta}\left(\zeta\boldsymbol{\Gamma}\left(\bar{\mathbf{x}}^*(kT),\zeta\right)\right)\\&=\left[D\bar{\boldsymbol{\Gamma}}\left(\bar{\mathbf{x}}^*(kT),\zeta+kT\right)\right]\zeta\boldsymbol{\Gamma}\left(\bar{\mathbf{x}}^*(kT),\zeta\right)+\bar{\boldsymbol{\Gamma}}\left(\bar{\mathbf{x}}^*(kT),\zeta+kT\right)\end{aligned}\tag{5.15}$$

where $0\le\zeta<T$. Noting that $\zeta\boldsymbol{\Gamma}\left(\bar{\mathbf{x}}^*(kT),\zeta\right)=0$ at $\zeta=0$, a solution to the above linear differential equation in $\zeta\boldsymbol{\Gamma}\left(\bar{\mathbf{x}}^*(kT),\zeta\right)$ gives the following continuous-time function [30]:

$$\zeta\boldsymbol{\Gamma}\left(\bar{\mathbf{x}}^*(kT),\zeta\right)=\int_0^{\zeta}e^{\int_{\lambda}^{\zeta}D\bar{\boldsymbol{\Gamma}}(\mathbf{x}_k,\gamma+kT)d\gamma}\bar{\boldsymbol{\Gamma}}\left(\mathbf{x}_k,\lambda+kT\right)d\lambda.\tag{5.16}$$

Adopting this form of function, the discrete-time function is obtained as

$$\boldsymbol{\Gamma}\left(\mathbf{x}_k,T\right)=\frac{1}{T}\int_0^{T}e^{\int_{\lambda}^{T}D\bar{\boldsymbol{\Gamma}}(\mathbf{x}_k,\gamma+kT)d\gamma}\bar{\boldsymbol{\Gamma}}\left(\mathbf{x}_k,\lambda+kT\right)d\lambda\tag{5.17}$$

which is (5.5).

Remark 5.1: The proposed discrete-time function (5.5) can be written as

$$\begin{aligned}\boldsymbol{\Gamma}\left(\mathbf{x}_k,T\right)&=\frac{1}{T}\int_0^{T}e^{\int_{\lambda}^{T}D\bar{\boldsymbol{\Gamma}}(\mathbf{x}_k,\gamma+kT)d\gamma}\bar{\boldsymbol{\Gamma}}\left(\mathbf{x}_k,\lambda+kT\right)d\lambda\\&=\frac{1}{T}\int_0^{T}e^{\int_{\lambda+kT}^{(k+1)T}D\bar{\boldsymbol{\Gamma}}(\mathbf{x}_k,\gamma)d\gamma}\bar{\boldsymbol{\Gamma}}\left(\mathbf{x}_k,\lambda+kT\right)d\lambda\\&=\frac{1}{T}\int_{kT}^{(k+1)T}e^{\int_{\lambda}^{(k+1)T}D\bar{\boldsymbol{\Gamma}}(\mathbf{x}_k,\gamma)d\gamma}\bar{\boldsymbol{\Gamma}}\left(\mathbf{x}_k,\lambda\right)d\lambda\end{aligned}\tag{5.18}$$

The proposed discrete-time function is time-varying and is updated at each instant by the above integration from kT to $(k+1)T$.

Remark 5.2: The solution to (5.15) is also given by the following form:

$$\zeta\boldsymbol{\Gamma}\left(\bar{\mathbf{x}}^*(kT),\zeta\right)=\int_{kT}^{\zeta+kT}\Phi\left(\zeta+kT,\lambda\right)\bar{\boldsymbol{\Gamma}}\left(\mathbf{x}_k,\lambda\right)d\lambda\tag{5.19}$$

where $\Phi(\zeta,\lambda)$ is the transition matrix of linear time variant equation (5.15), which is called Peano-Baker series and defined as [33]

$$\begin{aligned}\Phi(\zeta,\lambda)&=\mathbf{I}+\int_{\lambda}^{\zeta}\left[D\bar{\boldsymbol{\Gamma}}\left(\bar{\mathbf{x}}^*(kT),\sigma_1\right)\right]d\sigma_1\\&+\int_{\lambda}^{\zeta}\left[D\bar{\boldsymbol{\Gamma}}\left(\bar{\mathbf{x}}^*(kT),\sigma_1\right)\right]\int_{\lambda}^{\sigma_1}\left[D\bar{\boldsymbol{\Gamma}}\left(\bar{\mathbf{x}}^*(kT),\sigma_2\right)\right]d\sigma_2d\sigma_1+\dots\\&+\int_{\lambda}^{\zeta}\left[D\bar{\boldsymbol{\Gamma}}\left(\bar{\mathbf{x}}^*(kT),\sigma_1\right)\right]\int_{\lambda}^{\sigma_1}\left[D\bar{\boldsymbol{\Gamma}}\left(\bar{\mathbf{x}}^*(kT),\sigma_2\right)\right]\cdots\int_{\lambda}^{\sigma_{i-1}}\left[D\bar{\boldsymbol{\Gamma}}\left(\bar{\mathbf{x}}^*(kT),\sigma_i\right)\right]d\sigma_i\cdots d\sigma_2d\sigma_1+\dots\end{aligned}\tag{5.20}$$

Thus the proposed discrete-time function (5.5) can be written as

$$\mathbf{\Gamma}\left(\mathbf{x}_k,T\right)=\frac{1}{T}\int_{kT}^{(k+1)T}\Phi\left((k+1)T,\lambda\right)\bar{\mathbf{\Gamma}}\left(\mathbf{x}_k,\lambda\right)d\lambda\,. \tag{5.21}$$

Remark 5.3: When (5.3) can be solved exactly, an exact discrete-time model can be found. For instance for a linear system, the proposed method gives the exact discrete-time model; i.e., for $\bar{\mathbf{\Gamma}}$ in (5.1) given as

$$\bar{\mathbf{\Gamma}}\left(\bar{\mathbf{x}}(t),t\right)=\bar{\mathbf{A}}(t)\bar{\mathbf{x}}+\bar{\mathbf{B}}(t)\bar{\mathbf{u}}(t)\,, \tag{5.22}$$

where $\bar{\mathbf{A}}$ is a system matrix of compatible dimension, (5.3) can be written exactly as a linear differential equation as

$$\begin{aligned}&\frac{d}{dt}\left((t-kT)\mathbf{\Gamma}\left(\bar{\mathbf{x}}^*(kT),t-kT\right)\right)\\&-\bar{\mathbf{A}}(t)\left((t-kT)\mathbf{\Gamma}\left(\bar{\mathbf{x}}^*(kT),t-kT\right)\right)-\left(\bar{\mathbf{A}}(t)\bar{\mathbf{x}}^*(kT)+\bar{\mathbf{B}}(t)\bar{\mathbf{u}}(t)\right)=0\end{aligned}\,, \tag{5.23}$$

whose solution is [30]

$$(t-kT)\mathbf{\Gamma}\left(\bar{\mathbf{x}}^*(kT),t-kT\right)=\int_{kT}^{t}e^{\int_{\lambda}^{t}\bar{\mathbf{A}}(\gamma)d\gamma}\left(\bar{\mathbf{A}}(\lambda)\bar{\mathbf{x}}^*(kT)+\bar{\mathbf{B}}(\lambda)\bar{\mathbf{u}}(\lambda)\right)d\lambda\,. \tag{5.24}$$

This leads to the exact discrete-time model [34] as

$$\begin{aligned}&\mathbf{\Gamma}\left(\mathbf{x}_k,T\right)\\&=\frac{1}{T}\int_{kT}^{(k+1)T}e^{\int_{\lambda}^{(k+1)T}\bar{\mathbf{A}}(\gamma)d\gamma}\left(\bar{\mathbf{A}}(\lambda)\bar{\mathbf{x}}^*(kT)+\bar{\mathbf{B}}(\lambda)\bar{\mathbf{u}}(\lambda)\right)d\lambda\\&=\frac{1}{T}\int_{T}^{(k+1)T}\Phi\left((k+1)T,\lambda\right)\left(\bar{\mathbf{A}}(\lambda)\bar{\mathbf{x}}^*(kT)+\bar{\mathbf{B}}(\lambda)\bar{\mathbf{u}}(\lambda)\right)d\lambda\end{aligned} \tag{5.25}$$

where

$$\begin{aligned}\Phi(\zeta,\lambda)=\mathbf{I}&+\int_{\lambda}^{\zeta}\bar{\mathbf{A}}(\sigma_1)d\sigma_1+\int_{\lambda}^{\zeta}\bar{\mathbf{A}}(\sigma_1)\int_{\lambda}^{\sigma_1}\bar{\mathbf{A}}(\sigma_2)d\sigma_2d\sigma_1+\dots\\&+\int_{\lambda}^{\zeta}\bar{\mathbf{A}}(\sigma_1)\int_{\lambda}^{\sigma_1}\bar{\mathbf{A}}(\sigma_2)\cdots\int_{\lambda}^{\sigma_{i-1}}\bar{\mathbf{A}}(\sigma_i)d\sigma_i\cdots d\sigma_2d\sigma_1+\dots\end{aligned}\,. \tag{5.26}$$

Remark 5.4: When the Taylor series expansion of $\bar{\mathbf{\Gamma}}\left(\bar{\mathbf{x}}^*(kT)+(t-kT)\mathbf{\Gamma}\left(\bar{\mathbf{x}}^*(kT),t-kT\right),t\right)$ is truncated after the first term and noting that $\bar{\mathbf{\Gamma}}\left(\bar{\mathbf{x}}(t),t\right)$ is invariant in the interval $\left[kT,(k+1)T\right)$, (5.3) yields

$$\frac{d}{dt}\left((t-kT)\mathbf{\Gamma}\left(\bar{\mathbf{x}}^*(kT),t-kT\right)\right)=\bar{\mathbf{\Gamma}}\left(\bar{\mathbf{x}}^*(kT),kT\right) \tag{5.27}$$

so that

$$\boldsymbol{\Gamma}\left(\bar{\mathbf{x}}^{*}\left(kT\right),t-kT\right)=\bar{\boldsymbol{\Gamma}}\left(\bar{\mathbf{x}}^{*}\left(kT\right),kT\right). \tag{5.28}$$

This is known as the forward difference model.

Remark 5.5: When the continuous-time system (5.1) is an autonomous system $d\,\bar{\mathbf{x}}(t)/dt=\bar{\boldsymbol{\Gamma}}\left(\bar{\mathbf{x}}(t)\right)$, the proposed discrete-time function (5.5) leads to the discrete-time model for autonomous system proposed in [14]

$$\delta\mathbf{x}_k=\frac{1}{T}\int_0^T e^{D\bar{\boldsymbol{\Gamma}}(\mathbf{x}_k)\gamma d\gamma}d\lambda\bar{\boldsymbol{\Gamma}}\left(\mathbf{x}_k\right). \tag{5.29}$$

Remark 5.6: When the continuous-time system (5.1) is given in the form of a forced nonlinear oscillator with the system function being

$$\bar{\boldsymbol{\Gamma}}\left(\bar{\mathbf{x}}(t),t\right)=\bar{\mathbf{f}}\left(\bar{\mathbf{x}}(t)\right)+\bar{\mathbf{g}}(t), \tag{5.30}$$

the proposed discrete-time function (5.5) yields the following discrete-time function:

$$\begin{aligned}\boldsymbol{\Gamma}\left(\mathbf{x}_k,T\right)&=\frac{1}{T}\int_0^T e^{\int_\lambda^T D\bar{\boldsymbol{\Gamma}}(\mathbf{x}_k,\gamma+kT)d\gamma}\bar{\boldsymbol{\Gamma}}\left(\mathbf{x}_k,\lambda+kT\right)d\lambda\\&=\frac{1}{T}\int_0^T e^{\int_\lambda^T D\bar{\mathbf{f}}(\mathbf{x}_k)d\gamma}\left(\bar{\mathbf{f}}\left(\mathbf{x}_k\right)+\bar{\mathbf{g}}\left(\lambda+kT\right)\right)d\lambda\\&=\frac{1}{T}\left(\int_0^T e^{D\bar{\mathbf{f}}(\mathbf{x}_k)(T-\lambda)}d\lambda\right)\bar{\mathbf{f}}\left(\mathbf{x}_k\right)+\frac{1}{T}\int_0^T e^{D\bar{\mathbf{f}}(\mathbf{x}_k)(T-\lambda)}\bar{\mathbf{g}}\left(\lambda+kT\right)d\lambda,\end{aligned} \tag{5.31}$$

which is identical to one proposed in [13].

5.2 Discrete-time model for an inverted pendulum subjected to high-frequency excitations

Open-loop stabilization of an unstable equilibrium state of an inverted pendulum was shown to be possible in [35], where a high frequency excitation is used in the vertical axis with no feedback. This excited pendulum, shown in Fig. 5.1, is a nonlinear non-autonomous system, which consists of a point mass m attached to the top end of a massless rod of length l. The bottom end is periodically excited along the vertical axis with the amplitude and angular frequency of excitation being a_e and ω, respectively. Its equation of motion is given by [35]

$$\frac{d^2\theta}{dt^2}+\frac{c}{ml}\frac{d\theta}{dt}+\left(-\frac{g}{l}+\frac{a_e\omega^2}{l}\cos\omega t\right)\sin\theta=0 \tag{5.32}$$

where c is a viscous damping coefficient of the pivot at bottom. The system (5.32) can be rewritten

in a vector form as

$$\begin{cases} \dot{\theta} = \rho \\ \dot{\rho} = -\dfrac{c}{ml}\rho - \left(-\dfrac{g}{l} + \dfrac{a_e \omega^2}{l} \cos \omega t \right) \sin \theta \end{cases}, \tag{5.33}$$

for which the proposed discrete-time model is obtained as

$$\begin{bmatrix} \delta\theta_k \\ \delta\rho_k \end{bmatrix} = \frac{1}{T} \int_{kT}^{(k+1)T} \Phi\big((k+1)T, \lambda\big) \bar{\mathbf{\Gamma}}\left(\mathbf{x}_k, \lambda\right) d\lambda , \tag{5.34}$$

where

$$\bar{\mathbf{\Gamma}}\left(\mathbf{x}_k, t\right) = \begin{bmatrix} \rho_k \\ -\dfrac{c}{ml}\rho_k - \left(-\dfrac{g}{l} + \dfrac{a_e \omega^2}{l} \cos \omega t \right) \sin \theta_k \end{bmatrix} \tag{5.35}$$

Peano-Baker series $\Phi(\zeta, \lambda)$ is given by (5.20) with Jacobian matrix being

$$D\bar{\mathbf{\Gamma}}\left(\mathbf{x}_k\right) = \begin{bmatrix} 0 & 1 \\ -\left(-\dfrac{g}{l} + \dfrac{a_e \omega^2}{l} \cos \omega t \right) \cos \theta_k & -\dfrac{c}{ml} \end{bmatrix}. \tag{5.36}$$

The forward difference model of continuous-time system (5.33) is given by

$$\begin{bmatrix} \delta\theta_k \\ \delta\rho_k \end{bmatrix} = \begin{bmatrix} \rho_k \\ -\dfrac{c}{ml}\rho_k - \left(-\dfrac{g}{l} + \dfrac{a_e \omega^2}{l} \cos\left(\omega k T\right) \right) \sin \theta_k \end{bmatrix}. \tag{5.37}$$

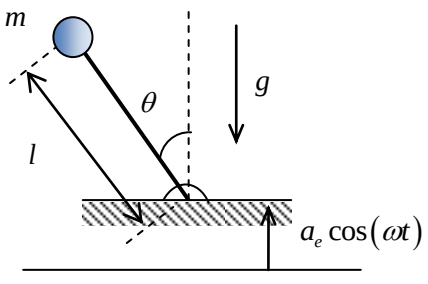

Fig. 5.1: The inverted pendulum subjected to high-frequency excitation at the base

Simulations have been carried out where m, l, and c are, respectively, $2.35\times10^{-2}\,kg$, $5.37\times10^{-2}\,m$ and 0.03. Yabuno et al. [35] have shown that the unstable equilibrium point ($\theta=0$) of the inverted pendulum can be stabilized without feedback by applying a high-frequency excitation with the amplitude of $a_e=4.5\times10^{-3}m$ and the frequency of $\omega=35Hz$. Figures 5.2 to 5.5 to be given below show the time responses for the first 0.2 seconds, starting from the initial condition of $\theta_0=0.3$ and $\dot{\theta}_0=0$. The sum of differences between continuous-time and discrete-time responses is used to assess the error ER, as

$$ER=T\sum_{k=0}^{kT=tl}\left|\theta(t)\big|_{t=kT}-\theta_k\right| \tag{5.38}$$

where tl is the time length of the simulation run.

From simulations, it was found that, in many cases, only a single term suffices in the calculation of Peano-Baker series. Fig. 5.2 shows that when the sampling interval is $\mathrm{T}=0.001$ second, the response of the proposed model is very close to that of the continuous-time model even with $\mathrm{i}=1$ in Peano-Baker series. The continuous-time response was calculated using the ode45 method (Runge-Kutta, Dormand Prince (4,5) pair) in Matlab/Simulink. The performance of the forward difference method is not good even at such a small sampling interval; the sampling interval should be reduced to $0.00005\mathrm{s}$ to obtain a response comparable to that of the original continuous-time system. When the sampling interval is increased to $0.0025\mathrm{s}$ (Fig. 5.3), the proposed model still gives almost exact responses at the sampling instants with $\mathrm{i}=1$. When the sampling interval is increased to $0.005\mathrm{s}$ (Fig. 5.4), the forward difference model becomes unstable, whereas the proposed model still yields stable responses. The response can be improved by increasing i, as shown in Fig. 5.5 where $\mathrm{i}=3$.

Fig. 5.6 shows the error evaluated by (5.38) where $\mathrm{tl}=0.2\mathrm{s}$. The error becomes smaller as the sampling period does in all cases. The proposed model with $\mathrm{i}=1$ has the error whose magnitude is orders of magnitude smaller than that of the forward-difference model, and the difference between the two models becomes larger as the sampling period is reduced. The figure also shows that increasing i beyond two or three does not reduce the error much further. It takes about 20, 65, 118, and 225 seconds, respectively for $\mathrm{i}=2$, 3, 4, and 5, to calculate the coefficients of the Peano-Baker series off-line, as measured by the "cputime" command. The time it takes for Matlab to compute the response in Fig. 5.4 is $2.18\mathrm{s}$ for the proposed model and 0.95s for the forward difference model.

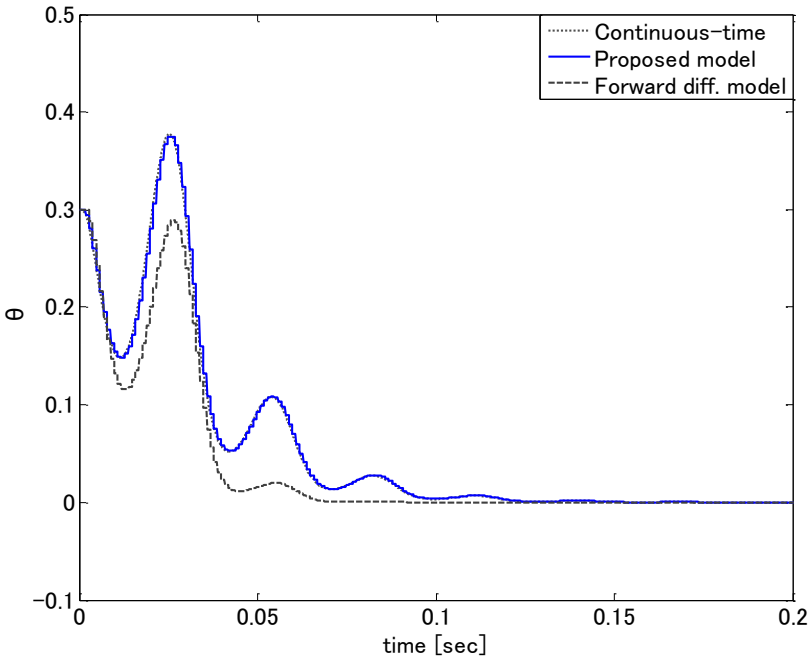

Fig. 5.2: Responses of the continuous-time, the proposed, and the forward difference discrete-time models for $T = 0.001\text{s}$, $i = 1$

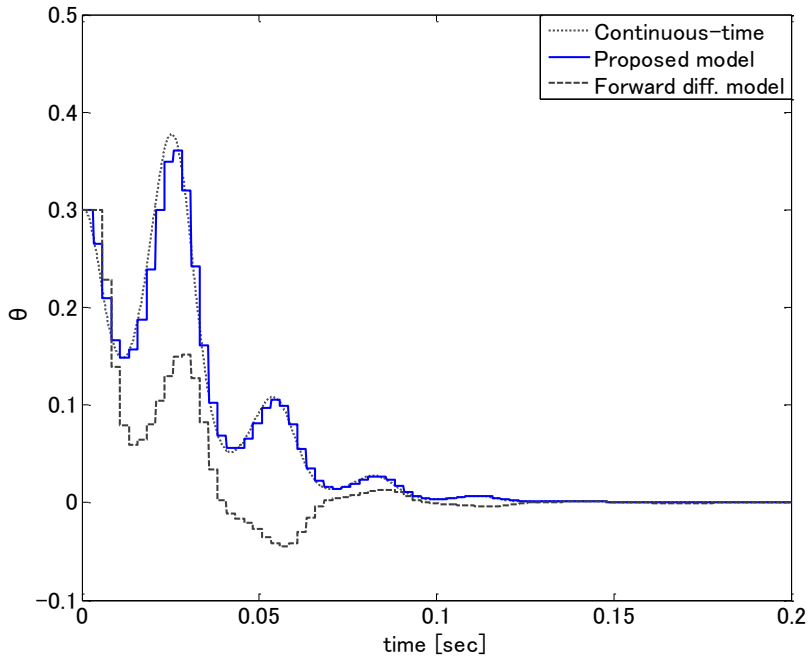

Fig. 5.3: Responses of the continuous-time, the proposed, and the forward difference discrete-time models for $T = 0.0025\text{s}$, $i = 1$

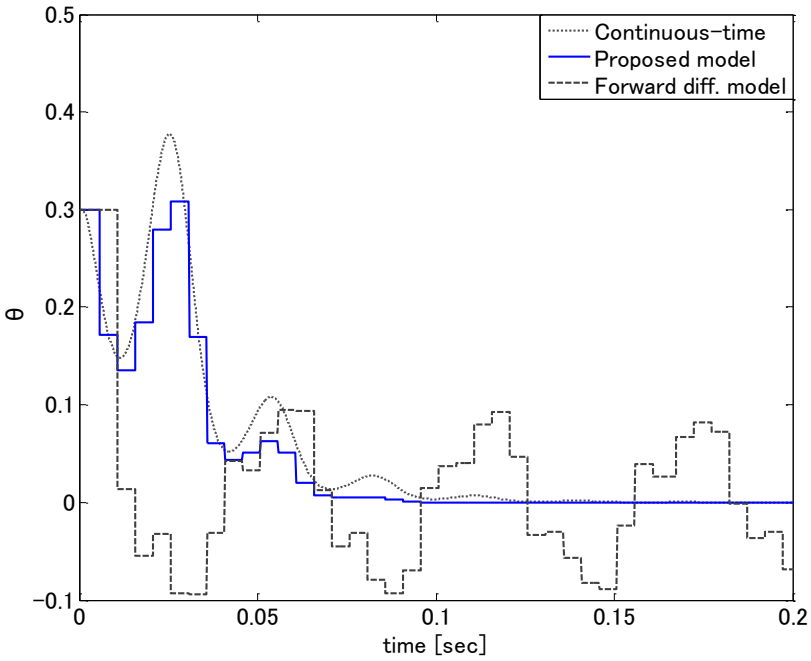

Fig. 5.4: Responses of the continuous-time, the proposed, and the forward difference discrete-time models for $T = 0.005\text{s}$, $i = 1$

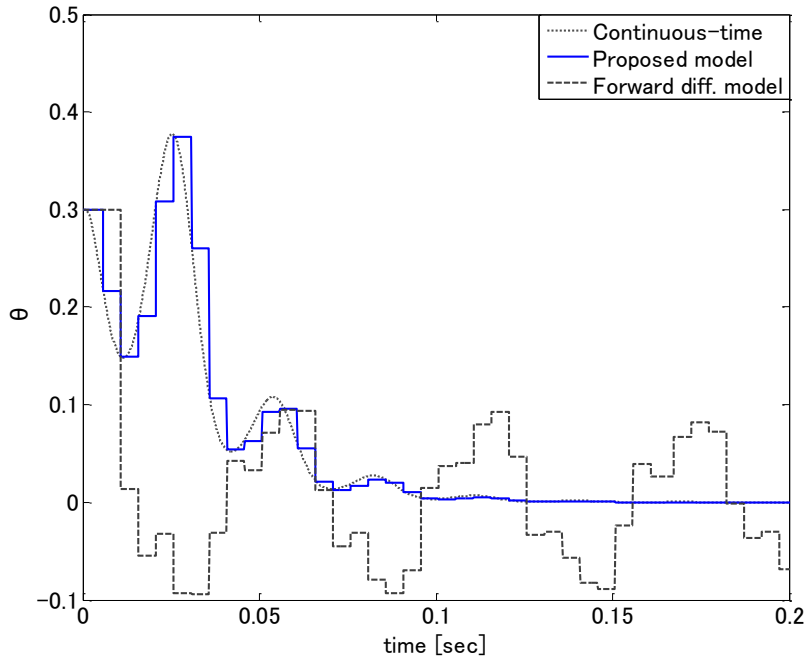

Fig. 5.5: Responses of the continuous-time, the proposed, and the forward difference discrete-time models for $T = 0.005\text{s}$, $i = 3$

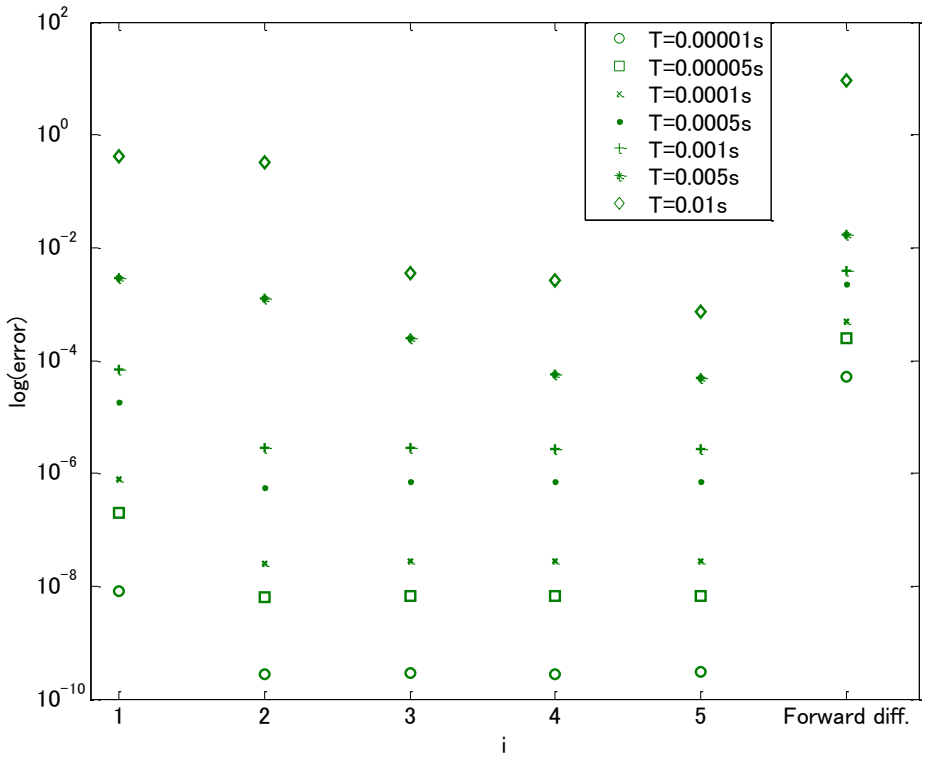

Fig. 5.6: Errors with the proposed and the forward difference discrete-time models for different values of sampling periods

5.3 Summary

A method of obtaining an on-line computable discrete- time model has been proposed for a rather general class of nonlinear non-autonomous systems. The proposed method offers an accurate model that is alternative to the popular forward-difference model, which has been practically the only on-line computable technique to such systems. This method is an extension of that introduced in Chapter 4 for forced nonlinear oscillators, a special class of non-autonomous nonlinear systems. The proposed discrete-time model can be exact when a certain condition equation can be solved exactly, such as for linear systems. When this condition can be solved approximately an approximate discrete-time model can be derived. The approximate model can always be obtained as long as the Jacobian matrix exists for the continuous-time system and Peano-Baker series can be computed. As an example, the proposed method was applied to open-loop control of an inverted pendulum under high-frequency excitation. Simulations show that the proposed model gives good performances even for relatively large sampling intervals. It was also found that, for sufficient small sampling intervals, only a single term is needed in the Peano-Baker series computation. When a larger sampling interval is used, higher order Peano-Baker series can used to improve the performance of the proposed method.

Chapter 6

Improved nonlinear discrete-time models based on Riccati approximation of integration-gains

The discretization method presented in Chapter 3, which is based on linear approximation, is improved in this chapter by using a Riccati approximation of sufficient condition for discrete-time integration gain. The resulting model is shown to have a smaller norm of the approximation error than the one based on the linear approximation. Simulation results are presented for a Lotka-Volterra system to demonstrate that the improved model has better performances than the existing methods obtained by the forward-difference, Kahan's, and Mickens' models, as well as one in Chapter 3.

6.1 Proposed model

Let the autonomous nonlinear continuous-time system be given by the following differential equation:

$$\frac{d\bar{\mathbf{x}}(t)}{dt} = \bar{\mathbf{\Gamma}}\left(\bar{\mathbf{x}}(t)\right), \quad \bar{\mathbf{x}}(t_0) = \bar{\mathbf{x}}_0, \tag{6.1}$$

where t is the independent continuous-time variable, $\bar{\mathbf{x}} \in R^n$ the continuous-time state vector, and $\bar{\mathbf{x}}_0$ an arbitrary constant vector. Function $\bar{\mathbf{\Gamma}}: R^n \to R^n$ is assumed to be expandable into Taylor series, which assures to satisfy Lipschitz condition so that a unique solution exists for a given initial condition $\bar{\mathbf{x}}_0$. A system under digital control, whose input is a piece-wise constant input applied through the zero-order-hold, can be expressed in the form of system (6.1) for each interval $kT \le t < (k+1)T$.

In Chapter 3, the discrete-time model is based on the use of the discrete-time integration gain expressed in delta operator form as

$$\delta \mathbf{x}_k = \frac{\mathbf{x}_{k+1} - \mathbf{x}_k}{T} = \mathbf{G}\left(\mathbf{x}_k, T\right)\bar{\mathbf{\Gamma}}\left(\mathbf{x}_k\right), \quad \mathbf{x}_{k_0} = \bar{\mathbf{x}}_0. \tag{6.2}$$

Theorem 3.2 shows that the discrete-time system (6.2), is an exact model of a continuous-time system (6.1), if the discrete-time integration gain $\mathbf{G}$ in (6.2) is chosen to satisfy that

$$\dot{\mathbf{H}}\left(\bar{\mathbf{x}}^*\left(kT\right),t-kT\right)\bar{\mathbf{\Gamma}}\left(\bar{\mathbf{x}}^*\left(kT\right)\right)=\bar{\mathbf{\Gamma}}\left(\bar{\mathbf{x}}^*\left(kT\right)+\mathbf{H}\left(\bar{\mathbf{x}}^*\left(kT\right),t-kT\right)\bar{\mathbf{\Gamma}}\left(\bar{\mathbf{x}}^*\left(kT\right)\right)\right) \tag{6.3}$$

for each interval $kT \le t < (k+1)T$, where $\bar{\mathbf{x}}^*(t)$ is the continualization of discrete-time state $\mathbf{x}_k$ as Definition 2.3, and the continuous-time function $\mathbf{H}\left(\bar{\mathbf{x}}^*\left(kT\right),t-kT\right)$ is defined as

$$\mathbf{H}\left(\bar{\mathbf{x}}^*\left(kT\right),t-kT\right)=\left(t-kT\right)\mathbf{G}\left(\bar{\mathbf{x}}^*\left(kT\right),t-kT\right). \tag{6.4}$$

If the integration gain can be chosen to satisfy condition (6.3) exactly, the resulting discrete-time model will be exact. When this is difficult, it may be solved approximately. To this end, let the right-hand side of eq. (6.3) be expanded, by assumption, into Taylor's series, as

$$\bar{\mathbf{\Gamma}}\left(\bar{\mathbf{x}}^*\left(kT\right)+\mathbf{H}\left(\bar{\mathbf{x}}^*\left(kT\right),t-kT\right)\bar{\mathbf{\Gamma}}\left(\bar{\mathbf{x}}^*\left(kT\right)\right)\right)=\bar{\mathbf{\Gamma}}\left(\bar{\mathbf{x}}^*\left(kT\right)\right)+D\bar{\mathbf{\Gamma}}\left(\bar{\mathbf{x}}^*\left(kT\right)\right)\boldsymbol{\varphi}+\mathbf{e}_2, \tag{6.5}$$

where $D\bar{\mathbf{\Gamma}}(\mathbf{x})$ is Jacobian matrix of function $\bar{\mathbf{\Gamma}}(\mathbf{x}) \triangleq \left[\bar{\Gamma}_1,...,\bar{\Gamma}_n\right]^T$,

$$\boldsymbol{\varphi} \triangleq \left[\varphi_1 \quad \dots \quad \varphi_n\right]^T \triangleq \mathbf{H}\left(\bar{\mathbf{x}}^*\left(kT\right),t-kT\right)\bar{\mathbf{\Gamma}}\left(\bar{\mathbf{x}}^*\left(kT\right)\right), \tag{6.6}$$

and $\mathbf{e}_2$ represents the second and higher order terms of $\bar{\mathbf{x}}^*$. In the Chapter 3, a discrete-time model called former model was proposed based on the solution of the first-order approximation, where $\mathbf{e}_2$ is simply ignored, as:

$$\mathbf{G}\left(\mathbf{x}_k,T\right)=\frac{1}{T}\int_0^T e^{D\bar{\mathbf{\Gamma}}(\mathbf{x}_k)\tau}d\tau \tag{6.7}$$

Taylor's expansion of the right-hand side of eq. (6.3) can be written more explicitly as

$$\bar{\mathbf{\Gamma}}\left(\bar{\mathbf{x}}^*\left(kT\right)+\mathbf{H}\left(\bar{\mathbf{x}}^*\left(kT\right),t-kT\right)\bar{\mathbf{\Gamma}}\left(\bar{\mathbf{x}}^*\left(kT\right)\right)\right)=\bar{\mathbf{\Gamma}}\left(\bar{\mathbf{x}}^*\left(kT\right)\right)+D\bar{\mathbf{\Gamma}}\left(\bar{\mathbf{x}}^*\left(kT\right)\right)\boldsymbol{\varphi}+\boldsymbol{\chi}+\mathbf{e}_3, \tag{6.8}$$

where $\boldsymbol{\chi} \triangleq \left[\chi_1,...,\chi_n\right]^T$ is the second-order term, which can be written as

$$\chi_i \triangleq \frac{1}{2}\left(\sum_{j=1}^{n}\varphi_j\frac{\partial}{\partial\bar{x}_j^*}\right)^2\Gamma_i\left(\bar{\mathbf{x}}^*\left(kT\right)\right)=\frac{1}{2}\sum_{j,l=1}^{n}\frac{\partial^2\Gamma_i\left(\bar{\mathbf{x}}^*\left(kT\right)\right)}{\partial\bar{x}_j^*\partial\bar{x}_l^*}\varphi_j\varphi_l, \tag{6.9}$$

and $\mathbf{e}_3$ represents the third and higher-order terms. While the first-order term in the Taylor series expansion of a vector function of multiple-variables can be written in a simple matrix-vector form using Jacobian matrix, the second and higher-order terms are not, in general. The use of multi-index [36] alleviates this issue and is used in the following, where the second-order term is further broken into two parts and one is included in the gain-condition equation, while the other is ignored.

Let the coefficient $\partial^2\Gamma_i\left(\bar{\mathbf{x}}^*\right)/\left(\partial\bar{x}_j^*\partial\bar{x}_l^*\right)$ of $\varphi_j\varphi_l$ in eq. (6.9) be expanded into Maclaurin's series in $\bar{\mathbf{x}}^*$ as

$$\frac{\partial^2 \Gamma_i\left(\overline{\mathbf{x}}^*(kT)\right)}{\partial \overline{x}_j^* \partial \overline{x}_l^*} = \sum_{order(\upsilon)\geq 0} {}_{ijl}\mu_\upsilon \overline{\mathbf{x}}^{*\upsilon}, \tag{6.10}$$

where

$${}_{ijl}\mu_\upsilon \triangleq \frac{1}{\upsilon!}\partial^\upsilon \left(\frac{\partial^2 \Gamma_i\left(\overline{\mathbf{x}}^*(kT)\right)}{\partial \overline{x}_j^* \partial \overline{x}_l^*} \right)\Bigg|_{\overline{\mathbf{x}}^*=\mathbf{0}}, \tag{6.11}$$

and the multi-index υ is defined [36] such that

$$\begin{aligned}
&\upsilon \triangleq (\upsilon_1, \upsilon_2, ..., \upsilon_n),\ \upsilon_i \in \{0,1,2,...\} \\
&order(\upsilon) \triangleq \upsilon_1 + \upsilon_2 + ... + \upsilon_n \\
&\upsilon! \triangleq \upsilon_1!\upsilon_2! \cdots \upsilon_n! \\
&\overline{\mathbf{x}}^\upsilon \triangleq \overline{x}_1^{\upsilon_1} \overline{x}_2^{\upsilon_2} \cdots \overline{x}_n^{\upsilon_n} \\
&\partial^\upsilon \triangleq \frac{\partial^{order(\upsilon)}}{\partial_{x_1}^{\upsilon_1} \partial_{x_2}^{\upsilon_2} \cdots \partial_{x_n}^{\upsilon_n}}.
\end{aligned} \tag{6.12}$$

In eq. (6.10), $order(\upsilon) \geq 0$ implies that the summation is taken over all combination of the multi-index whose order is zero or positive.

Theorem 6.1: Vector $\boldsymbol{\chi}$ in eq. (6.8) can be expressed uniquely as

$$\boldsymbol{\chi} = \frac{1}{2}\boldsymbol{\varphi}\mathbf{b}^T\left(\overline{\mathbf{x}}^*\right)\boldsymbol{\varphi} + \boldsymbol{\theta}, \tag{6.13}$$

where $\mathbf{b}\left(\overline{\mathbf{x}}^*\right)$ is chosen such that

$$\mathbf{b}\left(\overline{\mathbf{x}}^*\right) \triangleq \left[b_1\left(\overline{\mathbf{x}}^*\right) \quad \cdots \quad b_n\left(\overline{\mathbf{x}}^*\right) \right]^T, \quad b_i\left(\overline{\mathbf{x}}^*\right) = \sum_{order(\upsilon)\geq 0} {}_i\lambda_\upsilon \overline{\mathbf{x}}^{*\upsilon}, \tag{6.14}$$

and coefficients ${}_i\lambda_\upsilon$ as

$$\begin{aligned}
&\text{(i)}\ \ sgn({}_i\lambda_\upsilon) = sgn({}_{jij}\mu_\upsilon) \\
&\text{(ii)}\ \ |{}_i\lambda_\upsilon| = \min\left(|{}_{jij}\mu_\upsilon|\right),\ \ j = 1,2,...,n.
\end{aligned} \tag{6.15}$$

Under eq. (6.15), eq. (6.13) satisfies

$$\|\boldsymbol{\theta}\| \leq \|\boldsymbol{\chi}\|, \tag{6.16}$$

where $\|\cdot\|$ is a polynomial norm [37]. □

Proof: While the second-order term $\boldsymbol{\chi}$ may be broken into portions in different ways, this is done in a particular way such that the coefficient ${}_i\lambda_\upsilon$ is uniquely determined in eq. (6.15), making vector $\mathbf{b}(\mathbf{x})$ unique. Thus, given the second-order term $\boldsymbol{\chi}$, $\boldsymbol{\theta}$ in eq. (6.13) is unique.

Defining $\boldsymbol{\theta} \triangleq [\theta_1 \quad \cdots \quad \theta_n]^T$, eq. (6.13) yields

$$\theta_i = \chi_i - \frac{1}{2}\varphi_i \mathbf{b}^T\left(\bar{\mathbf{x}}^*\right)\boldsymbol{\varphi} = \frac{1}{2}\sum_{j,l=1}^{n}\frac{\partial^2\Gamma_i\left(\bar{\mathbf{x}}^*\right)}{\partial\bar{x}_j^*\partial\bar{x}_l^*}\varphi_j\varphi_l - \frac{1}{2}\varphi_i\sum_{j=1}^{n}b_j\varphi_j$$

$$= \frac{1}{2}\sum_{j,l=1}^{n}\left(\sum_{order(\upsilon)\geq 0}{}_{ijl}\mu_\upsilon\bar{\mathbf{x}}^{*\upsilon}\right)\varphi_j\varphi_l - \frac{1}{2}\varphi_i\sum_{j=1}^{n}b_j\varphi_j$$

$$= \frac{1}{2}\sum_{j=1}^{n}\left(\sum_{order(\upsilon)\geq 0}{}_{iji}\mu_\upsilon\bar{\mathbf{x}}^{*\upsilon} - b_j\right)\varphi_i\varphi_j + \frac{1}{2}\sum_{\substack{j,l=1\\ j,l\neq i}}^{n}\left(\sum_{order(\upsilon)\geq 0}{}_{ijl}\mu_\upsilon\bar{\mathbf{x}}^{*\upsilon}\right)\varphi_j\varphi_l \tag{6.17}$$

$$= \frac{1}{2}\sum_{j=1}^{n}\left(\sum_{order(\upsilon)\geq 0}{}_{iji}\mu_\upsilon\bar{\mathbf{x}}^{*\upsilon} - \sum_{order(\upsilon)\geq 0}{}_{j}\lambda_\upsilon\bar{\mathbf{x}}^{*\upsilon}\right)\varphi_i\varphi_j + \frac{1}{2}\sum_{\substack{j,l=1\\ j,l\neq i}}^{n}\left(\sum_{order(\upsilon)\geq 0}{}_{ijl}\mu_\upsilon\bar{\mathbf{x}}^{*\upsilon}\right)\varphi_j\varphi_l$$

$$= \frac{1}{2}\sum_{j=1}^{n}\left(\sum_{order(\upsilon)\geq 0}\left({}_{iji}\mu_\upsilon - {}_{j}\lambda_\upsilon\right)\bar{\mathbf{x}}^{*\upsilon}\right)\varphi_i\varphi_j + \frac{1}{2}\sum_{\substack{j,l=1\\ j,l\neq i}}^{n}\left(\sum_{order(\upsilon)\geq 0}{}_{ijl}\mu_\upsilon\bar{\mathbf{x}}^{*\upsilon}\right)\varphi_j\varphi_l$$

Since $b_i\left(\bar{\mathbf{x}}^*\right)$ as defined in eq. (6.14)-(6.15) implies that

$$\left\|\sum_{order(\upsilon)\geq 0}\left({}_{iji}\mu_\upsilon - {}_{j}\lambda_\upsilon\right)\bar{\mathbf{x}}^{*\upsilon}\right\| \leq \left\|\sum_{order(\upsilon)\geq 0}{}_{iji}\mu_\upsilon\bar{\mathbf{x}}^{*\upsilon}\right\|, \tag{6.18}$$

eqs. (6.9), (6.10), and (6.17) yield

$$\|\theta_i\| \leq \|\chi_i\|,$$

$$\|\boldsymbol{\theta}\| = \sum_{i=1}^{n}\|\theta_i\| \leq \sum_{i=1}^{n}\|\chi_i\| = \|\boldsymbol{\chi}\|. \tag{6.19}$$

Example 1: Consider a model given by

$$\begin{cases}\dot{\bar{x}}_1 = f_1\left(\bar{x}_1,\bar{x}_2\right) = \bar{x}_1\left(1-2\bar{x}_1-3\bar{x}_2-4\bar{x}_1^2-5\bar{x}_1\bar{x}_2-6\bar{x}_2^2\right)\\ \dot{\bar{x}}_2 = f_2\left(\bar{x}_1,\bar{x}_2\right) = \bar{x}_2\left(6-5\bar{x}_1-4\bar{x}_2-3\bar{x}_1^2-2\bar{x}_1\bar{x}_2-\bar{x}_2^2\right),\end{cases} \tag{6.20}$$

for which $\boldsymbol{\chi}$ is found to be

$$\boldsymbol{\chi} = \begin{bmatrix}\chi_1\\ \chi_2\end{bmatrix} = \frac{1}{2}\begin{bmatrix}-\left(4+24\bar{x}_1^*+10\bar{x}_2^*\right)\varphi_1{}^2 - 2\left(3+10\bar{x}_1^*+12\bar{x}_2^*\right)\varphi_1\varphi_2 - 12\bar{x}_1^*\varphi_2{}^2\\ -6\bar{x}_2^*\varphi_1{}^2 - 2\left(5+6\bar{x}_1^*+4\bar{x}_2^*\right)\varphi_1\varphi_2 - \left(8+4\bar{x}_1^*+6\bar{x}_2^*\right)\varphi_2{}^2\end{bmatrix}. \tag{6.21}$$

In the present example, the coefficients of $\varphi_i\varphi_j$ are already in the power series in $\bar{\mathbf{x}}^*$, so that Maclausin's expansion is unnecessary, and give

$$\begin{Bmatrix} -\left(4+24\bar{x}_1^*+10\bar{x}_2^*\right)\varphi_1^{\,2} \\ -2\left(3+10\bar{x}_1^*+12\bar{x}_2^*\right)\varphi_1\varphi_2 \\ -12\bar{x}_1^*\varphi_2^{\,2} \\ -6\bar{x}_2^*\varphi_1^{\,2} \\ -2\left(5+6\bar{x}_1^*+4\bar{x}_2^*\right)\varphi_1\varphi_2 \\ -\left(8+4\bar{x}_1^*+6\bar{x}_2^*\right)\varphi_2^{\,2} \end{Bmatrix} \rightarrow \begin{Bmatrix} {}_{111}\mu_{(0.0)}=-4,\ {}_{111}\mu_{(1.0)}=-24,\ {}_{111}\mu_{(0.1)}=-10 \\ {}_{112}\mu_{(0.0)}=-6,\ {}_{112}\mu_{(1.0)}=-20,\ {}_{112}\mu_{(0.1)}=-24 \\ {}_{122}\mu_{(1.0)}=-12 \\ {}_{211}\mu_{(0,1)}=-6 \\ {}_{212}\mu_{(0.0)}=-10,\ {}_{212}\mu_{(1.0)}=-12,\ {}_{212}\mu_{(0.1)}=-8 \\ {}_{222}\mu_{(0.0)}=-8,\ {}_{222}\mu_{(1.0)}=-4,\ {}_{222}\mu_{(0.1)}=-6 \end{Bmatrix}. \tag{6.22}$$

Other terms ${}_{ijl}\mu_{\upsilon}$ that do not appear in eq. (6.22) are zero. An element $b_i\left(\bar{\mathbf{x}}^*\right)$ has the form of

$$b_i\left(\bar{\mathbf{x}}^*\right)={}_i\lambda_{(0,0)}+{}_i\lambda_{(1,0)}\bar{x}_1^*+{}_i\lambda_{(0,1)}\bar{x}_2^*, \tag{6.23}$$

where the coefficients ${}_i\lambda_{(j,l)}$ satisfies conditions (6.15). For example, ${}_1\lambda_{(0,0)}$ is chosen to be -4, since

$$\begin{aligned} &\operatorname{sgn}\left({}_1\lambda_{(0,0)}\right)=\operatorname{sgn}\left({}_{111}\mu_{(0.0)}\right)=\operatorname{sgn}\left({}_{212}\mu_{(0.0)}\right)=-1 \\ &\left|{}_1\lambda_{(0,0)}\right|=\min\left(\left|{}_{111}\mu_{(0.0)}\right|,\left|{}_{212}\mu_{(0.0)}\right|\right)=\min\left(4,10\right)=4. \end{aligned} \tag{6.24}$$

In this manner, $\mathbf{b}\left(\bar{\mathbf{x}}^*\right)$ is found uniquely to be

$$\mathbf{b}\left(\bar{\mathbf{x}}^*\right)=\begin{bmatrix} b_1 \\ b_2 \end{bmatrix}=\begin{bmatrix} -4-12\bar{x}_1^*-8\bar{x}_2^* \\ -6-4\bar{x}_1^*-6\bar{x}_2^* \end{bmatrix}. \tag{6.25}$$

Thus, the second-order term $\boldsymbol{\omega}$ expressed as in eq. (6.13) is given by

$$\boldsymbol{\chi}=\frac{1}{2}\begin{bmatrix} \varphi_1 \\ \varphi_2 \end{bmatrix}\begin{bmatrix} -4-12\bar{x}_1^*-8\bar{x}_2^* \\ -6-4\bar{x}_1^*-6\bar{x}_2^* \end{bmatrix}^T\begin{bmatrix} \varphi_1 \\ \varphi_2 \end{bmatrix}+\frac{1}{2}\begin{bmatrix} -\left(12\bar{x}_1^*+2\bar{x}_2^*\right)\varphi_1^{\,2}-\left(16\bar{x}_1^*+18\bar{x}_2^*\right)\varphi_1\varphi_2-12\bar{x}_1^*\varphi_2^{\,2} \\ -6\bar{x}_2^*\varphi_1^{\,2}-6\varphi_1\varphi_2-2\varphi_2^{\,2} \end{bmatrix}. \tag{6.26}$$

The polynomial norms of $\boldsymbol{\chi}$ and $\boldsymbol{\theta}$ are calculated to be 154 and 84, respectively.

The main point of Theorem 1 is to separate the second-order term into the quadratic part and the rest, and to include the former part in the computation of the discrete-time integration gain. The resulting gain equation is of the Riccati form for which exact discretization is known [38]. The fact that this yields a smaller norm in the approximation is shown in the following theorem:

Theorem 6.2: When the integration-gain is approximated as

$$\dot{\mathbf{H}}\left(\bar{\mathbf{x}}^*\left(kT\right),t-kT\right)\bar{\boldsymbol{\Gamma}}\left(\bar{\mathbf{x}}^*\left(kT\right)\right)=\bar{\boldsymbol{\Gamma}}\left(\bar{\mathbf{x}}^*\left(kT\right)\right)+D\bar{\boldsymbol{\Gamma}}\left(\bar{\mathbf{x}}^*\left(kT\right)\right)\boldsymbol{\varphi}+\frac{1}{2}\boldsymbol{\varphi}\mathbf{b}^T\left(\bar{\mathbf{x}}^*\left(kT\right)\right)\boldsymbol{\varphi}, \tag{6.27}$$

the polynomial norm [37] of the error term is smaller than that with the first-order Taylor approximation. □

Proof: The approximation error $\mathbf{e}$ of eq. (6.27) can be written as

$$\mathbf{e}=\boldsymbol{\theta}+\mathbf{e}_2. \tag{6.28}$$

Since the approximation error of the first-order Taylor approximation is

$$\mathbf{e}_2 = \boldsymbol{\chi} + \mathbf{e}_3, \tag{6.29}$$

and $\mathbf{e}_2$ contains the third-order or higher derivatives, while $\boldsymbol{\chi}$ and $\boldsymbol{\theta}$ only the second-order derivatives, the polynomial norms [37] satisfy

$$\begin{aligned} \|\mathbf{e}_1\| &= \|\mathbf{e}_2 + \boldsymbol{\chi}\| = \|\mathbf{e}_2\| + \|\boldsymbol{\omega}\| \\ \|\mathbf{e}\| &= \|\mathbf{e}_2 + \boldsymbol{\theta}\| = \|\mathbf{e}_2\| + \|\boldsymbol{\theta}\|. \end{aligned} \tag{6.30}$$

Using the result of Theorem 6.1, eq. (6.30) leads to

$$\|\mathbf{e}\| = \|\mathbf{e}_2\| + \|\boldsymbol{\theta}\| \le \|\mathbf{e}_2\| + \|\boldsymbol{\chi}\| = \|\mathbf{e}_1\|, \tag{6.31}$$

which proves the theorem.

When the integration-gain is obtained by solving eq. (6.27) exactly, a new discrete-time model is obtained as follows:

Theorem 6.3 (Proposed Model): A discrete-time system (6.2), with the integration-gain given by the following, is a discrete-time model of system (6.1):

$$\mathbf{G}(\mathbf{x}_k, T) = \mathbf{M}_{21}(\mathbf{x}_k, T)\left(\mathbf{I} - T\mathbf{M}_{11}(\mathbf{x}_k, T)\right)^{-1}, \tag{6.32}$$

where $\mathbf{M}_{ij}(\mathbf{x}, \tau)$ are $n \times n$ matrices and satisfy

$$\mathbf{M}(\mathbf{x}, \tau) \triangleq \begin{bmatrix} -\mathbf{M}_{11}(\mathbf{x}, \tau) & -\mathbf{M}_{12}(\mathbf{x}, \tau) \\ \mathbf{M}_{21}(\mathbf{x}, \tau) & \mathbf{M}_{22}(\mathbf{x}, \tau) \end{bmatrix} \triangleq \frac{e^{\mathbf{Q}(\mathbf{x})\tau} - \mathbf{I}}{\tau}, \tag{6.33}$$

$$\mathbf{Q}(\mathbf{x}) \triangleq \begin{bmatrix} \mathbf{0} & -\mathbf{C}(\mathbf{x}) \\ \mathbf{I} & D\bar{\boldsymbol{\Gamma}}(\mathbf{x}) \end{bmatrix} \tag{6.34}$$

$$\mathbf{C}(\mathbf{x}) \triangleq \frac{1}{2}\bar{\boldsymbol{\Gamma}}(\mathbf{x})\mathbf{b}^T(\mathbf{x}). \tag{6.35}$$

Proof: Noting the definition of $\boldsymbol{\varphi}$ as in eq. (6.6), eq. (6.27) can be written as

$$\begin{aligned} &\dot{\mathbf{H}}\left(\bar{\mathbf{x}}^*(kT), t - kT\right)\bar{\boldsymbol{\Gamma}}\left(\bar{\mathbf{x}}^*(kT)\right) \\ &= \bar{\boldsymbol{\Gamma}}\left(\bar{\mathbf{x}}^*(kT)\right) + D\bar{\boldsymbol{\Gamma}}\left(\bar{\mathbf{x}}^*(kT)\right)\mathbf{H}\left(\bar{\mathbf{x}}^*(kT), t - kT\right)\bar{\boldsymbol{\Gamma}}\left(\bar{\mathbf{x}}^*(kT)\right) \\ &\quad + \frac{1}{2}\mathbf{H}\left(\bar{\mathbf{x}}^*(kT), t - kT\right)\bar{\boldsymbol{\Gamma}}\left(\bar{\mathbf{x}}^*(kT)\right)\mathbf{b}^T\left(\bar{\mathbf{x}}_k^*\right)\mathbf{H}\left(\bar{\mathbf{x}}^*(kT), t - kT\right)\bar{\boldsymbol{\Gamma}}\left(\bar{\mathbf{x}}^*(kT)\right) \\ &= \bar{\boldsymbol{\Gamma}}\left(\bar{\mathbf{x}}^*(kT)\right) + D\bar{\boldsymbol{\Gamma}}\left(\bar{\mathbf{x}}^*(kT)\right)\mathbf{H}\left(\bar{\mathbf{x}}^*(kT), t - kT\right)\bar{\boldsymbol{\Gamma}}\left(\bar{\mathbf{x}}^*(kT)\right) \\ &\quad + \mathbf{H}\left(\bar{\mathbf{x}}^*(kT), t - kT\right)\mathbf{C}\left(\bar{\mathbf{x}}^*(kT)\right)\mathbf{H}\left(\bar{\mathbf{x}}^*(kT), t - kT\right)\bar{\boldsymbol{\Gamma}}\left(\bar{\mathbf{x}}^*(kT)\right). \end{aligned} \tag{6.36}$$

For this relationship to hold for arbitrary $\bar{\boldsymbol{\Gamma}}$, it suffices that

$$\begin{aligned} \dot{\mathbf{H}}\left(\bar{\mathbf{x}}^*(kT), t - kT\right) = \mathbf{I} &+ D\bar{\boldsymbol{\Gamma}}\left(\bar{\mathbf{x}}^*(kT)\right)\mathbf{H}\left(\bar{\mathbf{x}}^*(kT), t - kT\right) \\ &+ \mathbf{H}\left(\bar{\mathbf{x}}^*(kT), t - kT\right)\mathbf{C}\left(\bar{\mathbf{x}}^*(kT)\right)\mathbf{H}\left(\bar{\mathbf{x}}^*(kT), t - kT\right) \end{aligned} \tag{6.37}$$

is satisfied, which is a matrix Riccati equation. Noting that $\mathbf{H}\left(\bar{\mathbf{x}}^*\left(kT\right),t-kT\right)=0$ when $t=kT$, the solution of eq. (6.37) is given as [38]

$$\mathbf{H}\left(\bar{\mathbf{x}}^*\left(kT\right),t-kT\right)=\left(t-kT\right)\mathbf{M}_{21}\left(\bar{\mathbf{x}}^*\left(kT\right),t-kT\right)\left(\mathbf{I}-T\mathbf{M}_{11}\left(\bar{\mathbf{x}}^*\left(kT\right),t-kT\right)\right)^{-1}, \tag{6.38}$$

which leads to

$$\begin{aligned}\mathbf{G}\left(\bar{\mathbf{x}}^*\left(kT\right),t-kT\right)&=\frac{1}{\left(t-kT\right)}\mathbf{H}\left(\bar{\mathbf{x}}^*\left(kT\right),t-kT\right)\\&=\mathbf{M}_{21}\left(\bar{\mathbf{x}}^*\left(kT\right),t-kT\right)\left(\mathbf{I}-T\mathbf{M}_{11}\left(\bar{\mathbf{x}}^*\left(kT\right),t-kT\right)\right)^{-1}\end{aligned}. \tag{6.39}$$

Since [38],

$$\lim_{T\to 0}\frac{e^{\mathbf{Q}(\mathbf{x}_k)T}-\mathbf{I}}{T}=\mathbf{Q}\left(\mathbf{x}_k\right), \tag{6.40}$$

it follows that

$$\lim_{T\to 0}\mathbf{M}\left(\mathbf{x}_k,T\right)=\lim_{T\to 0}\frac{e^{\mathbf{Q}(\mathbf{x}_k)T}-\mathbf{I}}{T}=\mathbf{Q}\left(\mathbf{x}_k\right)=\begin{bmatrix}\mathbf{0} & -\mathbf{C}\left(\mathbf{x}_k\right)\\ \mathbf{I} & D\bar{\mathbf{\Gamma}}\left(\mathbf{x}_k\right)\end{bmatrix}. \tag{6.41}$$

Comparison of the above equation with eq. (6.33) yields

$$\lim_{T\to 0}\mathbf{M}_{11}\left(\mathbf{x}_k,T\right)=\mathbf{0},\quad \lim_{T\to 0}\mathbf{M}_{21}\left(\mathbf{x}_k,T\right)=\mathbf{I}, \tag{6.42}$$

which lead to

$$\lim_{T\to 0}\mathbf{G}(\mathbf{x}_k,T)=\lim_{T\to 0}\left[\mathbf{M}_{21}\left(\mathbf{x}_k,T\right)\left(\mathbf{I}-T\mathbf{M}_{11}\left(\mathbf{x}_k,T\right)\right)^{-1}\right]=\mathbf{I}. \tag{6.43}$$

The discrete-time system (6.2) satisfies Theory 3.1 and, in view of Definition 2.2, is a discrete-time model of continuous-time system (6.1).

Remark 6.1: For a scalar system, the term $\boldsymbol{\theta}$ in eq. (6.13) is zero, so that and the discrete-time model (6.2) will be based on the second-order Taylor expansion of eq. (6.3).

Remark 6.2: When the continuous-time system is given by a matrix Riccati differential equation, the terms $\mathbf{e}_3$ in eq. (6.8), and $\boldsymbol{\theta}$ in eq. (6.13) are zero. Therefore, the discrete-time model (6.2) with integration-gain given by eq. (6.32) will be an exact discrete-time model of the Riccati system [38].

Remark 6.3: The proposed model is equivalent to the former model when matrix $\mathbf{b}(\mathbf{x})$ in eq. (6.14) is forced to be a zero matrix.

6.2 Simulation results

Simulations are carried out to compare the proposed discrete-time model with the former model, the forward difference model, Kahan' model, and Mickens' model. The continuous-time system used for this purpose is the following Lotka-Volterra model [39]:

$$\begin{cases} \dot{\bar{x}}_1 = \bar{\Gamma}_1(\bar{x}_1, \bar{x}_2) = \bar{x}_1(r_1 - a_{11}\bar{x}_1 - a_{12}\bar{x}_2) \\ \dot{\bar{x}}_2 = \bar{\Gamma}_2(\bar{x}_1, \bar{x}_2) = \bar{x}_2(r_2 - a_{21}\bar{x}_1 - a_{22}\bar{x}_2) \end{cases}, \tag{6.44}$$

where $\bar{x}_1(t)$ and $\bar{x}_2(t)$ represent the numbers of individual in each specy at time t, r_i is the intrinsic growth-rate of the specy i, and a_{ij} are competition coefficients that indicates the extent to which the specy j affects the growth-rate of the specy i. The parameters used for simulations are $r_1 = 5$, $r_2 = 6$, $a_{11} = 1$, $a_{12} = 2$, $a_{21} = 3$, and $a_{22} = 4$, which makes the equilibrium points to be $E1 = (0,0)$, $E2 = (5,0)$, $E3 = (0,1.5)$, and $E4 = (-4,4.5)$. The initial condition is chosen to be $(\bar{x}_1(0), \bar{x}_2(0)) = (0.2, 0.4)$.

- Forward Difference Model [9]: For system (6.44), this model is given by

$$\begin{bmatrix} \delta x_{1,k} \\ \delta x_{2,k} \end{bmatrix} = \begin{bmatrix} x_{1,k}(r_1 - a_{11}x_{1,k} - a_{12}x_{2,k}) \\ x_{2,k}(r_2 - a_{21}x_{1,k} - a_{22}x_{2,k}) \end{bmatrix}; \tag{6.45}$$

  i.e., eq. (6.2) with $\mathbf{G} = \mathbf{I}$ for any T.

- Former Model [Chapter 3]: The model proposed in Chapter 3 is eq. (6.2), where $\boldsymbol{\Gamma}$ is as defined in eq. (6.7) with Jacobian matrix given by

$$D\bar{\boldsymbol{\Gamma}}(\mathbf{x}_k) = \begin{bmatrix} r_1 - 2r_1a_{11}x_{1,k} - r_1a_{12}x_{2,k} & -r_1a_{12}x_{1,k} \\ -r_2a_{21}x_{1,k} & r_2 - r_2a_{21}x_{1,k} - 2r_2a_{22}x_{2,k} \end{bmatrix}. \tag{6.46}$$

- Kahan Model [40]: This model is known to be accurate for Lotka-Volterra type systems, and is given by

$$\begin{cases} \delta x_{1,k} = r_1\left(\dfrac{x_{1,k} + x_{1,k+1}}{2}\right) - a_{11}x_{1,k}x_{1,k+1} - a_{12}\left(\dfrac{x_{1,k}x_{2,k+1} + x_{1,k+1}x_{2,k}}{2}\right) \\ \delta x_{2,k} = r_2\left(\dfrac{x_{2,k} + x_{2,k+1}}{2}\right) - a_{21}\left(\dfrac{x_{1,k}x_{2,k+1} + x_{1,k+1}x_{2,k}}{2}\right) - a_{22}x_{2,k}x_{2,k+1}, \end{cases} \tag{6.47}$$

  where $\bar{x}_1$, $\bar{x}_2$, $\bar{x}_1\bar{x}_2$, $\bar{x}_1^2$, and $\bar{x}_2^2$ in the continuous-time model are replaced, respectively, by $(x_{1,k} + x_{1,k+1})/2$, $(x_{2,k} + x_{2,k+1})/2$, $(x_{1,k}x_{2,k+1} + x_{1,k+1}x_{2,k})/2$, $x_{1,k}x_{1,k+1}$, and $x_{2,k}x_{2,k+1}$. Equation (6.47) can be expressed in the form of eq. (6.2) with the integration gain given by

$$\mathbf{G}(\mathbf{x}_k, T) = \left(\mathbf{I} - \frac{T}{2}D\bar{\boldsymbol{\Gamma}}(\mathbf{x}_k)\right)^{-1}, \tag{6.48}$$

  where $D\bar{\boldsymbol{\Gamma}}(\mathbf{x}_k)$ is given by eq. (6.46).

- Mickens Model [24]: This nonstandard discrete-time model is given by

$$\begin{cases} \dfrac{x_{1,k+1}-x_{1,k}}{\varphi_1} = r_1 x_{1,k} + a_{11} x_{1,k} x_{1,k+1} + a_{12} x_{1,k+1} x_{2,k} \\ \dfrac{x_{2,k+1}-x_{2,k}}{\varphi_2} = r_2 x_{2,k} + a_{21} x_{1,k} x_{2,k+1} + a_{12} x_{2,k} x_{2,k+1}, \end{cases} \tag{6.49}$$

where $\varphi_1 = \left(e^{r_1 T} - 1\right)/r_1$ and $\varphi_2 = \left(e^{r_2 T} - 1\right)/r_2$. This yields the discrete-time model eq. (6.2) with

$$\mathbf{G}\left(\mathbf{x}_k, T\right) = \begin{bmatrix} \dfrac{\varphi_1}{1-\varphi_1\left(a_{11}x_{1,k} + a_{12}x_{2,k}\right)} & 0 \\ 0 & \dfrac{\varphi_2}{1-\varphi_2\left(a_{21}x_{1,k} + a_{22}x_{2,k}\right)} \end{bmatrix}. \tag{6.50}$$

- Proposed Model: The second differentiation of functions f_1 and f_2 are given by

$$\frac{\partial^2 \bar{\Gamma}_1}{\partial \bar{x}_1^2} = -2r_1 a_{11}, \frac{\partial^2 \bar{\Gamma}_1}{\partial \bar{x}_1 \partial \bar{x}_2} = -r_1 a_{12}, \frac{\partial^2 \bar{\Gamma}_2}{\partial \bar{x}_2^2} = -2r_2 a_{22}, \frac{\partial^2 \bar{\Gamma}_2}{\partial \bar{x}_1 \partial \bar{x}_2} = -r_2 a_{21}. \tag{6.51}$$

Vector $\mathbf{b}$ that satisfies conditions (i) and (ii) in eq. (6.15) is determined uniquely as

$$\mathbf{b}^T = -2\left[\min\left(r_1 a_{11}, r_2 a_{21}\right), \min\left(r_1 a_{12}, r_2 a_{22}\right)\right]. \tag{6.52}$$

The proposed discrete-time model has the integration gain given by eq. (6.32) with $\mathbf{b}$ given by eq. (6.52).

Figs. 6.1 and 6.2 show the state-responses of the continuous-time system and (a) Mickens' model, (b) Kahan's model, (c) the former model, and (d) the proposed model for $T = 0.1s$ and $0.5s$ up to $t = 10s$. The widely-used forward difference model, although not shown here, has a decent performance for $T = 0.1s$ but starts to oscillate around the equilibrium $E2 = (0,5)$ for T larger than about $0.2s$. The response becomes chaotic at about $T = 0.28s$ and divergent for T larger than about $0.29s$. Mickens's model in (a) is less accurate than the forward difference model for $T = 0.1s$, but remains at least stable and converges to $E2$ for $T = 0.5s$. Kahan's model (b) is accurate for $T = 0.1s$, but converges to a different equilibrium $E4 = (-4, 4.5)$ for $T = 0.5s$. The response reaches $E2$ using $T = 0.486s$ but it changes suddenly to $E4$ using $T = 0.487s$. If the response diverges or computation stops, one would doubt the veracity of the obtained results. However, if the response converges to an erroneous equilibrium, it would be difficult to notice it. Therefore, such a change in the steady-state property can be detrimental in numerical investigations. As for both the former (c) and the proposed (d) models, the results are accurate for $T = 0.1s$, while the proposed model shows a better performance for $T = 0.5s$.

Figs. 6.3 and 6.4 show the state-responses of the same models for $T = 1.0s$ up to $t = 10s$. As in Figs. 6.1 and 6.2, Mickens' model has a large delay during the transient response without oscillation and converges to the correct equilibrium $E2$. Kahan's model yields an oscillatory response and

converges to a different equilibrium $E4$. The former and the proposed models have overshoots but converge to the correct equilibrium $E2$.

Figs. 6.5 and 6.6 are the same as Figs. 6.3 and 6.4 but for $T = 2.0s$ (note the different scales for the time axes). Mickens' model converges to the correct equilibrium $E2$ after about $16s$, while Kahan's model takes a larger time to reach the steady-state, which is $E4$. The former model seems to diverge during the transient stage, but actually settles in about $80s$, to $E4$. The proposed model yields the transient response that becomes slower as the sampling period increases, but without becoming too oscillatory. In fact, the response remains convergent to the correct equilibrium $E2$ at least up to $T = 50s$.

Table 6.1 shows the actual computation times elapsed in running the ten seconds of Simulink simulations on a desktop PC as measured by Matlab's cputime command using T = 0.01s. Relatively speaking, the proposed model can take up to about 16% more CPU time than the other models compared.

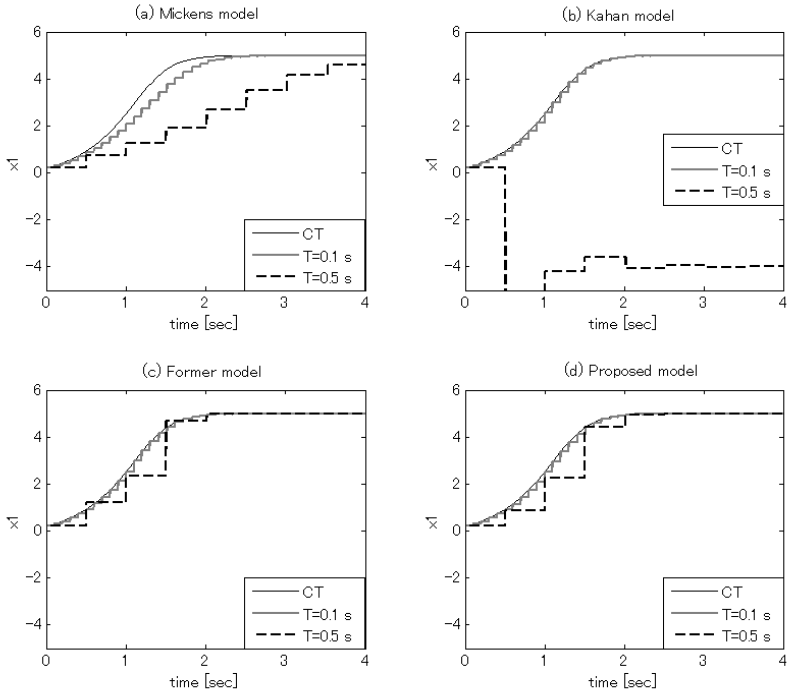

Fig. 6.1: State response x_1 of continuous-time, Mickens, Kahan, former and proposed models for $T = 0.1s$ and $T = 0.5s$

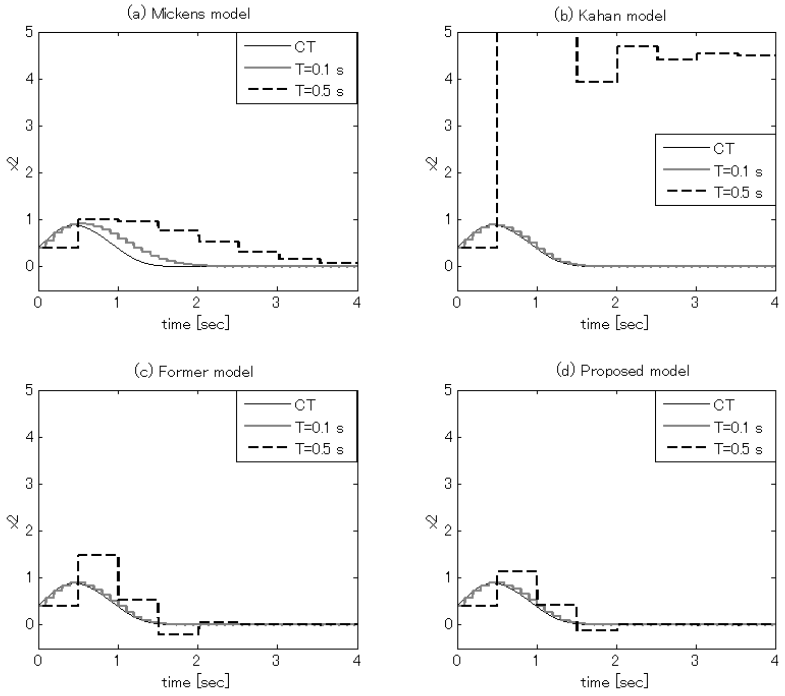

Fig. 6.2: State response x_2 of continuous-time, Mickens, Kahan, former and proposed models for $T = 0.1s$ and $T = 0.5s$

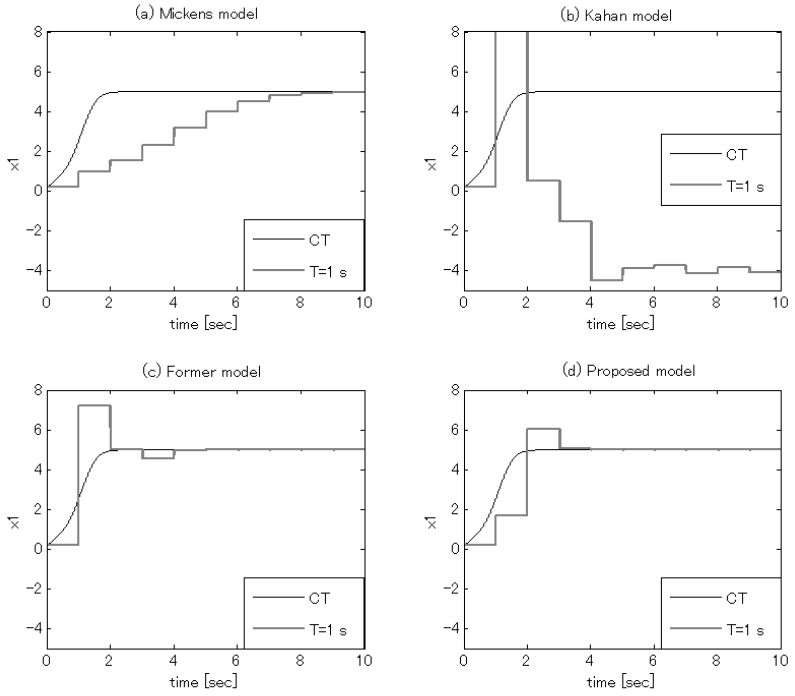

Fig. 6.3: State response x_1 of continuous-time, Mickens, Kahan, former and proposed models for $T = 1.0s$

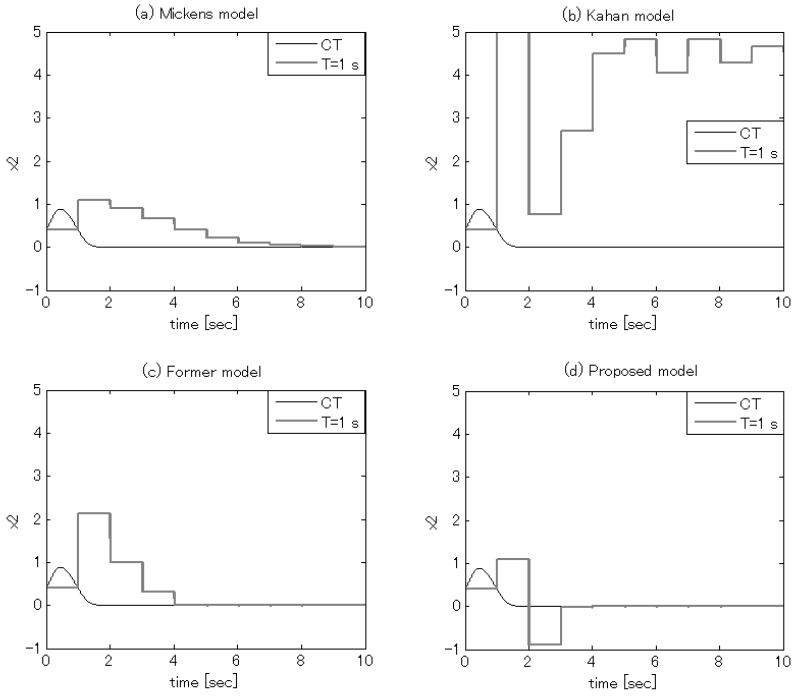

Fig. 6.4: State response x_2 of continuous-time, Mickens, Kahan, former and proposed models for $T = 1.0s$

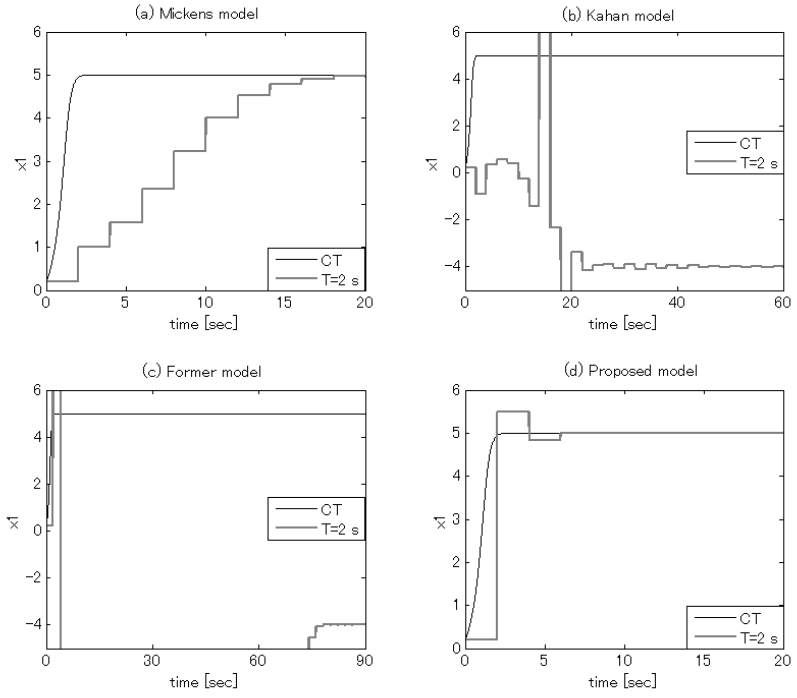

Fig. 6.5: State response x_1 of continuous-time, Mickens, Kahan, former and proposed models for $T = 2.0s$

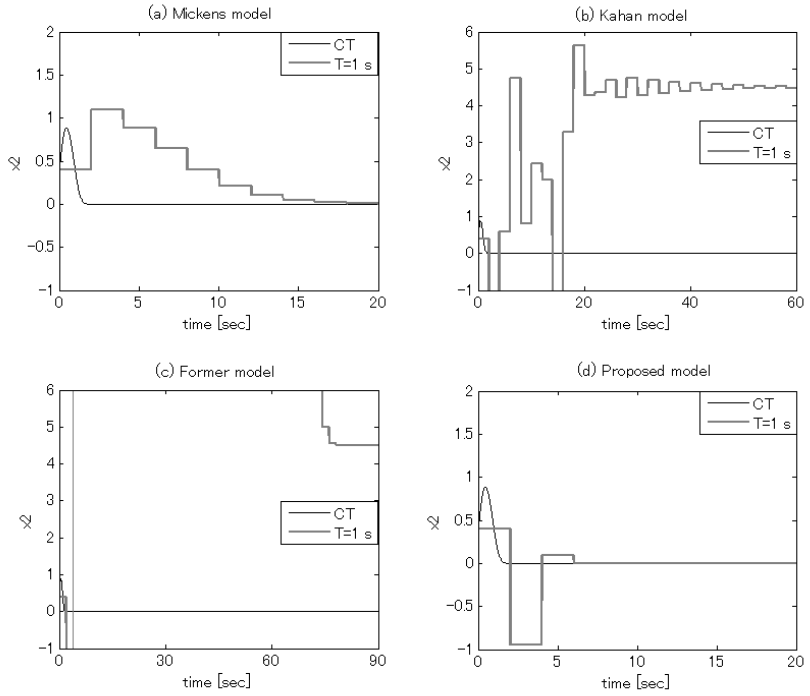

Fig. 6.6: State response x_2 of continuous-time, Mickens, Kahan, former and proposed models for $T = 2.0s$

Table 6.1: Duration of computation time

For. Diff. Model	Mickens Model	Kahan Model	Former Model	Proposed Model
0.7956 s	0.7956 s	0.7956 s	0.8892 s	0.9204 s

6.3 Summary

A discretization method has been proposed for nonautonomous nonlinear systems, where the resulting discrete-time model is expressed as the product of the integration-gain and the sampled version of the system function of the original continuous-time system. An equation for the integration-gain, which makes the discrete-time model exact when solved exactly, has been approximated as a Riccati differential equation, which can be discretized exactly. The proposed method has been shown to have a smaller error norm than the model proposed previously in Chapter 3, where the gain is approximated as the linear differential equation. As an example, a Lotka-Volterra model is considered and its state responses simulated to show a superior performance of the proposed model over the forward-difference, Kahan's, Mickens', and the former models, in terms of closer transient and steady-state responses to the continuous-time originals.

Chapter 7

A new discrete-time feedback control for scalar nonlinear systems

A new discrete-time feedback control is proposed for scalar nonlinear systems with constant parameters. The method uses the discretization method proposed in Chapter 3, where the so-called discrete-time integration gain is discretized such that the resulting model is approximate for nonlinear systems but exact for linear cases. It is shown that the proposed control law preserves the asymptotic stability of the desired discrete-time system at sampling instants, while the popular forward difference and accurate Mickens methods do not, in general. As an example, the proposed control law is applied for discrete-time feedback linearization of a scalar Riccati system. Simulation results demonstrate that the proposed method has better accuracy and tends to retain the desired dynamics for larger sampling intervals, than the other two methods.

7.1 Discrete-time feedback control

Consider a scalar nonlinear system with constant parameters given by

$$\dot{\bar{x}}(t) = f\left(\bar{x}(t)\right) + c\bar{u}_T(t) \tag{7.1}$$

where $c \neq 0$ and $\bar{u}_T(t)$ is a piece-wise constant input that is generated by applying a discrete-time sequence u_k with period T to the zero-order-hold (ZOH) synchronized with period T. This implies that

$$\bar{u}_T(t) = \bar{u}_T(kT), \quad \text{for } kT \le t < (k+1)T. \tag{7.2}$$

System (7.1) under input (7.2) can be considered as an autonomous system, since this input is constant between two successive sampling instants. However, while the continuous-time nonlinear system (7.1) may be linearized exactly by an exact-linearizing continuous-time feedback control, this is not possible in discrete-time form, since the exact discrete-time model of system (7.2) is generally non-affine in the input and, thus, the exact-linearizing discrete-time feedback control law cannot be derived. The three discrete-time models that are known to the authors as affine, but approximate, are the forward difference model, Mickens' model, and the one proposed in Chapter 3. Using this third discretization method, the affine discrete-time model of (7.1) is obtained as

$$\delta x_k = G(x_k, T)\left(f(x_k) + cu_k \right), \tag{7.3}$$

where

$$G(x_k, T) = \frac{1}{T}\int_0^T e^{\left[Df(x_k)\right]\tau} d\tau . \tag{7.4}$$

Let us assume that system (7.1) is to be controlled such that it behaves as if it were a desired system, which is given by

$$\dot{\bar{w}}(t) = h\left(\bar{w}(t), \bar{r}(t)\right) \tag{7.5}$$

where h is, in general, a nonlinear function of state $\bar{w}(t)$ and the reference input $\bar{r}(t)$. Its discrete-time model is derived by the proposed discretization method in Chapter 3 as

$$\delta \bar{w}_k = G_d \cdot h\left(\bar{w}_k, \bar{r}_k\right) \tag{7.6}$$

where

$$G_d = \frac{1}{T}\int_0^T e^{\left[Dh(w_k)\right]\tau} d\tau , \tag{7.7}$$

and $Dh(w_k)$ is Jacobian matrix of the system function $h(w_k)$.

The control law for system (7.1) is derived by equating the proposed discrete-time model (7.3) and the discrete-time model of the desired closed-loop system (7.6), and is obtained as

$$\bar{u}_T(t) = c^{-1}\left[G(\bar{x}_k, T)\right]^{-1} G_d \cdot h(\bar{x}_k, \bar{r}_k) - c^{-1} f(\bar{x}_k) \tag{7.8}$$

for each fixed k such that $kT \le t < (k+1)T$, and $\bar{x}_k = \bar{x}(kT)$. The schematic diagram of this controller is given in Fig. 7.1.

Theorem 7.1: When a piece-wise constant input generated by equation (7.8) is applied to continuous-time system (7.1), the asymptotic stability (instability) of the linearized discrete-time model of the resulting closed-loop system is equivalent to the asymptotic stability (instability) of the desired discrete-time system (7.5).

Proof: With the continuous-time input Eq. (7.8), the closed-loop system (7.1) can be written for $kT \le t < (k+1)T$ as

$$\dot{\bar{x}}(t) = f\left(\bar{x}(t)\right) + \left(\left[G(\bar{x}_k, T)\right]^{-1} G_d h(\bar{x}_k, \bar{r}_k) - f(\bar{x}_k)\right). \tag{7.9}$$

Expanding $f\left(\bar{x}(t)\right)$ in Eq. (7.9) into the Taylor series around $\bar{x}_k$, and keeping the first-derivative terms only, a linear approximation is obtained. Using $\bar{x}(t)$ for the state of this linearized system, this is written, for $kT \le t < (k+1)T$, as

$$\begin{aligned}\dot{\bar{x}}(t) &= f(\bar{x}_k) + Df(\bar{x}_k)\left(\bar{x}(t) - \bar{x}_k\right) + \left(\left[G(\bar{x}_k, T)\right]^{-1} G_d h(\bar{x}_k, \bar{r}_k) - f(\bar{x}_k)\right) \\ &= Df(\bar{x}_k)\bar{x}(t) + \mu\end{aligned} \tag{7.10}$$

where μ is a constant defined by

$$\mu = \left[G(\bar{x}_k, T)\right]^{-1} G_d h(\bar{x}_k, \bar{r}_k) - Df(\bar{x}_k)\bar{x}_k . \tag{7.11}$$

The analytical solution of linear differential equation (7.10) within $kT \le t < (k+1)T$ is known as

$$\bar{x}(t) = e^{\left[Df(\bar{x}_k)\right](t-kT)}\left(\bar{x}_k + \mu \int_{kT}^{t} e^{-\left[Df(\bar{x}_k)\right](\tau - kT)} d\tau\right). \tag{7.12}$$

This gives, for $t = (k+1)T$,

$$\begin{aligned}\bar{x}_{k+1} &= e^{\left[Df(\bar{x}_k)\right]T} x_k + \mu \int_0^T e^{\left[Df(\bar{x}_k)\right]\tau} d\tau \\ &= e^{\left[Df(\bar{x}_k)\right]T} \bar{x}_k + \left[G(\bar{x}_k, T)\right]^{-1} G_d h(\bar{x}_k, \bar{r}_k) \int_0^T e^{\left[Df(\bar{x}_k)\right]\tau} d\tau - Df(\bar{x}_k)\bar{x}_k \int_0^T e^{\left[Df(\bar{x}_k)\right]\tau} d\tau \\ &= e^{\left[Df(\bar{x}_k)\right]T} \bar{x}_k + \left[\frac{1}{T}\int_o^T e^{\left[Df(\bar{x}_k)\right]\tau} d\tau\right]^{-1} G_d h(\bar{x}_k, \bar{r}_k) \int_0^T e^{\left[Df(\bar{x}_k)\right]\tau} d\tau - Df(\bar{x}_k)\bar{x}_k \int_0^T e^{\left[Df(\bar{x}_k)\right]\tau} d\tau \\ &= TG_d h(\bar{x}_k, \bar{r}_k) + \left(e^{\left[Df(\bar{x}_k)\right]T} - Df(\bar{x}_k) \int_0^T e^{\left[Df(\bar{x}_k)\right]\tau} d\tau\right)\bar{x}_k \\ &= TG_d h(\bar{x}_k, \bar{r}_k) + \bar{x}_k ,\end{aligned} \tag{7.13}$$

which yields

$$\delta \bar{x}_k = G_d h(\bar{x}_k, \bar{r}_k), \tag{7.14}$$

thus proving Theorem 7.1.

Remark 7.1: Theorem 7.1 only shows that the linearized discrete-time model of closed-loop (7.1) under the proposed feedback control law of (7.8) is identical to the desired discrete-time system (7.6).

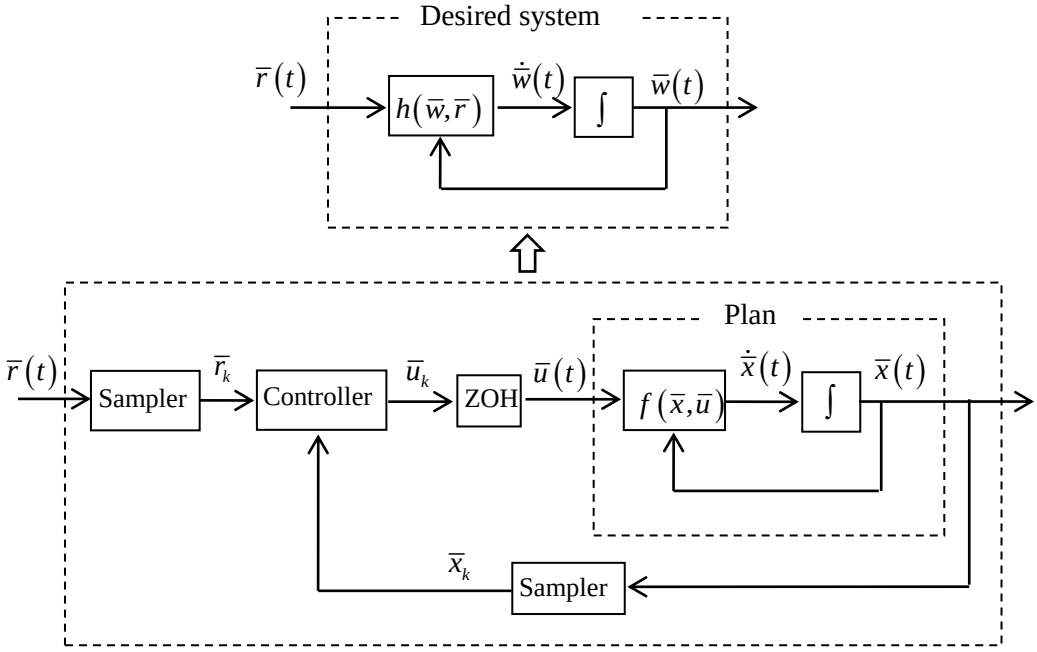

Fig. 7.1: Structure of discrete-time feedback controller

7.2 Discrete-time linearization feedback for Riccati System

To highlight the process of applying the discretization scheme described in the previous section to a nonlinear system, and as a first step towards its extension to a more practical system, a Riccati system with constant parameters is considered in this section. Riccati differential equations form an important class of mathematical models, which are used in such areas as mathematics [41], physics [42], and engineering [43]. To this end, let the Riccati system be given by

$$\dot{\bar{x}}(t) = f\left(\bar{x}(t)\right) + c\bar{u}_T(t) = a\bar{x}^2(t) + b\bar{x}(t) + c\bar{u}_T(t), \tag{7.15}$$

where $c \neq 0$ and $\bar{u}_T(t)$ is a piece-wise constant input. The proposed discrete-time model is given by

$$\delta x_k = \left[G(x_k, T)\right]\left(ax_k^2 + bx_k + cu_k\right), \tag{7.16}$$

where

$$Df(x_k) = 2ax_k + b. \tag{7.17}$$

Let us assume that the Riccati system (7.15) is to be controlled such that it behaves as if it were a linear system, which is given by

$$\dot{\bar{w}}(t) = h\left(\bar{w}(t), \bar{r}(t)\right) = \alpha\bar{w}(t) + \beta\bar{r}(t) \tag{7.18}$$

where α, β are non-zero constant parameters. The exact discrete-time model of the desired linear

system is given [9] by

$$\delta w_k = G_d\left(\alpha w_k + \beta \bar{r}_k\right) \tag{7.19}$$

where

$$G_d = \frac{e^{\alpha T} - 1}{\alpha T}. \tag{7.20}$$

Using the proposed control law (7.8), input $\bar{u}_k$ is given as

$$\bar{u}_k = \frac{1}{c}\left(\left[G\left(\bar{x}_k, T\right)\right]^{-1} G_d\left(\alpha \bar{x}_k + \beta \bar{r}_k\right) - a\bar{x}_k^2 - b\bar{x}_k\right), \tag{7.21}$$

which is applied to the continuous-time system through a ZOH.

Remark 7.2: If the forward difference method is used, the discrete-time model for system (7.1) and the corresponding discrete-time feedback control law are given by

$$\delta x_k = f\left(x_k, u_k\right) = ax_k^2 + bx_k + cu_k, \tag{7.22}$$

$$\bar{u}_k = \frac{1}{c}\left(G_d\left(\alpha \bar{x}_k + \beta \bar{r}_k\right) - a\bar{x}_k^2 - b\bar{x}_k\right). \tag{7.23}$$

The approximate solution of the resulting closed-loop system is

$$\bar{x}_{k+1} = \left[\int_0^T e^{\left[2a\bar{x}_k + b\right]\tau} d\tau\right] \Gamma_D\left(\alpha \bar{x}_k + \beta \bar{r}_k\right) + \bar{x}_k. \tag{7.24}$$

Remark 7.3: The semi-explicit discrete-time model and the corresponding feedback control law using the nonstandard finite difference scheme of Mickens [4] are given as

$$\delta x_k = \frac{\varphi}{T}\left(ax_k x_{k+1} + bx_k + cu_k\right), \tag{7.25}$$

$$\bar{u}_k = \frac{1}{\varphi c}\left[\left(1 - \varphi a\bar{x}_k\right)\left(\bar{x}_k + TG_d\left(\alpha \bar{x}_k + \beta \bar{r}_k\right)\right) - \left(1 + \varphi b\right)\bar{x}_k\right] \tag{7.26}$$

where $\varphi = 1 - e^{-T}$. The corresponding approximate solution of the closed-loop is obtained as

$$\bar{x}_{k+1} = \left[\int_0^T e^{\left[2a\bar{x}_k + b\right]\tau} d\tau\right]\left(\bar{u}_k + a\bar{x}_k^2 + b\bar{x}_k\right) + \bar{x}_k. \tag{7.27}$$

Theorem 7.1 does not hold using the forward-difference and Mickens' models.

7.3 Simulation results

Simulations have been carried out to assess performances of the digital controllers designed using the forward difference, Mickens, and the proposed discretization method, as compared with the behavior of the continuous-time closed-loop system. System parameters were chosen as $a = 2, b = -1, c = 1$, and the initial condition as $\bar{x}_0 = 1$. The desired closed-loop behavior was that of a

linear system (7.5) with $\alpha = -2$, $\beta = 3$, and the reference input $\bar{r}(t)$ was the unit step signal.

From Fig. 7.2 to Fig. 7.5, the responses are shown for the sampling interval of 0.2, 0.4, 0.6 and 1.0 seconds, respectively. At 0.2 seconds, all the methods give responses that are more or less similar to those of the desired behavior, although the proposed method gives the closest result (Fig. 7.2). When the sampling interval is increased to 0.4 seconds (Fig. 7.3), Mickens and forward difference methods deviate from the continuous-time response further, while the proposed method still yields a response close to the desired behavior. When the sampling interval is set at 0.6 second (Fig. 7.4), the response of the forward difference method shows chaotic behavior and that of Mickens method converges to a steady state, which differs from the desired behavior. In contrast, the response of the proposed method still shows a good performance. When the sampling interval is further increased to 1.0 second (Fig. 7.5), both the forward difference and Mickens methods become numerically unstable. However, the proposed method yields the result where the state reaches the correct steady value, although there is a large overshoot during the transient.

By the way, the common approach taken to deal with nonlinear systems is to linearize it around an intended equilibrium point and design a control law using the resulting linear model. This approach falls short of following comparison.

Linearization of system (7.15) around an equilibrium point $\bar{x}_e$ is given by

$$\dot{\bar{x}}(t) = (2a\bar{x}_e + b)\bar{x}(t) + c\bar{u}_T(t). \tag{7.28}$$

The discrete-time feedback control law for nonlinear system (7.15) based on the exact discrete-time model of the linear system (7.28) is obtained [9] as

$$u_k = \frac{1}{c}\left(\Gamma_e^{-1}\Gamma_d(\alpha x_k + \beta \bar{r}_k) - (2a\bar{x}_e + b)x_k\right), \tag{7.29}$$

where Γ_e is the discrete-time integrator gain of system (7.28) as given by

$$\Gamma_e = \frac{e^{(2a\bar{x}_e + b)T} - 1}{(2a\bar{x}_e + b)T}. \tag{7.30}$$

An important issue here is how one should choose the equilibrium point around which the control system is to be designed; should it be one of the open-loop system or the closed-loop system? When system (7.15) is linearized around the open-loop equilibrium points of $\bar{x}_e = 0$ and $\bar{x}_e = 0.5$, simulation studies revealed that the closed-loop systems with feedback control law of (7.29) are numerically unstable, even for a small sampling interval of $T = 0.01$ second.

When the linearization of system (7.15) is taken around the equilibrium point of desired linear system (7.5) at $\bar{x}_e = 1.5$, the response of the closed-loop system with feedback control law (7.29) becomes stable. However, the state converges to a value that differs from the desired steady-state behavior, as seen in Fig. 7.6.

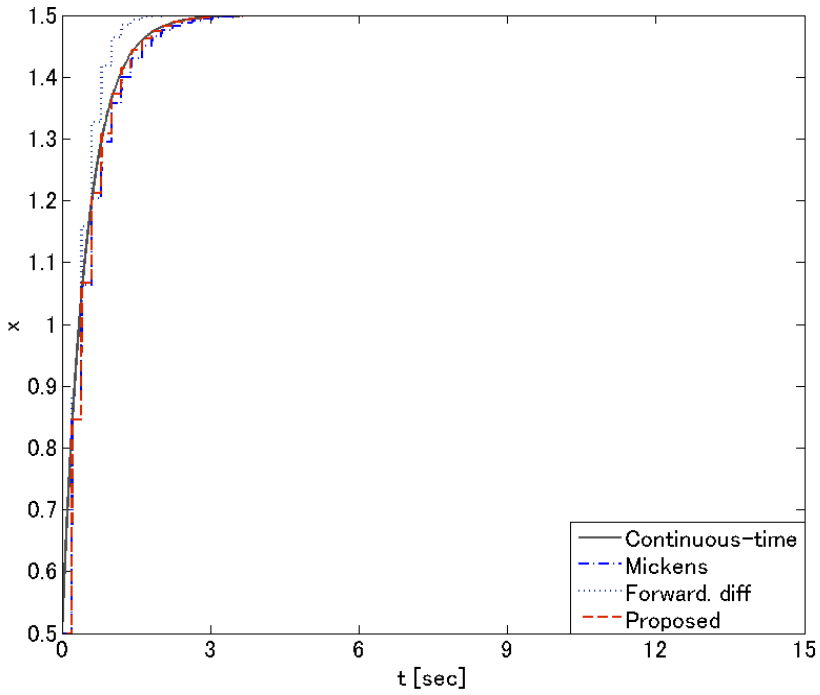

Fig. 7.2: Responses of the desired closed-loop, forward difference, Mickens', and proposed methods for $T = 0.2$ seconds

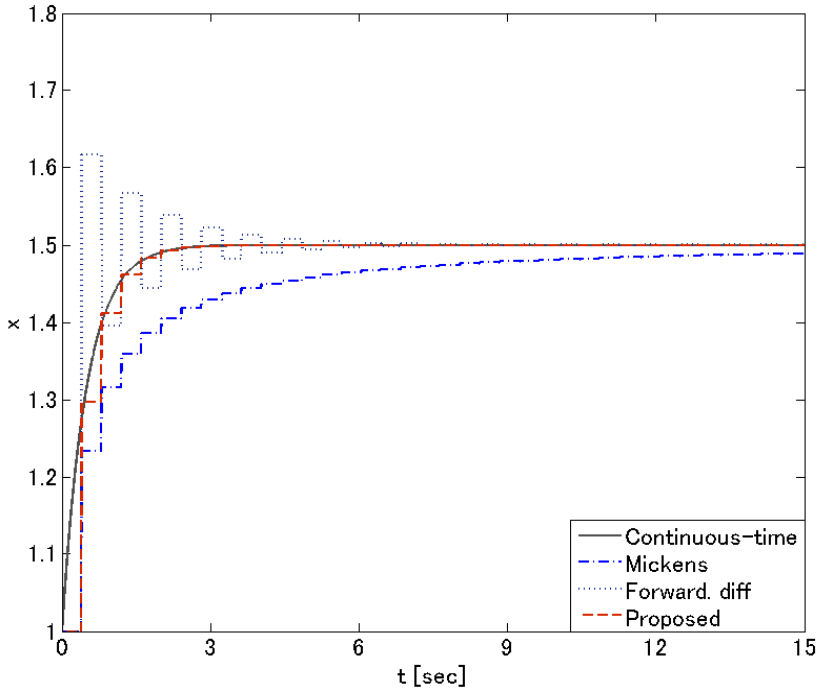

Fig. 7.3: Responses of the desired closed-loop, forward difference, Mickens', and proposed methods for $T = 0.4$ seconds

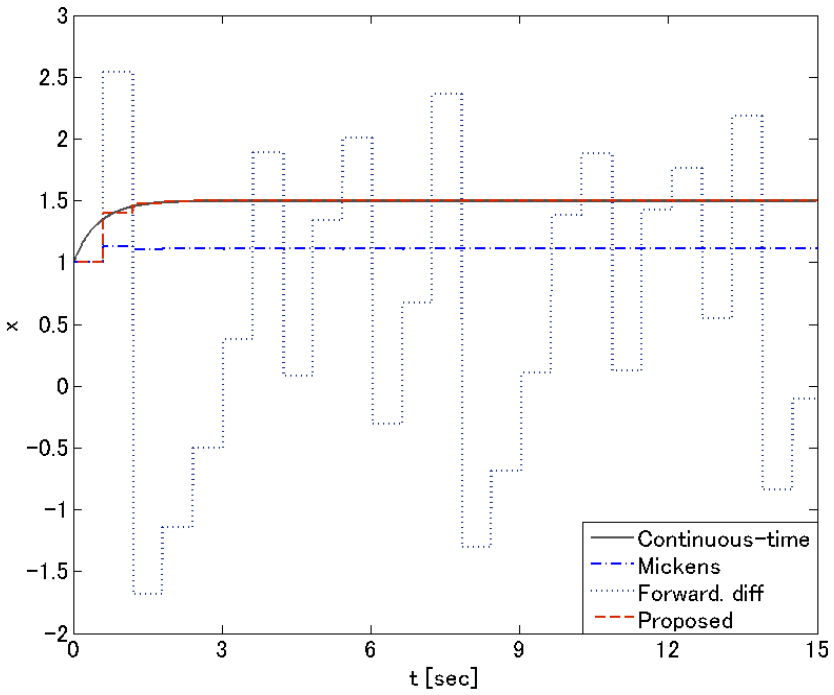

Fig. 7.4: Responses of the desired closed-loop, forward difference, Mickens', and proposed methods for $T = 0.6$ seconds

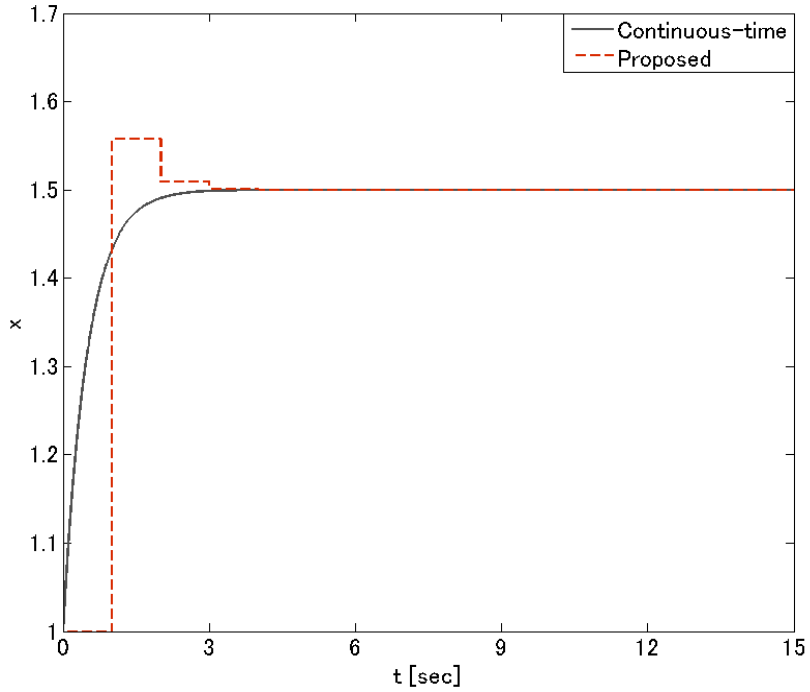

Fig. 7.5: Responses of the desired closed-loop and proposed methods for $T = 1$ second

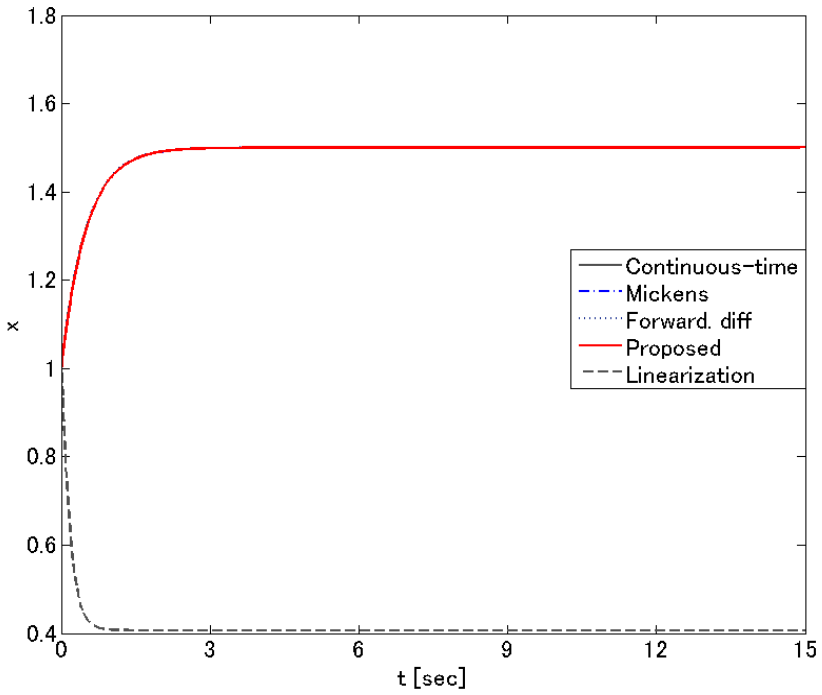

Fig. 7.6: Responses of the desired closed-loop, forward difference, Mickens', proposed and linearization-based methods for T=0.01 second

7.4 Summary

A discretization method proposed in Chapter 3 for autonomous nonlinear systems was used for designing a discrete-time feedback control law. The discrete-time model is affine in the input when the continuous-time model is, which is convenient for controller designs. The control law was show to retain the discrete-time asymptotic stability (instability) of the desired model for any sampling interval. Simulations were carried out for a nonlinear system whose dynamics are governed by Riccati differential equations. They showed that the proposed method produced state responses that were closer to the desired behavior than the forward difference and Mickens method at all sampling periods tested.

Chapter 8

Conclusions

Digital computations inevitably involve conversions of a continuous-time system into an equivalent discrete-time system, on which a large number of researchers have worked, mostly from a discretization point of view. Such a view paid off in filling a gap between discrete-time and continuous-time domains for linear systems. However, one for nonlinear systems is still lacking, especially for on-line computable algorithms. The present thesis has proposed an approach that is opposite to the conventional ones in the sense that the problem is looked at from a continuous-time point of view. This is the continualization technique explained in Chapter 2 and used in all the subsequent chapters. By looking at the problem as that of bridging the two time domains, their gap can be narrowed and the construction of the bridge can be managed more efficiently (Fig. 8.1). The key is the derivation of the condition for the discrete-time model to be exact, which made the shortest (but may be steepest) path to stand out. In addition, and perhaps more importantly, this sheds light into how approximate solutions can be obtained, as longer (but usually easier) paths.

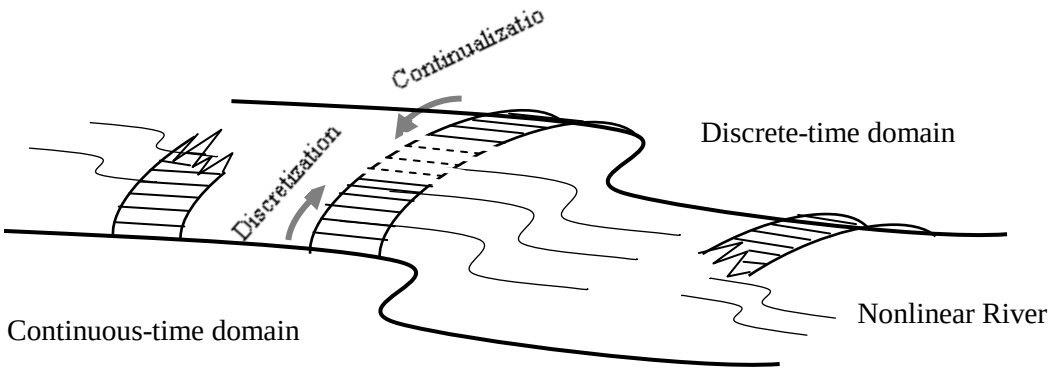

Fig. 8.1: Bridging the continuous-time and discrete-time domains for nonlinear system

Important techniques used in the thesis are, the use of the delta operator and the clarification of the definition of exact and general discretization, which together light up the roles of a discrete-time integration gain, and the concept of continualization. Chapter 3 treated the nonlinear autonomous case, Chapter 4 considered a class of non-autonomous systems, and Chapter 5 dealt with its generalization to a wider class of non-autonomous systems. Chapter 6 took the solution of the condition equation for autonomous case more seriously, using the Riccati approximation. Chapter 7 illustrates how these models could be used for the design of a control system.

Although the proposed models are developed based on the first order Taylor approximation of the sufficient condition derived in Chapters 3 and 5, the form of the discrete-time model is non-linear. This is different from the linearization of a nonlinear system itself based on Taylor approximation. The model explained in Chapter 3 (for autonomous systems) and in Chapter 5 (for non-autonomous systems) corresponds to one with the first two terms in the series expansion in a differential equation concerning continualized system, and can always be found as long as the expansion exists, whereas the well-known forward difference model corresponds to one with the first term only.

In all these chapters, simulations showed that the proposed models out-performed the existing methods in almost all cases. However, evaluation and comparisons of proposed method with the others needs to be carried out via real engineering examples for better test and examine the obtained theory. Analysis for the effect of sampling interval on properties of discrete-time model such as accuracy and numerical stability should be investigated further. The issues of how to apply the proposed discretization techniques in digital controller design methodology, and practical control engineers are important scopes for our future research.

References

[1] T. T. Hartley, Beale, G.O., Chicatelli, S.P., *Digital simulation of dynamic systems – a control theory approach*. New York: Prentice-Hall, Englewood Cliffs, 1994.

[2] R. Hirota, *Lectures on Difference Equations—From Continuous to Discrete Domains*. Tokyo: Science Publishing, 2000.

[3] J. D. Lambert, *Computational methods in ordinary differential equations*. London, New York,: Wiley, 1973.

[4] R. E. Mickens, *Nonstandard finite difference models of differential equations*. Singapore: World Scientific, 1994.

[5] D. Nesic and A. R. Teel, "Sampled-data control of nonlinear systems: An overview of recent results," *Perspectives in Robust Control,* vol. 268, pp. 221-239, 2001.

[6] J. J. E. Slotine, Li, W., *Applied nonlinear control*. New York: Prentice-Hall, Englewood Cliffs, 1991.

[7] J. Yuz, Goodwin, Graham C., *Sampled-Data Models for Linear and Nonlinear Systems*. Heidelberg: Springer, 2014.

[8] N. Hori, T. Mori, and P. N. Nikiforuk, "A New Perspective for Discrete-Time Models of a Continuous-Time System," *Ieee Transactions on Automatic Control,* vol. 37, pp. 1013-1017, Jul 1992.

[9] R. H. Middleton, Goodwin, G.C., *Digital control and estimation – a unified approach*. New York: Prentice-Hall, Englewood Cliffs, 1990.

[10] D. Nesic and A. R. Teel, "A framework for stabilization of nonlinear sampled-data systems based on their approximate discrete-time models," *Ieee Transactions on Automatic Control,* vol. 49, pp. 1103-1122, Jul 2004.

[11] N. Hori, C. A. Rabbath, and P. N. Nikiforuk, "Exact discretisation of a scalar differential Riccati equation with constant parameters," *Iet Control Theory and Applications,* vol. 1, pp. 1219-1223, Sep 2007.

[12] T. Nguyen-Van and N. Hori, "A new discrete-time model for a van del Pol Oscillator," in *SICE Annual Conference 2010, Proceedings of*, 2010, pp. 2699-2704.

[13] T. Nguyen-Van and N. Hori, "Discretization of Nonautonomous Nonlinear Systems Based on Continualization of an Exact Discrete-Time Model," *Journal of Dynamic Systems, Measurement, and Control,* vol. 136, p. 021004, 2013.

[14] T. Nguyen-Van and N. Hori, "New class of discrete-time models for non-linear systems through discretisation of integration gains," *Iet Control Theory and Applications,* vol. 7, pp. 80-89, Jan 2013.

[15] T. Nguyen-Van and N. Hori, "A Discrete-Time Model for Lotka-Volterra Equations With Preserved Stability of Equilibria," in *ASME 2013 International Mechanical Engineering Congress and Exposition*, San Diego, California, USA, 2013, pp. V04AT04A006; 7 pages.

[16] T. Nguyen-Van, N. Hori, and M. Nahon, "A Discrete-Time Model of Nonlinear Non-Autonomous Systems," in *Proc. American Control Conf*, pp. 5150-5155, 2014.

[17] T. Nguyen-Van and N. Hori, "Improved Nonlinear Discrete-Time Models based on Riccati

Approximation of Integration-Gains," *Iet Control Theory and Applications*, submitted.

[18] T. Nguyen-Van and N. Hori, "A new discrete-time linearization feedback law for scalar Riccati systems," in *SICE Annual Conference (SICE), 2013 Proceedings of*, 2013, pp. 2560-2565.

[19] J. I. Yuz and G. C. Goodwin, "On sampled-data models for nonlinear systems," *Ieee Transactions on Automatic Control*, vol. 50, pp. 1477-1489, Oct 2005.

[20] V. Lakshmikantham and D. Trigiante, *Theory of difference equations : numerical methods and applications*. Boston: Academic Press, 1988.

[21] T. Mori, P. N. Nikiforuk, M. M. Gupta, and N. Hori, "A Class of Discrete-Time Models for a Continuous-Time System," *Iee Proceedings-D Control Theory and Applications*, vol. 136, pp. 79-83, Mar 1989.

[22] A. H. Nayfeh, D. T. Mook, and Wiley InterScience (Online service). (1995). *Nonlinear oscillations*. Available: http://dx.doi.org/10.1002/9783527617586

[23] S. Wiggins, *Introduction to applied nonlinear dynamical systems and chaos*. New York: Springer-Verlag, 1990.

[24] R. E. Mickens, *Applications of nonstandard finite difference schemes*. Singapore: World Scientific, 2000.

[25] T. Chen and B. A. Francis, *Optimal sampled-data control systems*. London ; New York: Springer, 1995.

[26] A. Isidori, *Nonlinear control systems*, 3rd ed. Berlin ; New York: Springer, 1995.

[27] A. J. Lotka, *Elements of physical biology*. Baltimore,: Williams & Wilkins company, 1925.

[28] V. Volterra, *Lecons sur le theorie mathematique pour la vie*. Paris: Gauthiers-Villars, 1931.

[29] P. Z. Liu and S. N. Elaydi, "Discrete competitive and cooperative models of Lotka-Volterra type," *Journal of Computational Analysis and Applications*, vol. 3, pp. 53-73, Jan 2001.

[30] D. Zwillinger, *Handbook of differential equations*. San Diego, Calif.: Academic Press, 1989.

[31] H. Shiobara and N. Hori, "Exact Time-Discretization of Differential Riccati Equations with Variable Coefficients," in *Control and Applications - 2011*, Vancouver, BC, Canada 2011, pp. pp. 90–95.

[32] Y. Morimoto, "Frequency pulling of quasi-periodic oscillation in forced van der Pol oscillator," *Ieice Transactions on Fundamentals of Electronics Communications and Computer Sciences*, vol. E83a, pp. 1479-1482, Jul 2000.

[33] W. J. Rugh, *Linear system theory*, 2nd ed. Upper Saddle River, N.J.: Prentice Hall, 1996.

[34] H. Shiobara and N. Hori, "Numerical exact discrete-time-model of linear time-varying systems," in *Control, Automation and Systems, 2008. ICCAS 2008. International Conference on*, 2008, pp. 2314-2318.

[35] H. Yabuno, M. Miura, and N. Aoshima, "Bifurcation in an inverted pendulum with tilted high-frequency excitation: analytical and experimental investigations on the symmetry-breaking of the bifurcation," *Journal of Sound and Vibration*, vol. 273, pp. 493-513, Jun 7 2004.

[36] G. B. Folland, *Real analysis : modern techniques and their applications*, 2nd ed. New York: Wiley, 1999.

[37] P. B. Borwein and T. Erdēlyi, *Polynomials and polynomial inequalities*. New York: Springer

Verlag, 1995.
[38] K. Kittipeerachon, N. Hori, and Y. Tomita, "Exact Discretization of a Matrix Differential Riccati Equation With Constant Coefficients," *Ieee Transactions on Automatic Control,* vol. 54, pp. 1065-1068, May 2009.
[39] J. D. Murray and ebrary Inc. (2002). *Mathematical biology 1, An introduction (3rd ed.)*.
[40] W. Kahan, *Unconventional numerical methods for trajectory calculations*: Lecture Notes, CS Division, Department of EECS, Univ. of California at Berkley, 1993.
[41] M. I. Zelikin, *Control theory and optimization I : homogeneous spaces and the Riccati equation in the calculus of variations*. Berlin ; London: Springer, 2000.
[42] M. Nowakowski and H. C. Rosu, "Newton's laws of motion in the form of a Riccati equation," *Physical Review E,* vol. 65, Apr 2002.
[43] W. T. Reid, *Riccati differential equations*. New York: Academic Press, 1972.

Associated publications

The materials presented in this thesis covers all results from the following relevant publications:

Journal papers:

1. T. Nguyen-Van and N. Hori, "New class of discrete-time models for non-linear systems through discretisation of integration gains," *Iet Control Theory and Applications,* vol. 7, pp. 80-89, Jan 2013.
2. T. Nguyen-Van and N. Hori, "Discretization of Nonautonomous Nonlinear Systems Based on Continualization of an Exact Discrete-Time Model," *Journal of Dynamic Systems, Measurement, and Control*, vol. 136, p. 021004, 2013.
3. T. Nguyen-Van and N. Hori, "Improved Nonlinear Discrete-Time Models based on Riccati Approximation of Integration-Gains," *Iet Control Theory and Applications,* submitted.

Conference papers:

1. T. Nguyen-Van and N. Hori, "A new discrete-time linearization feedback law for scalar Riccati systems," in *SICE Annual Conference (SICE), 2013 Proceedings of*, 2013, pp. 2560-2565.
2. T. Nguyen-Van and N. Hori, "A Discrete-Time Model for Lotka-Volterra Equations With Preserved Stability of Equilibria," in *ASME 2013 International Mechanical Engineering Congress and Exposition*, San Diego, California, USA, 2013, pp. V04AT04A006; 7 pages.
3. T. Nguyen-Van, N. Hori, and M. Nahon, "A Discrete-Time Model of Nonlinear Non-Autonomous Systems," in *Proc. American Control Conf*, pp. 5150-5155, 2014.

Other works published by the author are detailed as follows:

Journal papers:

1. M. Senda and T. V. Nguyen, "Reproduction of PC Monitor-image from Common-mode Noise using Transfer Function Method," *Journal of JACT*, vol. 14 (4), pp. 55-60, 2009. (Japanese)

Conference papers:

1. T. Nguyen-Van and N. Hori, "A New Discrete-Time Model for a van del Pol Oscillator," *Proc. SICE Annual Conference 2010*, pp. 2699-2704, Taipei, Taiwan, 2010.
2. T. Nguyen-Van and N. Hori, "Linear-Form Discretization and its Application to Lewis Oscillators," *Proc. CA2011, IASTED Int. Conf. on Control and Application*, pp. 126-131, Vancouver, Canada, 2011.